
# ADDIS ABABA UNIVERSITY

## Addis Ababa Institute of Technology

## Energy Center

# WIND RESOURCE DATA ANALYSIS FOR MOSOBO-HARENA WIND FARM

**MASTER OF SCIENCE THESIS**

**PRESENTED IN PARTIAL FULFILLMENT OF THE REQUIREMENTS FOR THE DEGREE OF MASTER OF SCIENCE IN ENERGY TECHNOLOGY**

**By: Mezid Abdella**

**Advisor: Dr.-Ing.Abebayehu Assefa**

October 2015

Addis Ababa

# ABSTRACT

Ethiopia has been relied much on hydroelectric plants for of its power demand. But Hydro power is exposed to the effects of climatic change. Problem of water level fluctuation is increasing continuously in most of the hydropower dams resulting from the climate change. As the demand for safe and clean electricity increases due to industrial development and population growth in the country, expanding wind energy industry is greatly helpful to Ethiopia to meet its growing massive energy demand and to promote sustainable development. The country has enormous potential to generate electricity from wind.

This study investigates the wind energy resource potential for Mosobo-Harena using different statistical methods and software. MS-Excel and MATLAB programs were used to generate time-series graphs of wind speed and direction , frequency distributions of wind speeds (wind speed histogram) and a wind rose for 12 continuous months from January 1/2007 to December 31/ 2007. And WAsP (The Wind Atlas Analysis and Application Program) was used for predicting wind resources, wind atlas generation, develop site wind resource map, identify wind potential sites, sitting of wind turbines and estimating farm annual energy production (AEP). The analysis was conducted based on one year 10 minutes interval wind speed collected data from mast at Mosobo-Harena at heights of 10m and 40m above ground level. This site has an average wind speed of 5.47 m/s and annual wind power density is 161w/m2 at mast height of 10m.

The digital map of the study area was prepared by digital map generating software called Global Mapper considering an area of 20km by 20 km. Grid resource map for the wind farm was generated at some standard heights of 10m, 40m, 60m, 80m and 100m. Then from these standard heights, the hub height of the turbine was decided to be 60m for this project. And thus wind turbine Vestas V60-850kw was selected from WAsP documentation catalogue.

The proposed wind farm has 72 turbines. At the selected turbine hub height of 60m, the annual mean wind speed and wind power density of the farm are 6.79m/s and 316W/m2 respectively, this is categorized as IEC class-III wind resource at this height. And the farm installed capacity is 61.8 MW, the net farm AEP is estimated to be 201686.7 MWhr and the average capacity factor was calculated to be 37.6%.

# ACKNOWLEDGMENT

First of all, I would like to thank the almighty Allah for granting me all that it takes physically and spiritually to complete this thesis. The first person to be acknowledged is my thesis advisor, Dr.-Ing. Abebayehu Assefa, for his intellectual guidance and technical support with helpful comments so that this thesis is accomplished successfully. And I sincerely wish him a healthy long life. I also wish to thank Mr. Muaz Bedru. (Lecturer in the Mechanical Engineering Department, Addis Ababa University) for providing me guidance, direction, comments and giving me some necessary materials at the very beginning of this work.

I express my warm thanks to DTU Wind Energy, Technical University of Denmark especially, their sales assistance Ms. Heidi Serny Jacobsen who arranged the provision of a 6 month educational license to me for use of the WAsP Climate Analyst software, free of charge.

I would like to thank Mr. Addisu, Lecture in Debre-Markos University Mechanical Engineering Department for providing me the wind speed and direction data of Mesobo-Harena wind farm. I would like also to thank my friends who are directly or indirectly supported me in carrying out this thesis work successfully specially Mr. Mengesha Wudu for sharing me constructive ideas on a number of issues related to the project.

Most importantly, none of this could have happened without my family specially Mahmoud Teyib and his wife Amina Sherif. I will be ever grateful for their invaluable assistance, love and tolerance over the last several years. Again I say “thank you” to you all.

# Table Contents

# LIST OF FIGURES

# LIST OF TA`BLES

# NOMENCLATURE AND ABBREVIATIONS

| | | |
|---|---|---|
| A | : | Area |
| a | : | Wind shear exponent |
| AEP | : | Annual energy production |
| C | : | Weibull scale parameter (m/s); |
| CF | : | Capacity factor |
| Cp | : | Power coefficient |
| DTU | : | Denmark Technical University |
| E | : | Energy |
| f (v) | : | Probability density function of the wind speed |
| F (v) | : | Cumulative distribution function |
| GTP | : | Transformation and growth plane |
| GW | : | Gigawatt |
| GWh | : | Gigawatt hour |
| g | : | Gravity constant |
| H | : | Hub height |
| IEA | : | International Energy Agency |
| k | : | Dimensionless Weibull shape parameter |
| kW | : | Kilowatt |
| kWh | : | Kilowatt hour |
| $kg/m^3$ | : | Kilograms per cubic meter |
| m | : | Meters |
| MW | : | Megawatt |
| m/s | : | Meters per second |
| Met | : | Meteorological |
| n | : | Number of observed wind data |
| OWC | : | Observed wind climate |
| P | : | Total Wind Power |
| $P_o$ | : | Standard sea level atmospheric pressure |
| R | : | Specific gas constant |

| | | |
|---|---|---|
| RIX | : | Ruggedness index |
| T | : | Temperature |
| Ti | : | Turbulence intensity |
| v | : | Wind speed (m/s) |
| Vm | : | Mean wind speed (m/s) |
| v(z) | : | Wind speed at height, z |
| WAsP | : | Wind Atlas Analysis and Application Program |
| $W/m^2$ | : | Watt per square meter |
| WTG | : | Wind turbine generator |
| $W/m^2$ | : | Watt per square meter |
| Z | : | Altitude above sea level |
| $\rho$ | : | Air density ($kg/m^3$) |
| $\sigma$ | : | Standard deviation |

# CHAPTER ONE

## 1.1 Background Information

Energy is the key input for technological, industrial, social and economical development of a nation. And energy resources are the basic drive of development of entire mankind and growth of countries' economy, also basis of survival of mankind. The current energy situation is greatly dependents on petroleum products, coal, nuclear energy, energy supplied by wood, etc. all these energy sources are found limited in nature and they create environmental pollution problems. This has led countries to focus on a renewable and cleaner energy sources like wind and solar energy. Wind energy is rapidly emerging as one of the most cost-effective forms of renewable energy with very significant increases in annual installed capacity around the world.

Hydro power currently makes up about 92.5 percent of Ethiopia's total power supply [5]. While hydroelectric power will remain a predominant energy source, the country is looking to diversify its production of renewable power. Hydro power is vulnerable to the effects of climatic change. The problem of water level fluctuation will not be solved completely even with the construction of large scale hydro power plants. Most of the dams face shortage of water due to hydrological problems resulting from climate change. And non-renewable fuels such as gasoline and charcoal are polluting and expensive. Hence, the power generation system has to be diversified. In the short-run it is necessary to increase the current power generation mix, to cover increasing and unsatisfied power demand and to avoid dependence on fuel imports [4].

Ethiopia, a country that relies on hydroelectric plants for the bulk of its power, is now developing significant wind energy capacities. Lack of reliable wind data covering the entire country has been one of the reasons for limited application of wind energy in Ethiopia, but recent studies have shown that Ethiopia has substantial potential to generate electricity from wind, geothermal, solar and hydropower [6]. For example, a recent 17-month study undertaken by Chinese firm Hydro China Corporation confirmed the high potential for wind power in the northern and southern parts of Ethiopia, particularly in the Somali region, with a huge estimated wind energy potential of 1.3 million MW.

Considering the substantial wind resource in the country, the Ethiopian government has committed itself to generate electricity from wind power plants by constructing eight wind farms with total capacities of 1116MW such as Ashegoda (Northern Ethiopia, Tigray region) and Adama (Central Ethiopia, Oromia region) as part the country's plan for diversification of energy generation mix to have reliable electricity supply and to create a "climate resilient" economy together with a number of hydropower plants over the five year Growth and Transformation Plan (GTP) period from 2011 to 2015 [6].

The first two wind farms, the 51MW Adama1 and the 120MW Ashegoda, with a combined capacity of 171MW have already began production of electricity. Ashegoda wind farm is the largest wind farm in Africa. These and other wind farms under construction are expected to ease Ethiopia's dependence on hydropower. This development of wind power is a part of the current energy sector policy of the country that aims at a five-fold increase in renewable energy production by the end of 2015.

This report focuses on analysis of wind resource potential for Mesobo-Harena Wind Farm. Published literatures, measured data sets and analysis techniques and software are the basic tools that shall be used as a method of solution during this analysis.

## 1.2 Problem Statement

In recent years, global renewable energy industry has developed rapidly. Many countries have taken developing wind energy and other renewable energy as important opportunity and means for responding to future dual challenges of energy and climate change and the continued depletion of fossil fuel which is world's major energy resource. Since Ethiopia is an oil importer country, the global oil price increase has significant impact on its economic growth and national security. Therefore searching local renewable energy sources, particularly wind energy, is greatly helpful to Ethiopia to meet its growing massive energy demand and pave the way for the future development of the country. Wind energy is an alternative form of energy which has the most valuable and promising choice for Ethiopia as it is cheap, environmentally friendly, inexhaustible, price stable and the country is an ideal location for application of wind power generation system.

The government of Ethiopia has put in place its Growth and Transformation Plan (GTP) to radically develop the Ethiopian economy. A radical growth in the provision of electricity is one of the cornerstones of the plan. The GTP targets to reach 10 000 MW installed electricity generating capacity by 2015 with large hydropower constituting the largest share, but also bringing in wind and geothermal power into the energy mix to play a vital role in meeting demand with a high degree of reliability. Regarding wind power, Ethiopia is endowed with a huge estimated potential of 100 GW technically feasible wind power [5].

In the context of the Ethiopian power system wind power will play a vital complementary role with hydro power in that the natural cycle of wind energy availability is such that it increases in the dry season when the hydropower reservoirs are low in water, and it decreases in the wet seasons when the reservoirs are rapidly filling up with water. This will make wind power a crucial ingredient of the grid energy mix by improving the reliability of the system even in dry years [5]. Wind power will thereafter continue to be developed as a significant component of the power system.

To this end, the purpose of this thesis is to conduct analysis of wind data for Mesobo-Harena Wind Farm.

## 1.3 Major and Specific Objective

### 1.3.1 Major objective

The major objective of the study is to analyze wind data and estimate site wind energy production potential for Mesobo-Harena Wind Farm based on collected data of 2007 using WAsP software.

### 1.3.2 Specific objectives

The study has the under listed objectives

- To determine wind class of the site based on measured data;
- To generate the wind atlas and the resource map of the site;
- To determine IEC (international electro technician commission) wind turbine classes based on analyzed data;
- To identify potential sites of turbines in the wind farm; and
- Estimation of annual energy production (AEP) and capacity factor (CF).

## 1.4 Methodology

To conduct this research, first related literature were reviewed on wind energy development and wind resource assessment. Then all necessary data were collected and carefully examined for reliability, accuracy and relevance. Then site visit was performed to observe site situation such as the roughness of the area, terrain feature, presence of obstacle around the site, etc. Statistical tools, Excel and MATLAB software have been implemented to process the collected data and format it in a meaningful and insightful manner. The MATLAB code was used to filter and plot the wind speed. WAsP software was the major tool to process one year 10min averaged wind speed and direction data that had been collected from the 10m tower height, to generate wind atlas, wind climate estimation, estimation of the amount of Energy Production and sitting of wind turbines.

## 1.5 Significance of the Study

The result of this study will assist Ethiopia's plan of developing new national energy development strategy to encourage the development of domestic renewable energy resources (especially wind energy) and promotes its development objective of "Energy Diversification". The project work shall contribute to Ethiopia's plan of creating a "climate resilient" economy by 2025, with adequate energy for the country's domestic needs and to reduce global warming. The study also supports in increasing the local value added in the engineering and technological inputs going into the development of wind farms, thereby ascertaining the long term future of large scale wind power development in Ethiopia.

## 1.6 Organization of the Research Report

The study is mainly organized as follows.

The first chapter is organized as discussed above. Chapter Two reviews theoretical and empirical literature on wind energy system and wind resource assessment. The third Chapter analyses the wind data using Excel and Matlab software and format the data in a meaningful manner. The forth chapter is modeling the wind data with WAsP software. Site wind map (resource grid) preparation is discussed in chapter five. Chapter six looks at turbine sitting and the wind farm layout whiles conclusion and recommendations are presented in chapter seven.

## 1.7 Site Description


Figure1-1: Location map of the study wind Park

The study wind park site considered in this project is located in the Mesobo-Harena area of Tigray Region, northern part of Ethiopia. The wind measuring mast has coordinates of 13.3N and 39.3E with elevation of 2400m a.s.l. And the wind farm, covers 20 by 20 km, is specifically bounded by geographic co-ordinates of 545340 m E to 565340 m E longitude and 1489974 m N to 1509974 m N latitude with altitude ranges from approximately 1800 to 2580 m a.s.l. This is presented in the figure below.

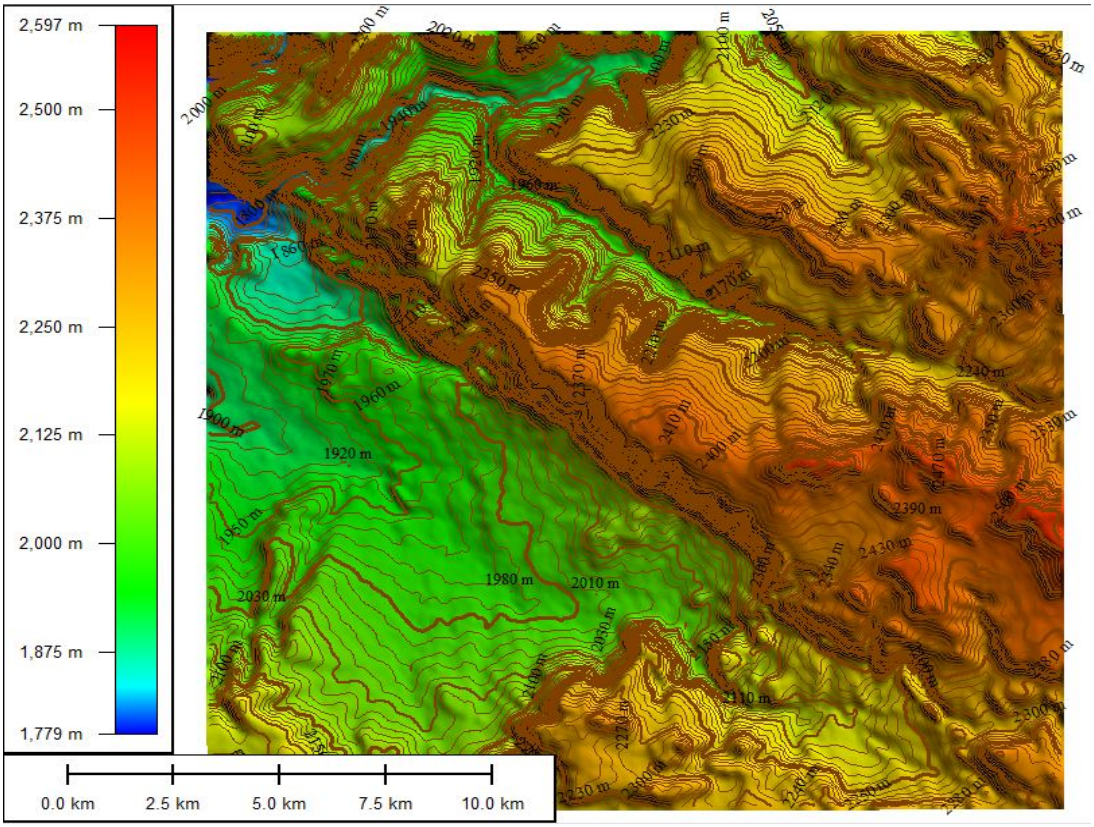


Figure1-2: Mesobo-Harena wind farm on scale of 1:50000 and with height contour density of 20m (Global Mapper Image)

The proposed area for the wind farm contains series of plateau and valley covered with small bushes and grass, with a scattering of small small villages. Most of the plain area is covered by agricultural land. The 3D Global Mapper Image in figure 1.3 shows the terrain feature of the wind farm and the image in figure 1.4 which was captured during site visit shows situation of vegetation cover for some part of study area.

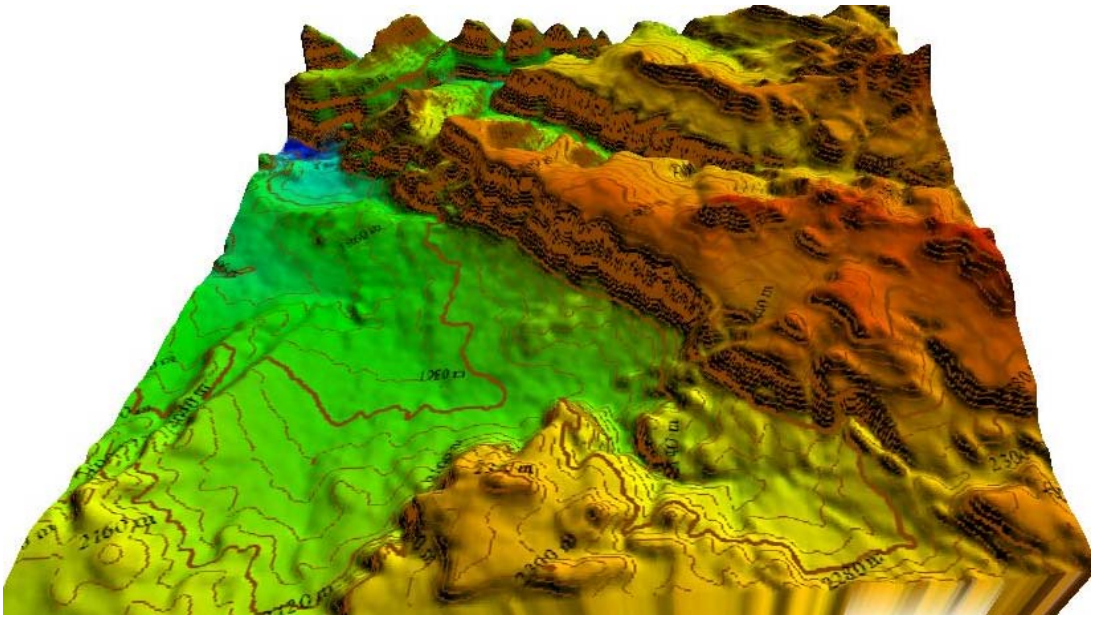

Figure1-3: Terrain feature of the wind farm (Global Mapper Image)

Figure1-4: Situation of vegetation covers for part of study area. (photograghed image, January 2015)

# CHAPTER TWO
# THEORETICAL BACKGROUND

## 2.1 Source of Wind Energy

Solar energy is considered to be the source for most of the renewable energy as the earth receives 1.7 x 10 *14 kW of power as a solar radiation [6].

Wind is the natural movement of air across the land or sea which is caused by uneven heating and cooling of the earth's surface by the sun and by the earth's rotation. Because the Earth's surface is made of very different types of land and water, it absorbs the sun's heat at different rates. Higher intensity of radiation on the equator warms up the earth surface. The air above these warmer areas heats up, then the density of the air became lighter. The light air rises up in the space for certain latitude and spreads around. The rising air creates a low pressure area. Cooler air from adjacent higher pressure areas moves to the low pressure areas. This air movement is called wind. The rotation of the earth changes the direction of the flow of air which produces prevailing winds. Surface features such as mountains and valleys can change the direction and speed of prevailing winds. This wind flow, or motion energy, when "harvested" by modern wind turbines, can be used to generate electricity.

## 2.2 How Wind Power is Generated

The term "wind energy" or "wind power" describes the process by which the wind is used to generate mechanical power or electricity. Wind turbine is a mechanical device that converts the kinetic energy of the wind into mechanical energy through the induced rotation of aerofoil-shaped blades. The turbine's blades are similar to the propeller blades on an airplane. The hub of the turbine is rotated as the wind blows on the angled blades of the rotor. When the wind blows, a pocket of low-pressure air is formed on the downwind side of the blade. The low-pressure air pocket then pulls the blade toward it, causing the rotor to turn. This rotating action of the rotor then spins a shaft, which connects to a generator. The generator converts some of the wind's kinetic energy into mechanical energy. This mechanical power can be used for specific tasks (such as grinding grain or pumping water) or the generator uses an electromagnetic field to convert this mechanical energy into electrical energy [12].

The electrical energy from the generator is transmitted along cables to a substation. Here, the electrical energy generated by all the turbines in the wind farm is combined and converted to a high voltage. The national grid uses high voltages to transmit electricity efficiently through the power lines to the homes and businesses that need it. Here, other transformers reduce the voltage back down to a usable level.

### 2.2.1 Power available in the wind spectra

The performance of a wind turbine is measured in terms of the rate of work done or energy transferred over a given period of time. With a wind turbine, kinetic energy of the wind is converted into electrical energy.

The power from the wind can be given as equation (2.1): [7]

$$P = \frac{1}{2}\rho A V^3 \tag{2.1}$$

This shows that the power (P) of the wind is a function of air density (***ρ***), the area swept by the turbine blades (A), and the velocity of the wind (V). As any one of these factors increase, so does the power available from the wind. Each variable in the power of the wind equation are described below.

**Mean wind speed**

The power possessed by the wind is directly proportional to the cube of the wind speed, as indicated in equation (2.1) above. It means that a relatively small increase in the mean wind speed can make a significant difference in energy output. Therefore, slight differences in the mean wind speed might determine whether a wind energy conversion project is viable or not. For example, if the wind speed is doubled, it will produce eight times the amount of energy captured by the wind turbine. Or if the wind speed at a site is increased by 10%, the energy output will be increased by approximately 30% higher.

**Air density**

Air density is a function of air pressure and temperature, which both are functions of the height above sea level. [10]

$$\rho(z) = {}^{P_0}\Big/_{(R.T)}\exp(-g.z/(R.T)) \tag{2.2}$$

where $\rho(z)$ = air density as a function of altitude (kg/m3); Po = standard sea level atmospheric pressure (kg/m3); R= specific gas constant for air (J/K mol); T= temperature (K); g = gravity constant (m/s2); z= altitude above sea level (m).

So that air density is higher for cold temperatures and low elevations. Increasing the air density increases the turbine's ability to generate power. The WAsP software Air Density Calculator calculates air density [kg/m$^3$] as a function of altitude (elevation) Z [m a.s.l.] and mean air temperature at the same altitude. A lapse rate of 6.5 K/km and a sea level pressure of 1013.25 hPa are assumed [9].

**Area swept**

The final variable in the 'power from the wind' equation is the area swept by the turbine blades. As this increases, so the energy captured increases by the same proportion. So if the area swept by the turbine blades is doubled, so will the potential power from the wind. It is therefore clear that either increasing the number of turbines or the individual blade diameters can increase the total 'area swept' for a wind farm and hence the power output.

### 2.2.2 Power coefficient

Theoretical power available in a wind stream is given by Eq. (2.1). However, the ability of a wind turbine to capture this energy completely from the wind is not perfect. Therefore for any wind turbine, the power output must also incorporate another term in the power of the wind equation, called the power coefficient ($\boldsymbol{C_p}$). Therefore, the power from a turbine can be given as:

$$P = C_p \frac{1}{2} \rho A V^3 \tag{2.3}$$

When the wind stream passes the turbine, a part of its kinetic energy is transferred to the rotor and the air leaving the turbine carries the rest away. Actual power produced by a rotor would thus be decided by the efficiency with which this energy transfer from wind to the rotor takes place. This efficiency is usually termed as the power coefficient (Cp). Thus, the power coefficient of the rotor can be defined as the ratio of actual power developed by the rotor to the theoretical power available in the wind. The power coefficient can be seen a measure of the turbine's efficiency. Hence, [9]

$$C_p = \frac{2\, P_T}{\rho_a\, A_T\, V^3} \tag{2.4}$$

where: $P_T$ is the power developed by the turbine. The power coefficient of a turbine depends on many factors such as the profile of the rotor blades, blade arrangement and setting etc [6]. The real power coefficient Cp is much lower than its theoretical limit, usually ranging from 30 to 45%. [11]

A designer would try to fix these parameters at its optimum level so as to attain maximum Cp at a wide range of wind velocities.

As it was first discovered by Betz in 1925, the theoretical maximum fraction power that can be extracted from the wind is 16/27 or about 59% of the maximum available power from the wind. This is called the Betz maximum**.** So, according to Betz, the theoretical maximum power that can be extracted from the wind is

$$P_{Betz} = \frac{1}{2}.\rho.A.v^3.C_{pBetz} = \frac{1}{2}.\rho.A.v^3.0.59 \quad (2.5)$$

Hence, even if a power extraction without any losses would be possible, only 59% of the power could be utilized by wind turbine.

## 2.3 Wind Speed Measurement

A precise knowledge of the wind characteristics at the prospective sites is essential for the successful planning and implementation of wind energy projects. The basic information required for such an analysis is the speed and direction of the prevailing wind at different time scales. Ecological factors and biological indicators may often be helpful in identifying a candidate site for wind power project. However, for a precise analysis, the wind velocity and direction at the specific site has to be measured with the help of accurate and reliable instruments. The measurement of wind on potential wind turbine sites is generally performed by mounting anemometers onto a mast commonly called a Met Mast. As the anemometers are installed onto the met mast at fixed heights, the wind-shear equation (Equation 2.16) can be used to extrapolate to higher elevations. Universally standard meteorological wind speed measurement height is 10m However, multiple measurement heights are encouraged for determining a site's wind shear characteristics [8].

One year wind data recorded at the site is sufficient to represent the long term variations in the wind profile within an accuracy level of 10 per cent, [6].

Among the various types of anemometer, the most common instrument used to measure wind speeds is the cup anemometer. The wind direction is detected with a wind vane, which is normally fitted together with the anemometer. A data logger collects wind speed and wind direction data from the anemometer and wind vane respectively. As the power is sensitive to the wind speed, good quality anemometers which are sensitive, reliable and properly calibrated should be used for wind measurements. Wind speeds are usually recorded as a 10 minute average basis, which is now the international standard period for wind measurement [8].

## 2.4 Wind Direction

It is very important to find out which directions have the best winds for the sitting of a wind energy conversion system. If we receive the major share of energy available in the wind from a certain direction, the turbine should exposed towards that direction and obstructions to the wind flow have to be avoided from this side.

Information on the velocity and direction of wind, in a combined form, can be presented in the wind roses. The wind rose is a helpful tool chart which indicates the distribution of wind in different directions.

## 2.5 Analysis of Wind Data

### 2.5.1 Average velocity

Due to its cubic relationship with power, the wind velocity is the most critical factor influencing the power developed by a wind energy conversion system. Even a small variation in the wind speed may result in significant change in power. Wind speed and direction are usually basic data required to identify wind resource in a site, but Wind is stochastic in nature. Speed and direction of wind at a location vary randomly from year to year, season to season, with the time of day, and with height above ground. Therefore these data need to be analyzed in a proper way to provide us better understanding of wind characteristics at a prospective site. In the long term, the mean annual wind speed at a particular site provides a good indication of the amount of energy likely to be captured by the wind. A candidate site must usually have a minimum annual average wind speed of 5 m/s [6].

Wind data can be grouped and averaged over time spans that we are interested to know wind profile over them. In simple terms, the average velocity (Vm) is given according to the equation, Eq. 2.6.

$$\boldsymbol{V_m = \frac{1}{n} \sum_{i=1}^{n} V_i} \qquad \textbf{(2.6)}$$

Where V is the wind velocity and *n* is the number of wind data.

The usage of equation, Eq. (2.6) underestimates the wind power production by twenty percent if it has been used for wind power calculations. Therefore for wind energy calculations, the velocity should be weighed for its power content while computing the average. Thus, the average wind velocity is given by equation, Eq. 2.7, [6].

$$\boldsymbol{V_m = \left[\frac{1}{n} \sum_{i=1}^{n} V_i^{3}\right]^{\frac{1}{3}}} \qquad \textbf{(2.7)}$$

### 2.5.2 Distribution of wind velocity

When calculating the wind power potential of a certain wind farm, it is important to take into account not only the average wind speed of that farm but also the wind speed distribution .Two different Wind farms having the same mean wind speed may give completely different energy output due to differences in the distribution of velocity within the regimes.

One measure for the variability of velocities in a given set of wind data is the Standard deviation $(\boldsymbol{\sigma_v})$. Standard deviation shows how much variation or dispersion of individual velocities from the average value.

Thus it is given by

$$\boldsymbol{\sigma_v}=\sqrt{\frac{\sum_{i=1}^{n}(v_i-v_m)^2}{n}} \quad \textbf{(2.8)}$$

Lower values of standard deviation indicates that the wind data points tend to be very close to mean and a higher value of standard deviation indicates that the data points are spread out over a large range of values.

For a better understanding on wind variability, the data are often grouped and presented in the form of frequency distribution. This gives us the information on the number of hours for which the velocity is within a specific range. If the velocity is presented in the form of frequency distribution, the average and standard deviation are given by Eq. (2.9& 2.6), [6].

$$\mathbf{v_m}=\left[\frac{\sum_{i=1}^{n}\mathbf{f_i v_i^3}}{\sum_{i=1}^{n}\mathbf{f_i}}\right]^{\frac{1}{3}} \quad \textbf{(2.9)}$$

And

$$\boldsymbol{\sigma_v} \;=\sqrt{\frac{\sum_{i=1}^{n}\mathbf{f_i}(\mathbf{v_i}-\mathbf{v_m})^2}{\sum_{i=1}^{n}\mathbf{f_i}}} \quad \textbf{(2.10)}$$

### 2.5.3 Frequency distribution of wind speed

It is logical to represent the wind velocity distributions by standard statistical functions. Various probability functions were fitted with the field data to identify suitable statistical distributions for representing wind regimes. It is found that the Weibull and Rayleigh distributions can be used to describe the wind variations in a regime with an acceptable accuracy level. This study is prepared by considering the Weibull distribution methods as it is widely accepted and extensively used for wind regime analysis, [6].

#### 2.5.3.1 Weibull distribution

The Weibull distribution is a two-parameter probability density function that models the observed or predicted frequency distribution of wind speeds at a particular site very well and it is characterized by the two functions as probability density function and cumulative distribution function. The probability density function (f (V)) indicates the fraction of time for which the wind is at a given velocity V.

Equation (2.11) gives the probability density function (PDF) of the wind speed [6].

$$\mathbf{f(V)=\frac{k}{c}\left[\frac{V}{c}\right]^{k-1} e^{-(V/c)^k}} \quad \textbf{(2.11)}$$

where:

f (V) = the probability density function of the wind speed;

C = the Weibull scale parameter (m/s);

V = wind speed (m/s);

k = the dimensionless Weibull shape parameter

In general, k specifies how steep the peak of the curve is, while c is a value close to the mean wind speed. The Weibull parameters k and c are empirically derived by statistical calculations based on the wind data.

Equation (2.12) defines the cumulative distribution function (F (V)) and it gives us the fraction of time (or probability) that the wind velocity is equal or lower than V. Thus the cumulative distribution F (V) is the integral of the probability density function [6].

Thus,

$$\mathbf{F(V) = \int_0^{\alpha} f(V)dV = 1 - e^{-(V/c)^K}} \quad \textbf{(2.12)}$$

For analyzing a wind regime following the Weibull distribution, we have to estimate the Weibull parameters k and c. Weibull shape and scale parameters k and c can estimated using graphical and other methods, but these factors can also be simply estimated from the mean and standard deviation of wind data with an acceptable approximation as follows [6].

$$\mathbf{k = \left(\frac{\sigma_v}{v_m}\right)^{-1.090}} \quad \textbf{(2.13)}$$

And

$$\mathbf{c = \frac{2v_m}{\sqrt{\pi}}} \quad \textbf{(2.14)}$$

More accuratly, C can be found using the expression [6].

$$\mathbf{c = \frac{v_{mk}{}^{2.6674}}{0.184+0.816k^{2.73855}}} \quad \textbf{(2.15)}$$

## 2.6 Characteristics of wind

A precise knowledge of the wind characteristics at the prospective sites is essential for the successful planning and implementation of wind energy projects. The understanding of the wind characteristics will help optimize wind turbine design, develop wind measuring techniques, and select wind farm sites. The basic information required for such an analysis is the speed and direction of the prevailing wind at different time scales. Velocity and direction of wind change with the geographical locations, time of day, season, and height above the earth's surface, weather, and local landforms. Due to these changes, the power and energy available from the wind also vary. Wind speed variations with height, and presence turbulence are discussed here in this section [6].

### 2.6.1 Variation of wind speed with height and surface roughness

One of the most important phenomena with respect to the utilization of wind energy is the increase in wind speed with height above ground. Wind does not flow smoothly over the Earth's surface. It encounters resistance that changes its velocity and direction over some distance from the surface. The friction of the moving air masses against the earth's surface slows down the wind speed from an undisturbed value at great altitude to zero directly at g round level. This resistance may be caused by the roughness of the ground itself or due to vegetations, buildings and other structures present over the ground, So that much less wind speed is available near the ground. A typical vertical wind profile at a site is shown in Figure 2.1. Theoretically, the mean horizontal wind speed is zero at the Earth's surface and increases with height in the atmospheric boundary layer.

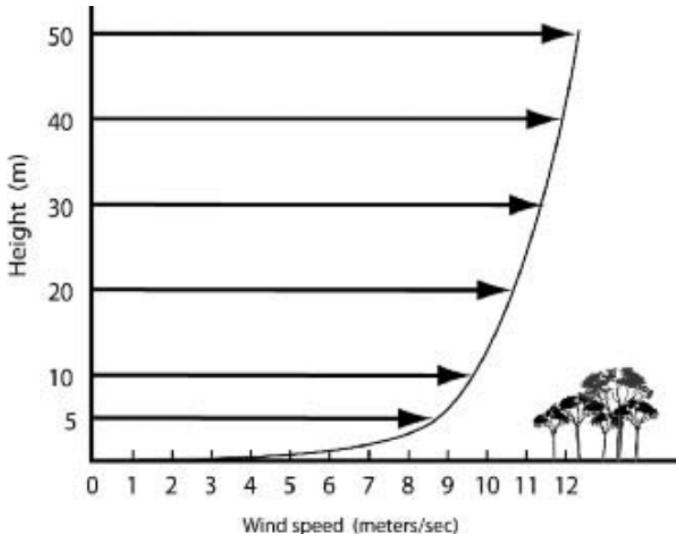


Figure2-1: Variation of wind velocity with height [1]

The increase in wind speed with height is in a logarithmic pattern. The wind data from a known reference height Z and the roughness height is $Z_0$, can be used to calculate the wind speed at another height using the following logarithmic formula: [3].

$$V(Z_R) = V(Z)\ \frac{\ln\left(Z_R/Z_o\right)}{\ln\left(Z/Z_o\right)} \qquad (2.16)$$

where:

V ($Z_R$) = is the predicted mean wind velocity at elevation $Z_R$ (m/s)

V (Z) = is the known mean wind speed at reference elevation Z (m/s)

$Z_R$ = height (m)

Z = reference elevation (measuring elevation) (m)

$Z_0$ = the roughness height at the site of interest

ln = natural logarithm (base e = 2.7183)

This resistance due to friction, however, varies considerably, depending on the roughness of the surface. The rougher or more irregular the surface is, the greater the friction. The surface roughness of a terrain is usually represented by the roughness class or roughness height. The roughness height of a surface may be close to zero (surface of the sea) or even as high as 2 (town centers).

Values of surface roughness length are empirically derived. Table below gives some examples of approximate values of the surface roughness length or height $Z_O$ (m) used in a study.

Table 2.1: Examples of surface roughness lengths

| Terrain surface characteristics | Roughness Class $z_0$ | specified in WAsP [m] |
|---|---|---|
| | **4** (1.5 m) | 1.5 |
| tall forest | | > 1 |
| city | | 1.00 |
| forest | | 0.80 |
| suburbs | | 0.50 |
| | **3** (0.40 m) | 0.40 |
| shelter belts | | 0.30 |
| many trees and/or bushes | | 0.20 |
| farmland with closed appearance | **2** (0.10 m) | 0.10 |
| farmland with open appearance | | 0.05 |
| farmland with very few buildings/trees | **1** (0.03 m) | 0.03 |
| airport areas with buildings and trees | | 0.02 |
| airport runway areas | | 0.01 |
| mown grass | | 0.008 |
| bare soil (smooth) | | 0.005 |
| snow surfaces (smooth) | | 0.003 |
| sand surfaces (smooth) | | 0.003 |
| (used for water surfaces in the Atlas) | **0** (0.0002 m) | 0.0 |
| water areas (lakes, fjords, open sea) | | 0.0 |

**Source:** (WAsP Reference Manual)

As discussed above, Roughness height is an important factor in estimating wind turbine energy production and should be considered in the design of wind energy plants. Obstacles in the vicinity of the point under study may play a paramount role in the assessment of wind climates. The magnitude of this effect depends on the dimensions of the object, its orientation and the distance to the point under study. This effect can be minimized by mounting a wind turbine on sufficiently tall tower so that it maximizes the electrical out-put of the machine.

### 2.6.2 Turbulence

Another natural phenomenon that affects the output of most wind turbines is turbulence. Turbulence is produced as air flowing through rough surfaces and obstructions, such as trees, buildings and rocks. Rapid changes in wind speed occur behind large obstacles and winds may even flow in the direction opposite to the wind. This highly disorganized wind flow is referred to as turbulence (Figure 2.2). The presence of turbulence reduces the harnessable energy of the wind and causes more wear, tear, vibration and unequal forces on the wind turbine.

Extent of this turbulence at the upstream and down-stream of the flow is shown in Figure 2.2.

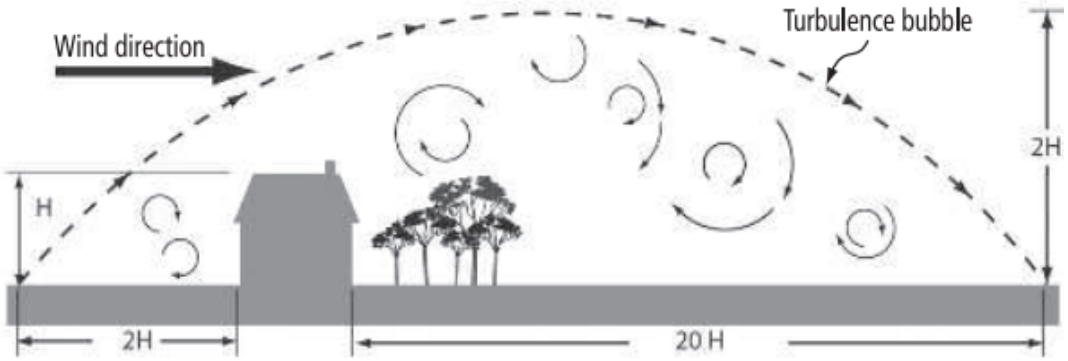


Figure2-2: Turbulence Bubble. The turbulence bubble extends upwind, downwind, and even above the clutter. The shifts when wind direction changes [1]

Turbulence intensity is frequently in the range of 0.1 to 0.4. In general the highest value of turbulence intensities occur at the lowest wind speeds, but the lower limiting value at a given location will depend on the specific terrain features and surface conditions at the site [5]. Based on its nature, the turbulent zone or "turbulence bubble" Can extend vertically about twice the height of the obstruction and extends downwind approximately 15 to 20 times the height of the obstruction [6].

The calculation formula for turbulence intensity is

$$I_r = \frac{\sigma}{V} \tag{2.17}$$

where, $\boldsymbol{\sigma}$: Standard deviation of wind speed (m/s) in a certain time period; V: Average wind speed (m/s) in a certain time period.

Before citing the turbine, the obstacles present in the nearby area should be taken into account and installers recommend that wind machines be mounted so that the complete rotor (the hub and the blades) of the wind generator is at least 30 feet (9 meters) above the closest obstacle within 500 feet (about 150 meters), or a tree line in [1].

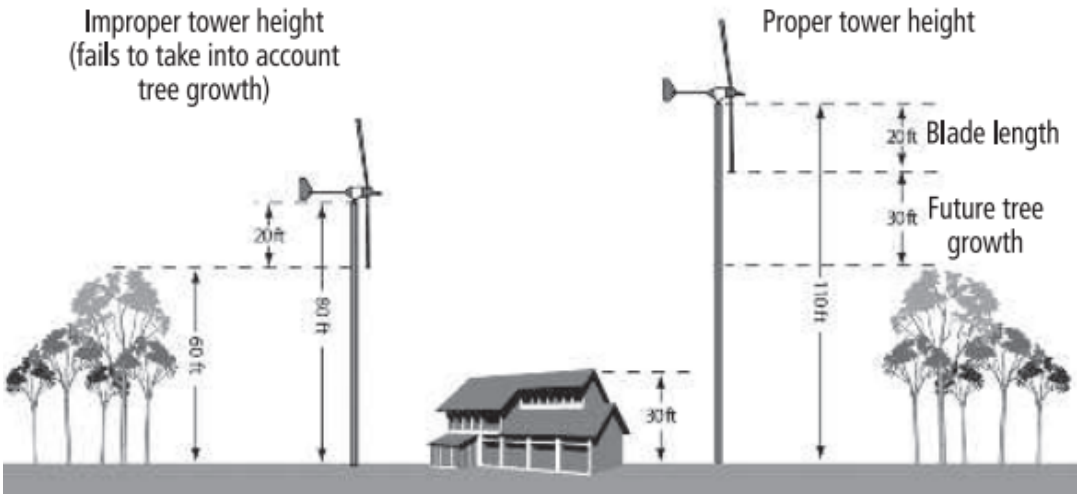


Figure2-3: Tree lines and wind speed [1]

## 2.7 Wind Turbine Selection

Wind turbines are subjected to environmental conditions which may affect their loading, durability and operation. To ensure an appropriate level of safety and reliability, the environmental parameters shall be taken into account during the selection of appropriate wind turbines. In addition wind turbines are selected to produce as much electricity as possible, as cheaply as possible, and so that it maximizes profits.

Wind turbines are grouped into four classes according to IEC 61400-1, Rev 3 depending on the design wind conditions. IEC creates and publishes standards for wind turbine among other electrical and electronics equipment. The IEC 61400 deals with wind turbine generators. The classes are defined by wind speed and turbulence data (Table 2.2) and characterized by:

- The mean annual wind speed ($V_w$)
- The maximum wind speed to be expected as a mean value over 10 min, the so called reference wind velocity ($V_{ref}$).
- The so called characteristic turbulence intensity at a wind speed of 15 m/s ($I_{15}$) at hub height [3].

Table 2.3: Basic wind parameters at rotor hub height for wind type classes

| WT Classes | | I | II | III | IV | S |
|---|---|---|---|---|---|---|
| $v_{ref}$ (m/s) | | 50 | 42.5 | 37.5 | 30 | |
| $\bar{v}_w$ (m/s) | | 10 | 8.5 | 7.5 | 6.0 | |
| $v_{G50} = 1.4v_{ref}$ | | 70 | 59.5 | 52.5 | 42 | values to be |
| $v_{G1} = 1.05v_{G50}$ | | 52.5 | 44.6 | 39.4 | 31.5 | specified by |
| A | $I_{15}$ | 0.18 | 0.18 | 0.18 | 0.18 | the designer |
| | $a$ | 2 | 2 | 2 | 2 | |
| B | $I_{15}$ | 0.16 | 0.16 | 0.16 | 0.16 | |
| | $a$ | 3 | 3 | 3 | 3 | |

**Source:** (Erich H., 2006)

For wind turbine designs in the standard wind turbine classes, the extreme wind speed, $V_{G50}$, with a recurrence period of 50 years, and the extreme wind speed, $V_{G1}$, with a recurrence period of 1 year ( annual gust), shall be computed as a function of height h, using the following equations: [3,4].

$$v_{G50}(h) = 1.4\, v_{ref} \cdot \left(\frac{h}{h_{hub}}\right)^{0.11} \quad (2.18)$$

$$v_{G1}(h) = 0.75 v_{G50}(h) \quad (2.19)$$

As the recommendation from IEC (1999) standard, 'reference wind speed' ($V_{ref}$) can be estimated as five times the annual mean wind speed.

## 2.8 Annual Energy Production (AEP)

It is common practice to specify the energy output of a wind turbine over one year as annual energy production (AEP). Annual Energy Production (AEP) is the total amount of energy produced by the wind turbine over the period of one year. It is a function of the velocity and distribution of wind in the regime. The annual energy production will be calculated by applying the measured power curve to different reference wind speed frequency distributions. In this study A Weibull distribution shall be used as the reference wind speed frequency distribution for AEP estimations as it is widely accepted and extensively used for wind regime analysis. And WAsP, the software used in this paper, uses Weibull distribution for calculating the power production of a wind turbine.

AEP estimations shall be made for hub height according to the equation [4].

$$APN = N_h \sum_{i=1}^{N} [F(V_i) - F(V_{i-1})] \left(\frac{P_{i-1} + P_i}{2}\right) \quad (2.20)$$

where

**AEP** = the annual energy production (MWh) ;

**Nh** = the number of hours in one year ≈ 8760;

**N** i= the number of bins;

**Vi** = the normalized and averaged wind speed in bin i (m/s) ;

**Pi** = the normalized and averaged power output in bin i.

The summation is initiated by setting Vi–1 equal to Vi – 0, 5 m/s and Pi–1 equal to 0,0 kW.

# CHAPTER THREE

# ANALYSIS OF MEASURED DATA USING EXCEL AND MATLAB SOFTWARE

Long term measurements of wind speed and direction are usually needed for a good wind energy assessment. The longer the period of collected data the more reliable are the estimated wind potentials. However, one year data is sufficient to predict the long-term trend of seasonal mean wind speed to within an accuracy of 10 % and a confidence level of 90 % [6].

The raw data gathered directly from the data loggers cannot be used unprocessed for the estimation of the energy yield as it may contain erroneous and incomplete recorded data. This is maybe due to inadequate installation anemometer or external effects like extreme weather conditions or vandalism may cause similar losses of data and data quality. Data losses over longer periods of time also distort the information. Therefore these data need to be checked carefully with erroneous values to be sorted out or to be replaced by suitable ones in a proper way to provide us better understanding of wind characteristics at a prospective site.

For this study one year wind data, collected from January 1 2007 up to December 31 2007, from mast at Mosobo-Harena was used. When this data was provided for this study it had been already inspected and validated, for completeness, reasonableness and the elimination of erroneous values, so that annually expected data of 52560 - 10 minutes average was achieved.

## 3.1 Analysis of Wind Speed Frequency Distribution

The frequency distribution of wind speed is essential in evaluating the availability of wind power at a site. It also permits the selection of appropriate wind machines for exploiting the wind for such application. A histogram is a graphical representation of measured time series wind data distribution. The wind speeds are sorted into wind speed intervals with bin width of 1 m/s. The histogram provides information how often the wind is blowing for each wind speed intervals. The following histogram below shows measured wind data distribution of Mosobo–Harena wind farm at 10 minutes interval.

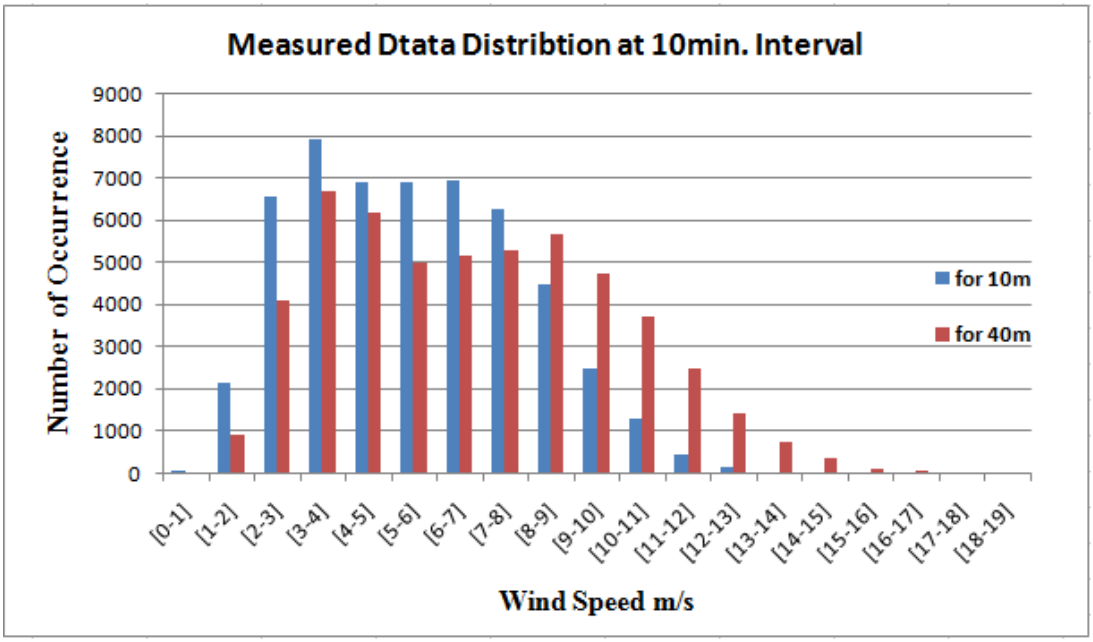


Figure3-1: Histogram of ten minutes average measured data distribution

The observed frequencies rise steadily, reaching maximum value of the wind speed between 3 and 4 m/s and the drop slowly. As can be seen from figure 3.1, smaller speed dominantly at lower height of 10m and higher speed interval dominates at higher height of 40m above ground level.

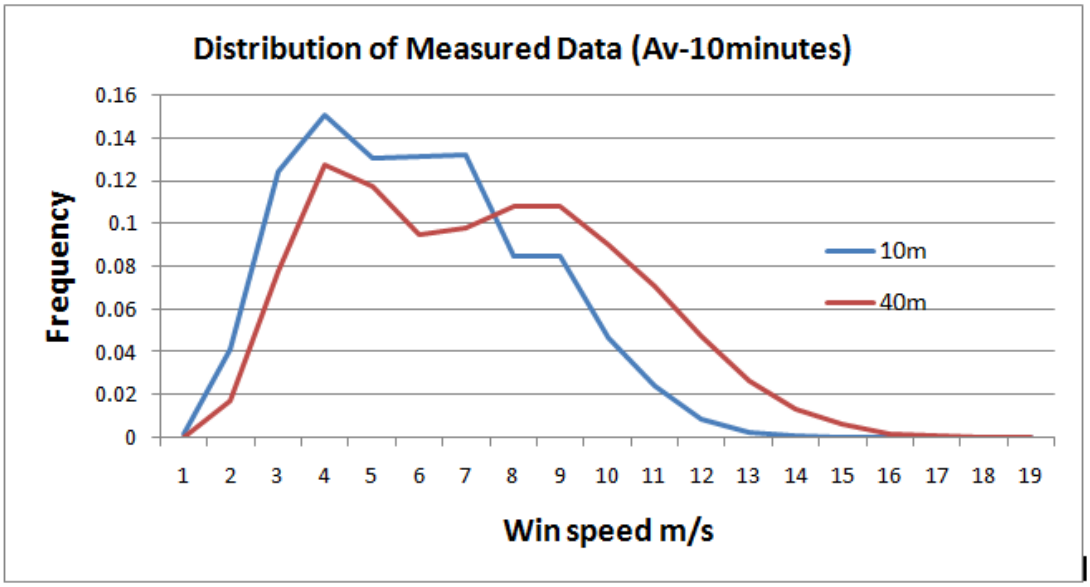


Figure3-2: Frequency distribution of 10 minutes average measured data

Table 3.1: Measured data distribution summary for ten minutes average

| 10min. average speed interval | Number of occurrence at 10m | Number of occurrence at 40m | 10min. Speed interval | Percent of occurrence (at 10m) | Percent of occurrence (at 40m) |
|---|---|---|---|---|---|
| [0-1] | 66 | 4 | [0-1] | 0.00125571 | 7.61E-05 |
| [1-2] | 2152 | 899 | [1-2] | 0.04094368 | 0.0171043 |
| [2-3] | 6560 | 4079 | [2-3] | 0.12480974 | 0.0776065 |
| [3-4] | 7945 | 6711 | [3-4] | 0.15116058 | 0.1276826 |
| [4-5] | 6899 | 6187 | [4-5] | 0.13125951 | 0.1177131 |
| [5-6] | 6923 | 5001 | [5-6] | 0.13171613 | 0.0951484 |
| [6-7] | 6943 | 5143 | [6-7] | 0.13209665 | 0.0978501 |
| [7-8] | 6261 | 5271 | [7-8] | 0.08510274 | 0.1082763 |
| [8-9] | 4473 | 5691 | [8-9] | 0.08510274 | 0.1082763 |
| [9-10] | 2466 | 4741 | [9-10] | 0.04691781 | 0.0902017 |
| [10-11] | 1275 | 3720 | [10-11] | 0.02425799 | 0.0707763 |
| [11-12] | 432 | 2491 | [11-12] | 0.00821918 | 0.0473935 |
| [12-13] | 131 | 1413 | [12-13] | 0.00249239 | 0.0268836 |
| [13-14] | 24 | 709 | [13-14] | 0.00045662 | 0.0134893 |
| [14-15] | 10 | 330 | [14-15] | 0.00019026 | 0.0062785 |
| [15-16] | 0 | 100 | [15-16] | 0 | 0.0019026 |
| [16-17] | 0 | 48 | [16-17] | 0 | 0.0009132 |
| [17-18] | 0 | 16 | [17-18] | 0 | 0.0003044 |
| [18-19] | 0 | 6 | [18-19] | 0 | 0.0001142 |

The hourly average wind speed distribution is presented as shown in Figure 3.3, Figure 3.4 and Table 3.2 below to see the variation of wind speed in hourly basis.

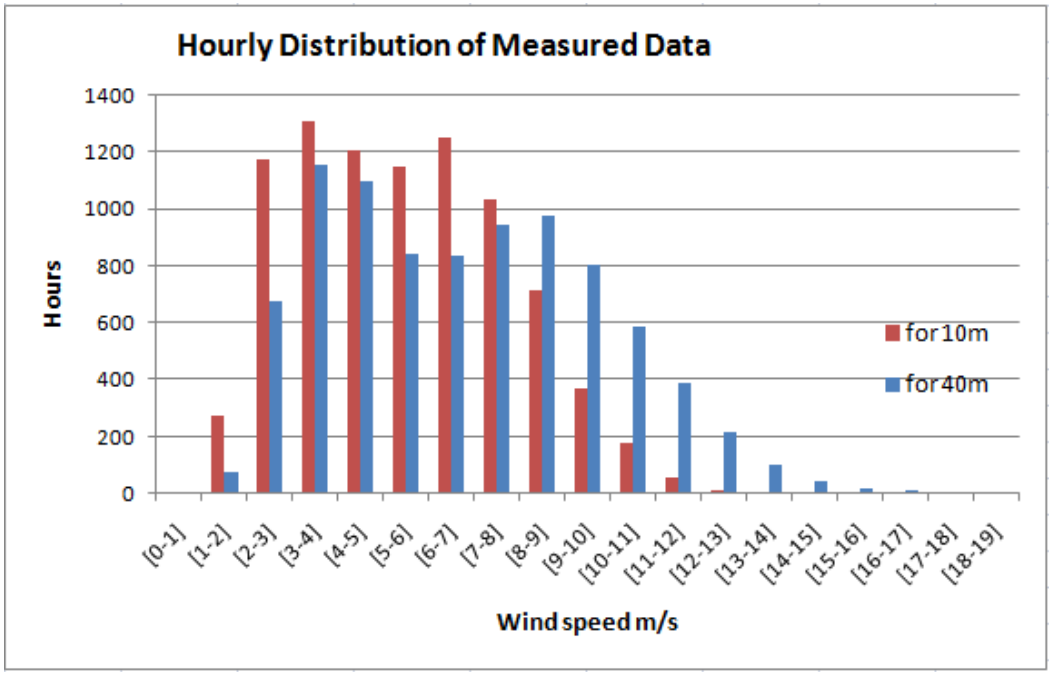


Figure3-3: Histogram of hourly average measured data distribution

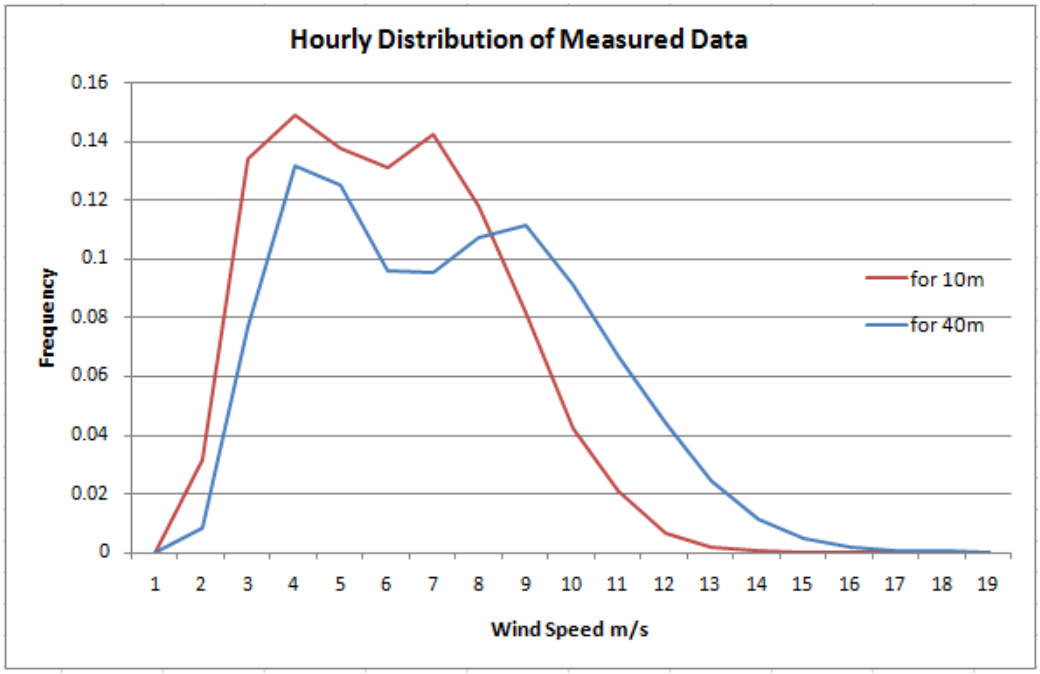


Figure3-4: Frequency distribution of hourly average measured data

Table 3.2: Measured data distribution summary for hourly average

| Speed interval | Number of hours(10m) | Number of hours(40m) | | Speed interval | Percent of occurrence (at 10m) | Percent of occurrence (at 40m) |
|---|---|---|---|---|---|---|
| [0-1] | 1 | 0 | | [0-1] | 0.00011416 | 0 |
| [1-2] | 276 | 73 | | [1-2] | 0.03150685 | 0.00833333 |
| [2-3] | 1176 | 677 | | [2-3] | 0.13424658 | 0.07728311 |
| [3-4] | 1308 | 1156 | | [3-4] | 0.14931507 | 0.13196347 |
| [4-5] | 1211 | 1097 | | [4-5] | 0.13824201 | 0.12522831 |
| [5-6] | 1153 | 844 | | [5-6] | 0.131621 | 0.09634703 |
| [6-7] | 1253 | 837 | | [6-7] | 0.14303653 | 0.09554795 |
| [7-8] | 1036 | 942 | | [7-8] | 0.11826484 | 0.10753425 |
| [8-9] | 715 | 977 | | [8-9] | 0.081621 | 0.11152968 |
| [9-10] | 370 | 802 | | [9-10] | 0.04223744 | 0.09155251 |
| [10-11] | 182 | 588 | | [10-11] | 0.02077626 | 0.06712329 |
| [11-12] | 59 | 387 | | [11-12] | 0.00673516 | 0.04417808 |
| [12-13] | 16 | 212 | | [12-13] | 0.00182648 | 0.02420091 |
| [13-14] | 4 | 100 | | [13-14] | 0.00045662 | 0.01141553 |
| [14-15] | 0 | 44 | | [14-15] | 0 | 0.00502283 |
| [15-16] | 0 | 14 | | [15-16] | 0 | 0.00159817 |
| [16-17] | 0 | 7 | | [16-17] | 0 | 0.00079909 |
| [17-18] | 0 | 3 | | [17-18] | 0 | 0.00034247 |
| [18-19] | 0 | 0 | | [18-19] | 0 | 0 |
| Total | 8760 | 8760 | | | 0.00011416 | 0 |

Variation of average wind speed on a daily basis over the year is plotted in Figure 3.5

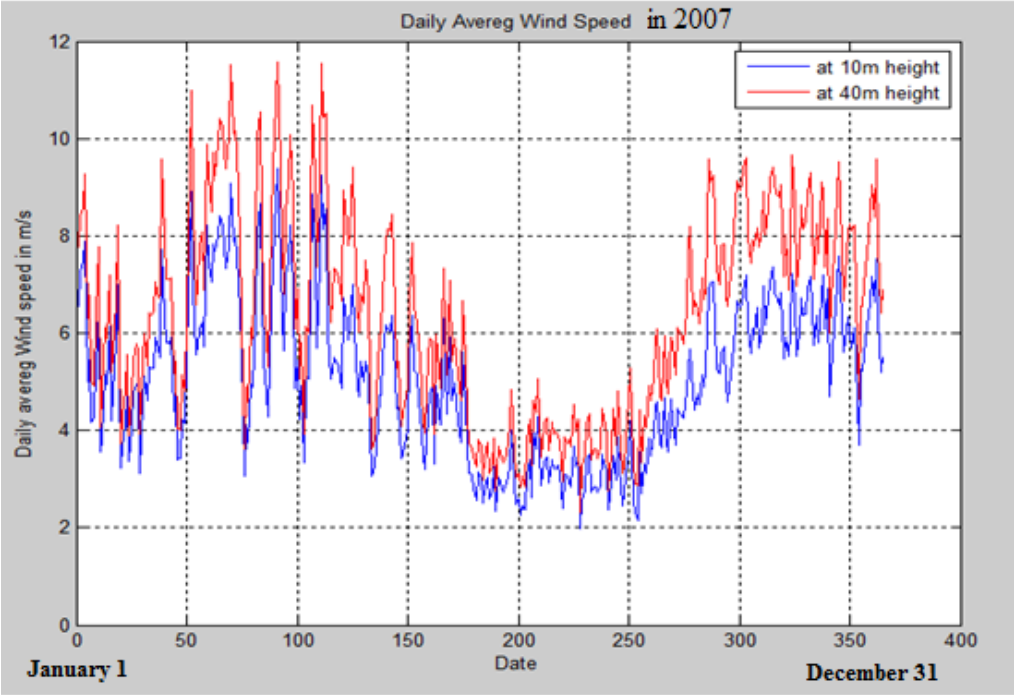


Figure3-5: Difference of annual daily average wind speeds (both heights)

Wind speed also varies in the daily hours as can be seen in the diurnal curve below.

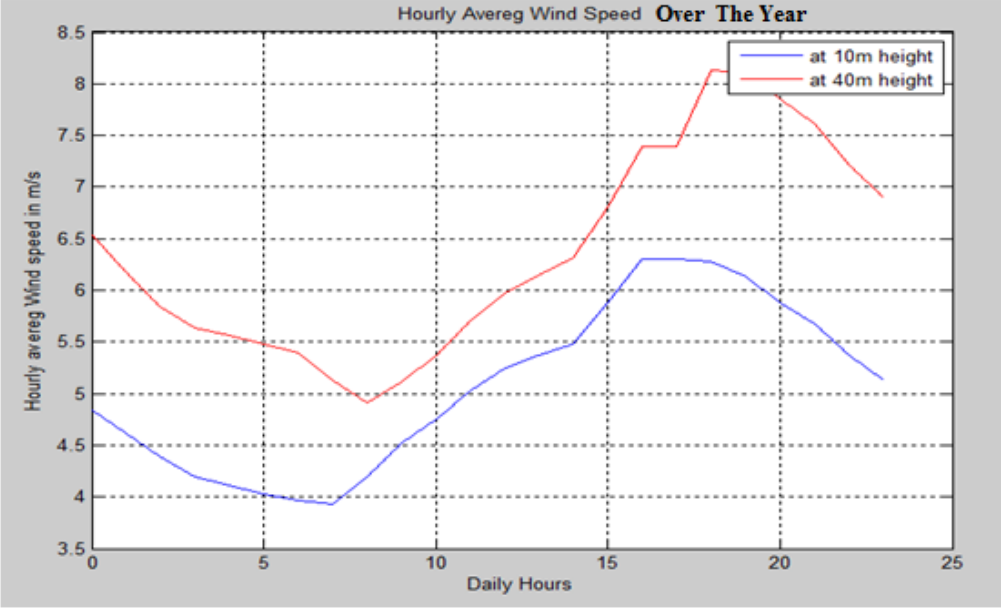


Figure3-6: Hourly average wind speed (both heights)

Figure 3.6 shows the means of day and night wind speed for the study wind site for the year. From the data presented big variation in day and night wind speeds can be seen. Wind speed starts to decrease from evening to the morning in the night time and reaches minimum around 7:00 Am. And then starts to increase from morning to evening in the day time and reaches maximum around 6:00 PM.

The diurnal variation can be advantageous for wind power production during the daytime as the demand for power is more in the daytime than nighttime [6].

Monthly wind speed profile of the study site is shown in Figure 3.7 , the seasonal change of wind speed as described in Mathew's book is due to variation of daylight caused by the earth's tilt and elliptical orbit [6].

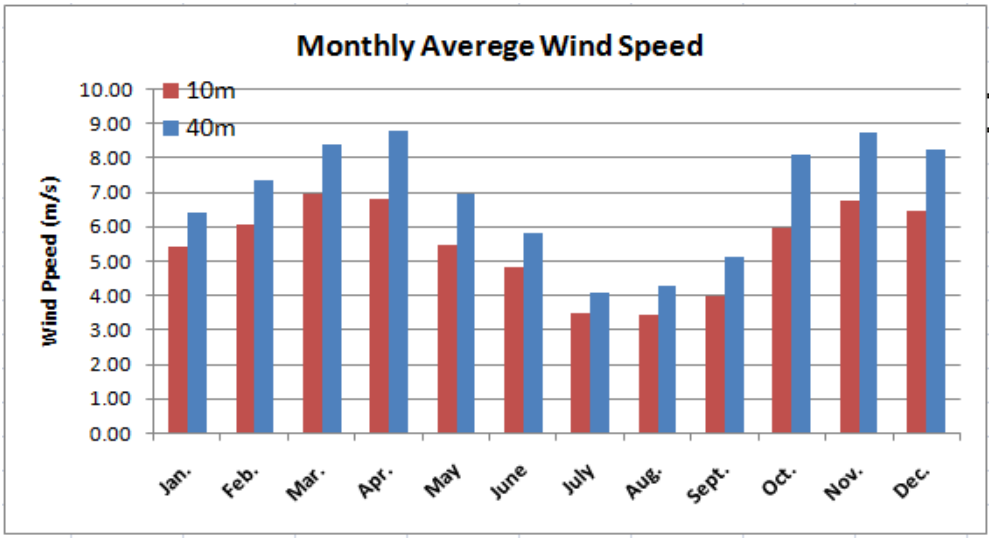


Figure3-7: Monthly variation of wind speed

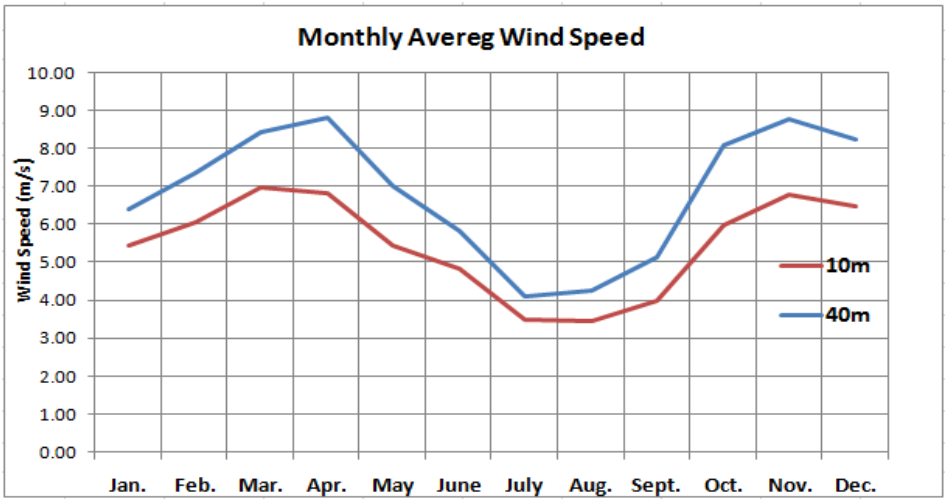


Figure3-8: Variation of the monthly average wind speed at 10 m and 40 m height

Figure 3.8 illustrates the seasonal variation of the site at height 10 and 40 m; slight difference in the monthly mean values have been noticed from the months July to September.

Table 3.3: Annual average wind speed

| Months | 10m | 40m |
|---|---|---|
| Jan. | 5.42 | 6.40 |
| Feb. | 6.06 | 7.34 |
| March | 6.97 | 8.43 |
| April | 6.81 | 8.81 |
| May | 5.45 | 6.99 |
| June | 4.82 | 5.81 |
| July | 3.49 | 4.09 |
| Aug. | 3.44 | 4.26 |
| Sept. | 3.96 | 5.14 |
| Oct. | 5.97 | 8.10 |
| Nov. | 6.77 | 8.76 |
| Dec. | 6.49 | 8.24 |
| **Annual** | 5.47 | 6.86 |

As shown in Table 3.3 above the resulting seasonal pattern in wind availability is characterized by high mean speeds during the dry season and the maximum monthly mean wind speed of 6.97 m/s and 8.81 m/s recorded in March and April corresponding to dry season for 10m and 40m heights respectively. The least windy months are generally July and August corresponding to the rainy and cold season.

## 3.2 Weibull Distribution

The Weibull distribution is a two-parameter probability function that models the observed or predicted frequency distribution of wind speeds at the wind site and it is characterized by the two functions as probability density function and cumulative distribution function. The two parameters of the Weibull distribution can be easily estimated using the wind speed data of the site. Table 3.4 summarizes the results for the site. And here below figures 3.9 and 3.10 show Weibull probability density curve and Weibull cumulative distribution curve of the site respectably.

Table 3.4: Summarized data

| Description | Value ( 10m) | Value (40m) |
|---|---|---|
| No. of data(n) | 52560 | 52560 |
| Sum ($\Sigma Vi^3$) | 13757008.76 | 26761524.3 |
| Mean speed(Vm) | 6.396703476 | 7.985188329 |
| Sum ($\Sigma(V_i-V_m)^2$) | 341726.0968 | 558189.4404 |
| Std.div($\sigma_v$) | 2.549830988 | 3.258840687 |
| k-10 | 2.725177901 | 2.656146448 |
| C-10 | 7.19522046 | 8.989072181 |

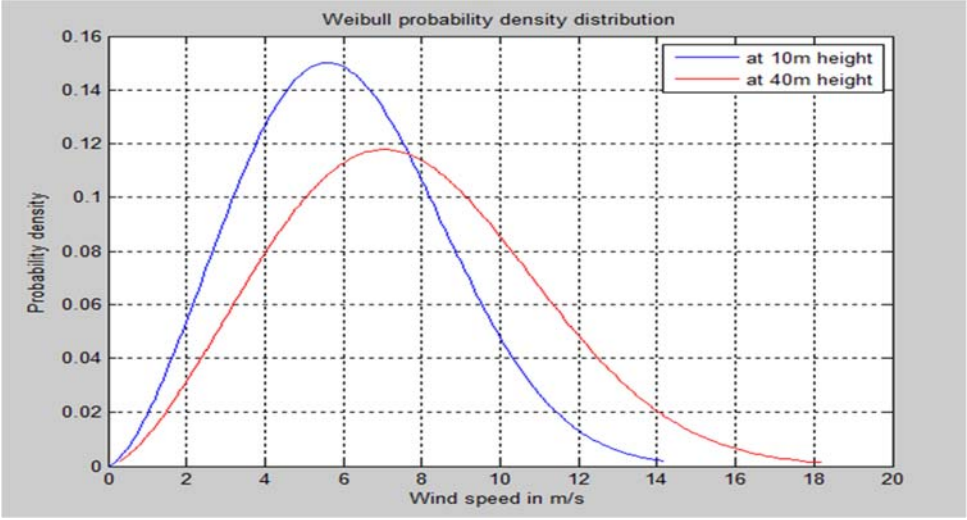


Figure3-9: Weibull probability density curves for both heights (10 minutes average)

From the figure the most frequent occurrence for 10m height is 5.7 m/s with 15% occurrence, and for 40 m height it is 7 m/s with 11.8%. The maximum speed is 14.2 m/s with 0.18% occurrence for 10m and 18.2 m/s with 0.13 % occurrence for 40m.

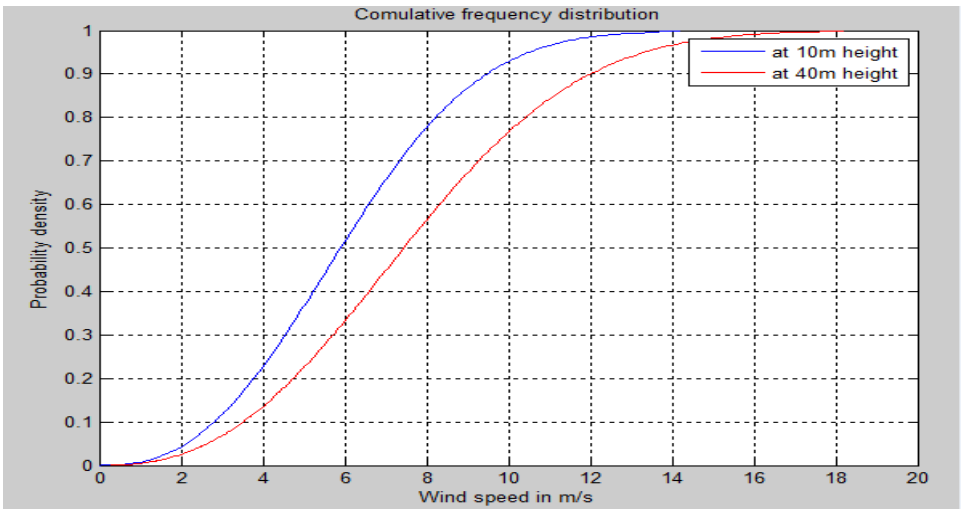


Figure3-10: Weibull cumulative distribution curves for both heights (10 minutes average)

From this cumulative distribution curve, it is presented that:

• 90% of the speeds are below 9.7 m/s and 50% are above 6 m/s for 10m sensor,

• 90% of the speeds are below 12 m/s and 50% are above 7 m/s for 40m sensor,

## 3.3 Wind shear exponent

Using measured wind data at the heights of 10 m and 40 m of Mesobo-Harena site, the average Wind shear exponent has been calculated to 0.1633 using equation 3.1, implying that the wind speed variation in vertical direction is very small at measuring location as shown in Figure 3.11 below.

$$\frac{V_2}{V_1} = \left(\frac{h_2}{h_1}\right)^{\alpha} \qquad 3.1$$

where: α is Wind shear exponent, and $v_2$ and $v_1$ are the mean wind speeds at heights $h_2$ and $h_1$ respectively.

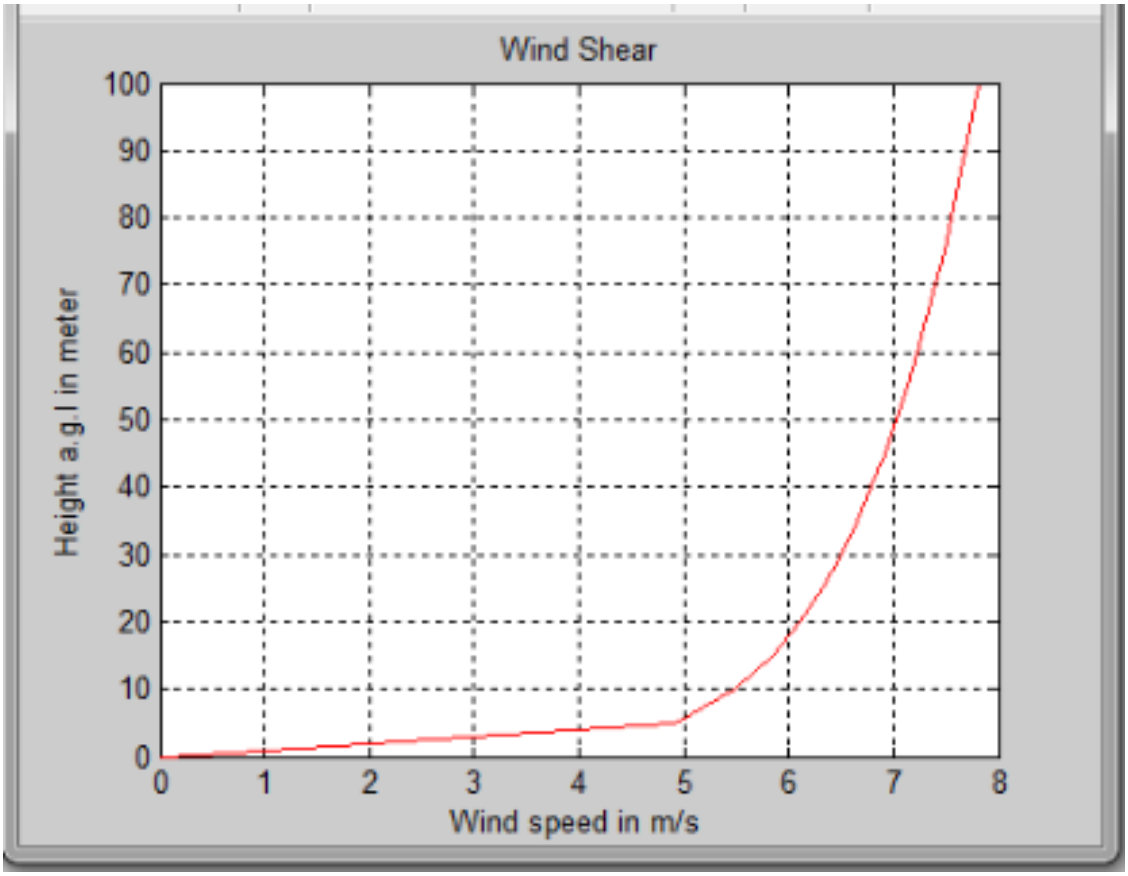


Figure3-11: Wind shear at mast location

## 3.4 Turbulence intensity

Turbulence is natural phenomenon that affects the output of most wind turbines. It is the rapid irregularity of wind speed and wind direction and it is the important wind regime index. The presence of turbulence reduces the harnessable energy of the wind and causes more wear, tear, vibration and unequal forces on the wind turbine. Turbulence intensity can be calculated using the following equation.

$$T_I = \frac{\sigma_v}{V_m} \qquad 3.2$$

Here below Figures are to show the turbulence intensities of both heights and the average turbulence intensity of the site is given in Table 3.5.

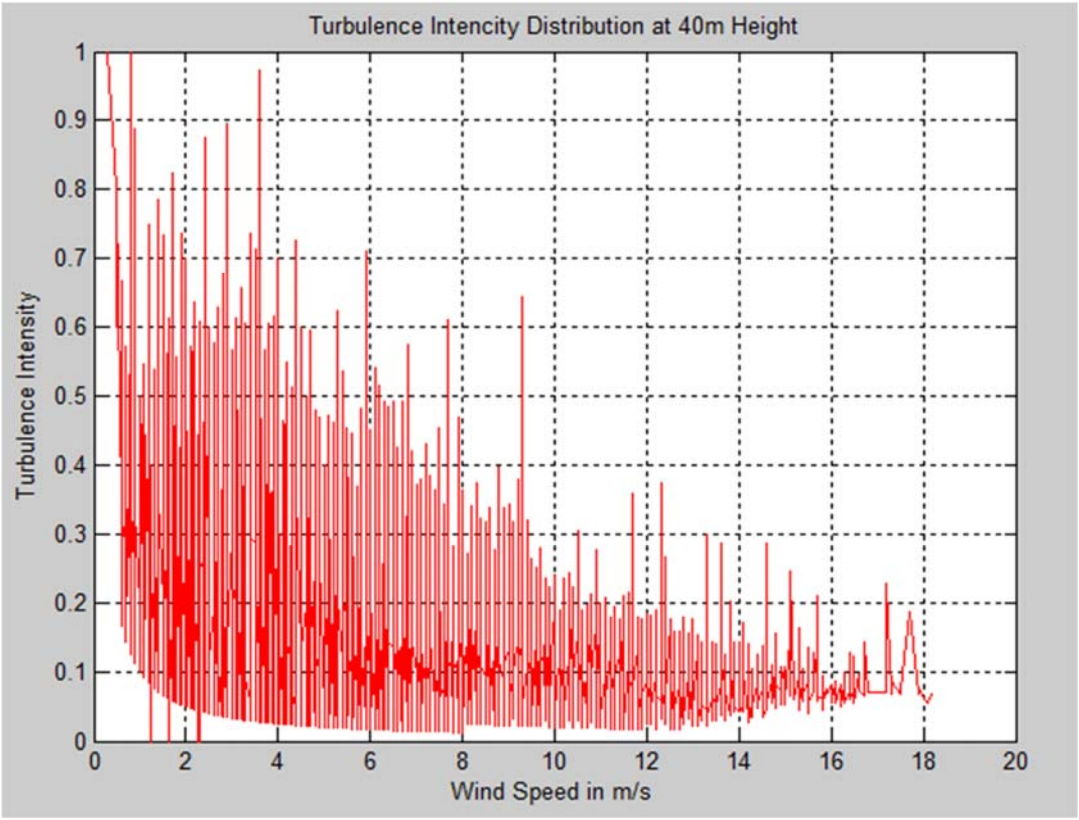


Figure3-12: Turbulence intensity at 40m height

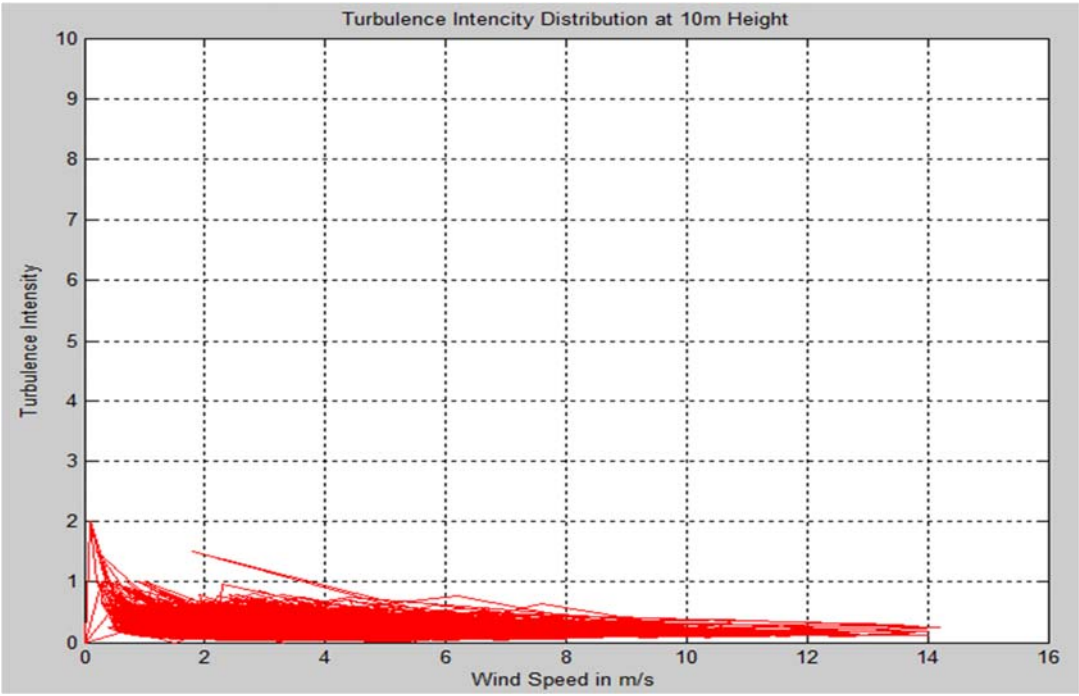


Figure3-13: Turbulence intensity at 10m height

Table 3.5: Average Turbulence intensity at both heights

| | | |
|---|---|---|
| Mosobo–Harena Wind Farm | Ti at 40m | Ti at10m |
| | 0.137758 | 0.177653 |

$T_I$ is a relative indicator of turbulence with low levels indicated by values less than or equal to 0.10, moderate levels to 0.25, and high levels greater than 0.25**.** Therefore, Mosobo-Harena wind mast site is considered as moderate turbulence intensity site.

## 3.5 Wind Power Density

Wind power density value for each 10min interval wind speed at both 10m and 40m heights is computed with the help of the following equation. The figure below shows the wind power density of the site.

$$\frac{P}{A} = \frac{1}{2}\rho * \frac{1}{N}\sum_{i=1}^{N} V_i^3 \qquad 3.3$$

where: P = power, A= swept area of rotor, $\rho$ = air density and V = wind velocity

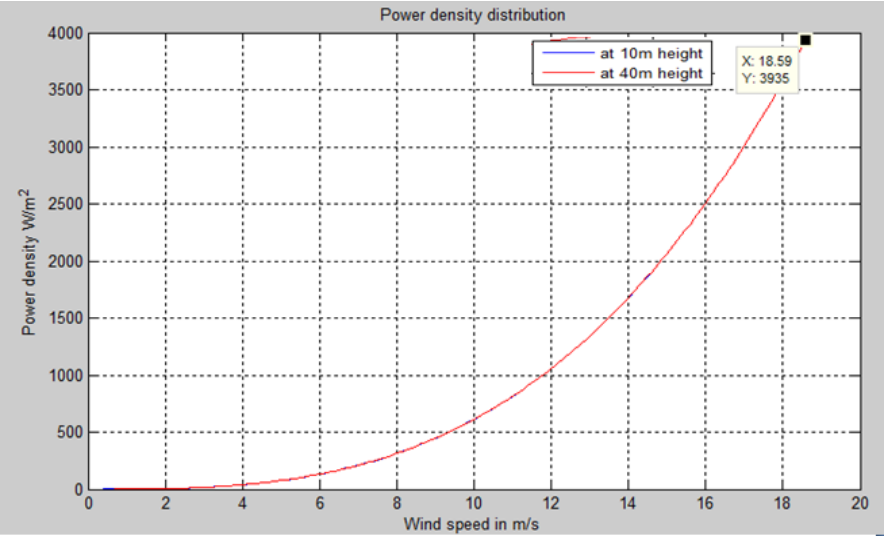


Figure3-14: Wind power density variation (both heights)

Based on equation 3.3, the average wind power density is computed to be 159.67 W/m$^2$ and 310.85 W/m$^2$ at heights of 10m and 40m respectively. Beside this the wind power density at each speed is plotted as shown in figure 3.14. The power density varies from 0 at 0m/s to 1902.3 W/m$^2$ and 3935 W/m$^2$ respectively at 10m and 40m height. In the figure above the curve for the 10m coincides with 40m and not shown clearly because the power density values at both heights are very closed each other.

## 3.6 Wind Rose

As can be seen from Figure 3.15, wind rose for the proposed site was prepared from the wind speed and direction data from the 10m tower height. This circular diagram displays the relative frequency of wind direction in 12 principle direction. As shown in Figure 3.15, 12 radial lines in the wind rose diagram, with 30$^0$ apart from each other are created. The length of each line is proportional to the frequency of wind direction.

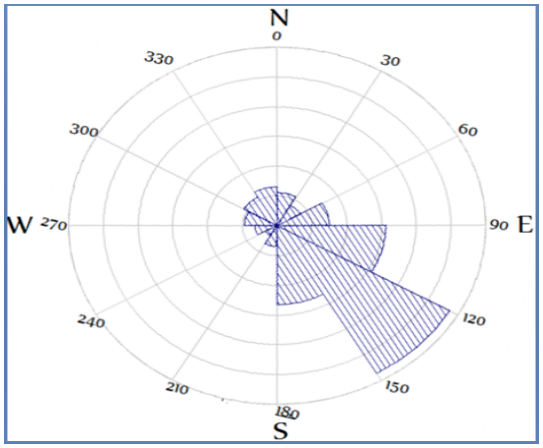


Figure3-15: Wind frequency rose at mast location

On an annual basis, we can see from the above wind rose diagram that the most frequent wind comes from east of southeast direction (120$^o$-150$^o$), and the next high frequent wind is from east of southeast direction (120$^o$-150$^o$), and the least frequent wind direction is south sector (180$^o$).

## 3.7 IEC Wind Turbine Class of the Site

Wind turbines are grouped into classes according to IEC 61400-1, depending to their ability to withstand defined wind speed and turbulence parameters under which the wind turbine might reasonably be expected to operate. Table 2.3 specifies the basic parameters, which define the wind turbine classes.

In the table below the mean wind speed (**$V_{hub}$**) at 10m mast height ($H_{hub}$) is extrapolated to some reference hub heights (H) applying equation 3.1.

For determining **IEC Wind Turbine Class**, based on Table 2.3, at some reference hub heights, the extreme wind speed with a recurrence period of 50 years (**$V_{G50}$**), and the extreme wind speed with a recurrence period of 1 year ($V_{G1}$), shall be computed as a function of height h, using equations 2.18 and 2.19. And the reference wind speed' ($V_{ref}$) is five times the annual mean wind speed [According to IEC (1999) standard].

In this case, the basic wind parameters are computed for different hub heights and their corresponding wind turbine classes as shown in table below.

Table 3.8: Basic wind parameters at rotor hub height and the corresponding WT class

| Reference height(m) | $V_m$ (m/s) | $V_{ref}$ (m/s) | $V_{G50}$(m/s) | $V_{G1}$(m/s) | WT Class |
|---|---|---|---|---|---|
| 10 | 5.47 | 27.4 | 38.36 | 28.77 | IV |
| 40 | 6.86 | 34.3 | 48.02 | 36.02 | III |
| 60 | 7.34 | 36.7 | 51.38 | 38.53 | III |
| 80 | 7.69 | 38.5 | 53.9 | 40.43 | II |
| 100 | 7.98 | 39.9 | 55.86 | 41.89 | II |

Therefore, at this site, low wind speed characteristic has been found. Based on the results in the above table, Mosobo-Harena site is to be classified according to the IEC wind class

regulations as class-IV for 10m, class-III for 40m and 60m, and class-II for 80m and 100m hub heights.

## 3.8 Suitable Tower Heights

Since wind speeds are higher with increasing heights above ground, higher towers can exploit higher wind speeds so that the annual energy production can be increased correspondingly. But higher towers need additional investment cost for the tower and the foundation.

Therefore the hub heights for wind turbines must be selected based on to find a higher wind energy, which is increasing with the hub height, and tower and foundation cost, which also increases as the hub height increases above ground. As it is presented in table 3.8, no significant wind speed increase is recorded after 60m height with these big increases in heights. Therefore, from the standard heights listed it is decided the hub height of the turbine to be 60m for this project. At this height the wind turbine class of the farm is class-III.

## 3.9 Wind Turbine Selection

For this project an appropriate wind turbine, which is class-III with 60m hub height, is available from WAsP wind turbine generators documentation catalogue. Therefore Vestas V60-850kw wind turbine with 3 m/s cut-in, 13m/s rated speed and 20 m/s cut-out speeds with 60m rotor diameter and 60m hub height was selected from WAsP documentation catalogue.

Figure 3-16 shows the performance curve of the selected wind turbine:

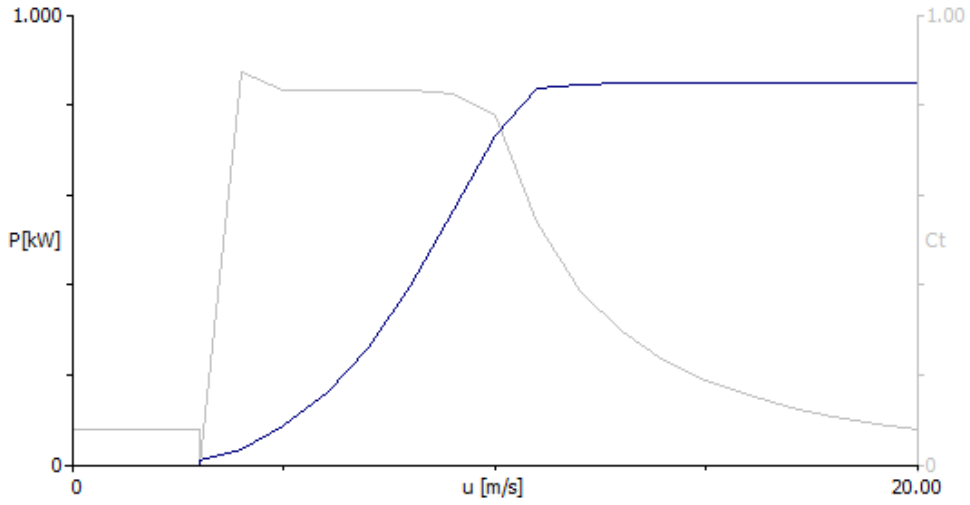


Figure3-16: Power performance curve of Vestas V60-850 kW wind turbine

In wind energy prediction of annual energy production (AEP) the air density is accounted for by using power curves valid for the site specific annual mean air density. The ratings for turbines in WAsP's wind turbines catalogue the default power curves available are valid at standard conditions of 15° C and 101.325 Kpa for which the standard air density is 1.225kg/$m^3$.

But the air density, ρ, changes slightly with air temperature and with air pressure, which both are functions of the height above sea level [6]. In practice a density correction should be made for higher elevations (at the selected hub height of the turbine a.s.l) as the air density change with elevation. This paper has not considered the site specific power curve adjustment of the air density.

# CHAPTER FOUR

# Modeling with WAsP

## 4.1 Overview of WAsP (Wind Atlas Analysis and Application Program)

WAsP is a program for the vertical and horizontal extrapolation of wind climate statistics and energy yield of wind turbines. The predictions are based on wind data measured on site or from stations in the same region and considers wind variations affected by features of the surface of the land such as topographic changes like surface roughness variations, and obstacles, like buildings and trees. WAsP uses equations to describe these variations of the Earth's surface and their effect on wind speed and direction. Weibull distribution is the standard all-sector distribution used for power production calculations by WAsP. [WAsP-10 help doc.]

**Model Input Parameters**

For the wind climate analyses as well as for the energy yield calculation, WAsP needs the following important input parameters.

- **The wind data**: - For this study 10 minutes averaged one year wind data from mast at Mosobo-Harena has been provided and processed into observed wind climate (OWC) wizard to make it compatible with WAsP.
- **Contour map of the area: -** For Mesobo-Harena case the digital map of the site was prepared by digital map generating software called Global Mapper as will be discussed in section 4.2
- **Roughness map of the area:-** A digitized roughness map that describes the terrain around the predicted site has been also prepared by the WAsP Map Editor tool as will be discussed later in section 4.3
- **A description of the power-generating characteristics of the turbine: -** in section 3.8 it has been mentioned that for this paper Vestas V60-850Kw turbine was selected from WAsP turbine data file. The data file also contains a power production curve and thrust coefficient curve for the turbine.

## 4.2 Preparing Map Files for Use in WAsP

WAsP uses vector maps to get information about the elevation (orography) and land cover (roughness) characteristics of the landscape in which the modeling is being done. Digital elevation models cannot be used directly by WAsP, but must be transformed to vector maps format that WAsP can use. Digital map-file of a wind farm can be established by digitization of lines from a map sheet or may be prepared by reformatting existing digital map information [WAsP help doc.]. For Mesobo-Harena case the digital map of the site

was prepared by map generating software called Global Mapper. The height contour map considered an area of 20 by 20 km on scale of 1:50000 and with height contour density of 20m. The elevation range within the map area is found to be 1800 to 2580m above sea level. This digital map is then exported to WAsP and saved as vector map file format (*.map) so that WAsP would accept it. The vector map is shown in the figure blow.

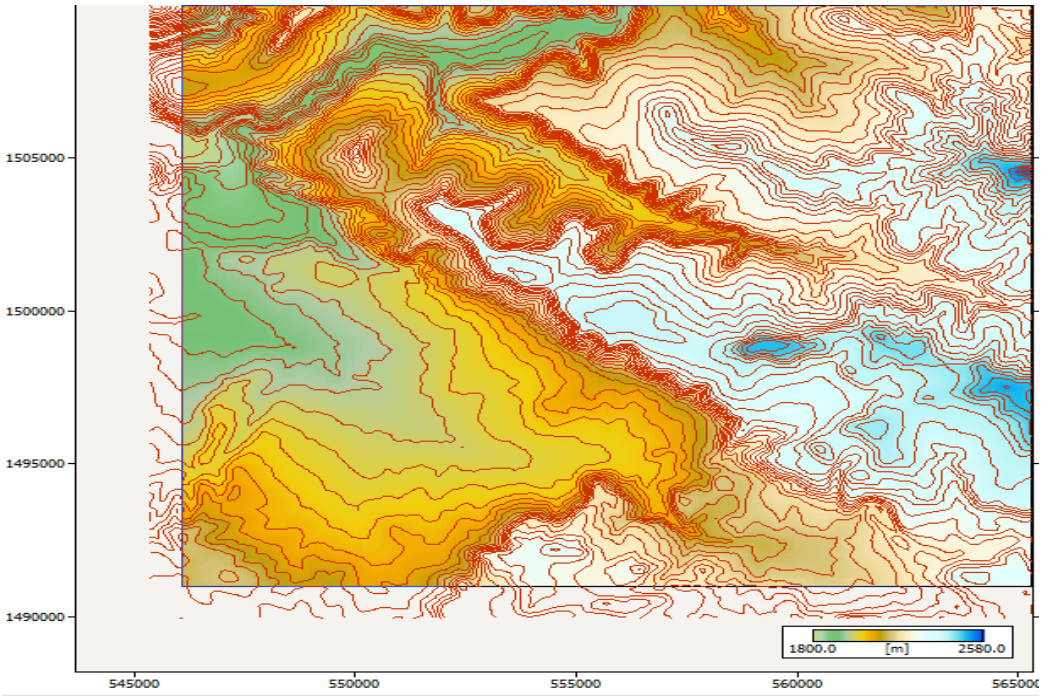


Figure 4-1: Vector map of Mesobo-Harena wind farm

## 4.3 The Roughness Change Model


Figure 4-2: Surface roughness of the project site (Google Earth image)

The overall effects of the terrain surface and obstacles that lead to resistance to the wind near the ground are referred to as the roughness of the terrain. The roughness of a particular surface area is determined by the size and distribution of the roughness elements it contains like vegetation, houses, open farmland, farmland with many shelter belts, forests, villages, and cities. In WAsP the different terrains have been divided into four types, each characterized by its roughness elements or roughness class. And it is parameterized by a length scale called the roughness length, $z_0$. The roughness length describes the height where the wind speed in a logarithmic wind profile is becoming zero; the coarser the surface, the higher the roughness length [WAsP-10 help doc.]. The relation between roughness length, terrain surface characteristics and roughness class is given in table 2.1. The table was served as a guideline for assigning roughness length values for the proposed wind farm.

## 4.4 Roughness Map

WAsP describes the roughness characteristics of the terrain in the form of a digital map of roughness-change lines, i.e. lines separating areas of equal roughness (length). So that WAsP is able to interpret the roughness conditions at any site within the map. As recommended by WAsP, roughness changes close to sites of interest should preferably extend to in radius of at least 10 km from any site likely to be investigated.

For Mesobo-Harena wind farm a digitized roughness map has been evaluated by dividing the landscape into three roughness classes of similar roughness on basis of the information obtained from Google Earth imagery (see Figure 4.3 and table 4.1). And roughness changes specified in a map file format that indicate the roughness change boundaries over the area of interest as shown in the figure 4.4. Then the roughness lengths were assigned to each class as follows.

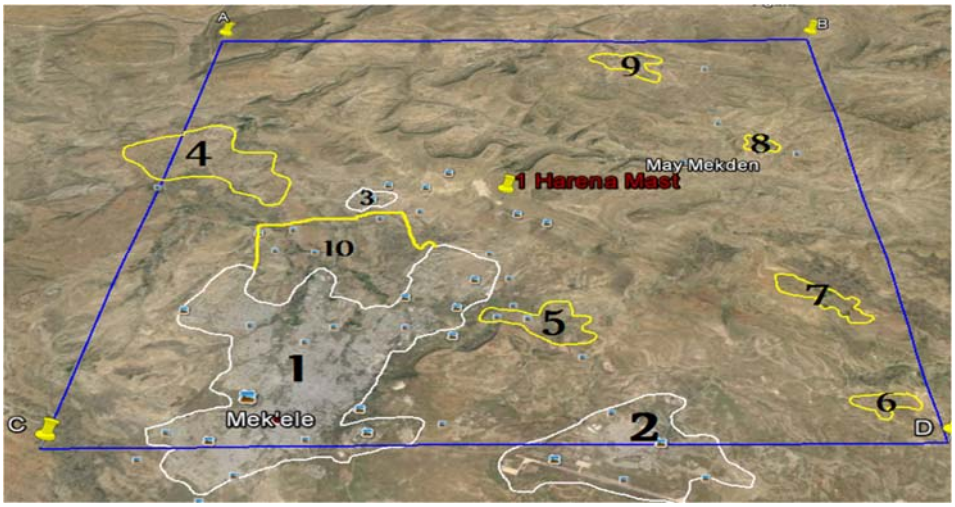


Figure 4-3: Google earth imagery showing roughness of the Mesobo-Harena wind farm

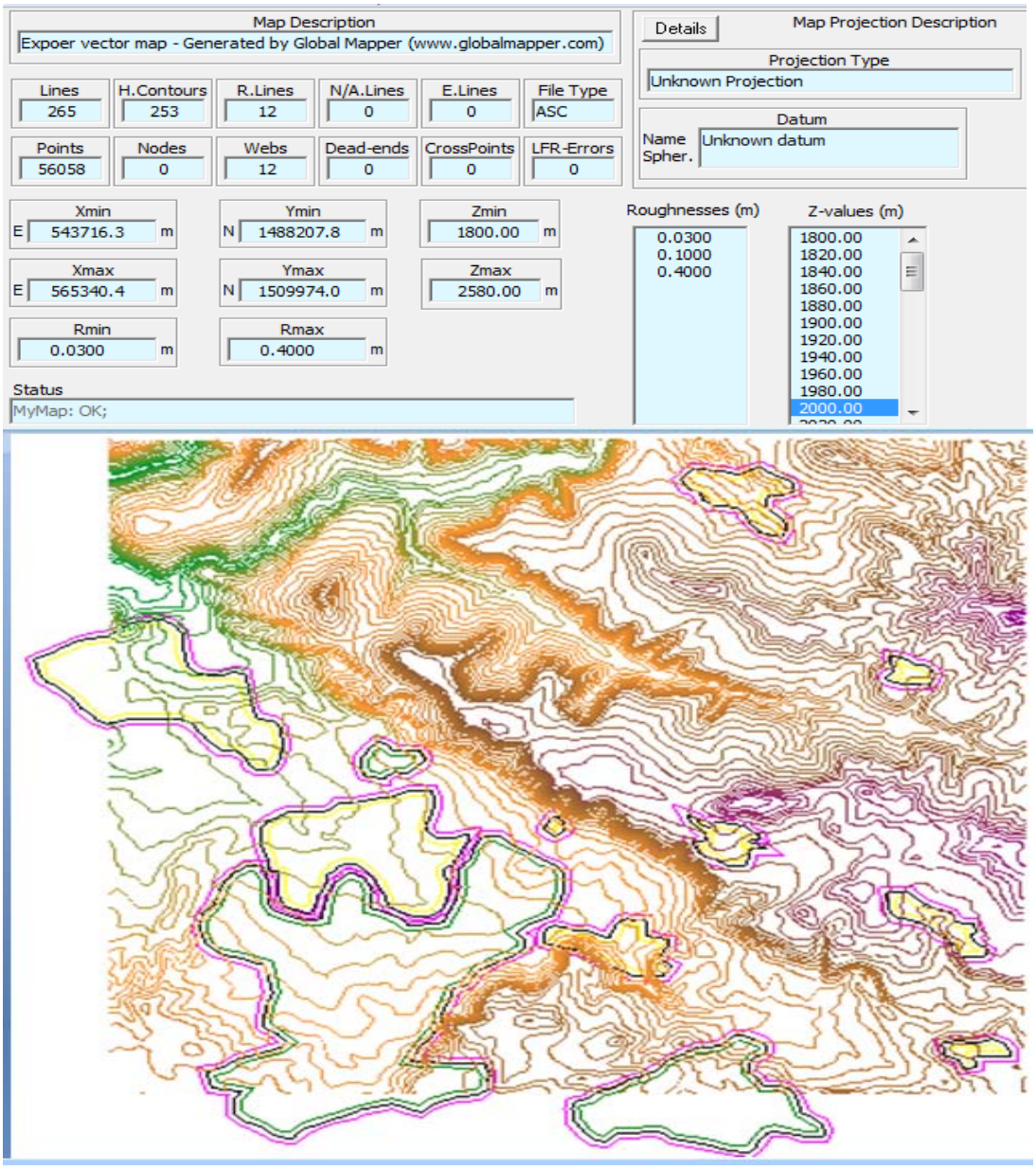


Figure 4-4: Roughness map of Mesobo-Harena wind farm

The terrain corresponding to roughness class 3 (labeled as 1, 2 and 3 in Figure 4-3): urban districts, forests. The farm land is characterized by the many closely spaced windbreaks. Mekele city and Mesobo-Cement Factory areas are made to be belonging to this class. The roughness length is $z_0 = 0.40$ m.

The terrain corresponding to roughness class 2 (labeled as 4 to 10 in figure 4.3): open areas with wind-breaks. The terrain is characterized by less open areas and many windbreaks with trees and houses. The roughness length is $z_0 = 0.10$ m.

The terrain corresponding to roughness class 1(for the rest of the land): very open areas with few windbreaks like Single farms and stands of trees and bushes can be found. The large portion of the wind farm land belongs to this class. The roughness length is $z_0 = 0.03$ m.

Table 4.1 below summarizes the relation between terrain feature and roughness classes and describes the corresponding roughness length values assigned in this study.

Table 4.1: Standard roughness class of Mesobo-Harena wind farm

| **Terrain description** | **Roughness class** | **Roughness length $z_0$ (m)** |
|---|---|---|
| **Urban areas** | 3 | 0.40 |
| **Less open farmland with trees and houses** | 2 | 0.10 |
| **Open farm land with very few buildings/trees** | 1 | 0.03 |

## 4.5 Obstacle Group

Met-stations and (less commonly) turbine sites can have sheltering obstacles in their surroundings. As mentioned in WAsP help facility, if the point of interest (anemometer or wind turbine hub) is closer than about 50 obstacle heights to the obstacle and closer than about three obstacle heights to the ground, the object should probably be included as an obstacle. But in the case of Mesobo-Harena site there are no such obstacles.

## 4.6 Modeling Mesobo-Harena Wind Farm with WAsP Hierarchy Members

There are several hierarchy members, which can appear in the WAsP workspace. The organization of the members in the hierarchy forms associations between the members to perform the calculation. The hierarchy members of Mesobo-Harena wind farm WAsP model were associated as shown in Figure 4-5 below.

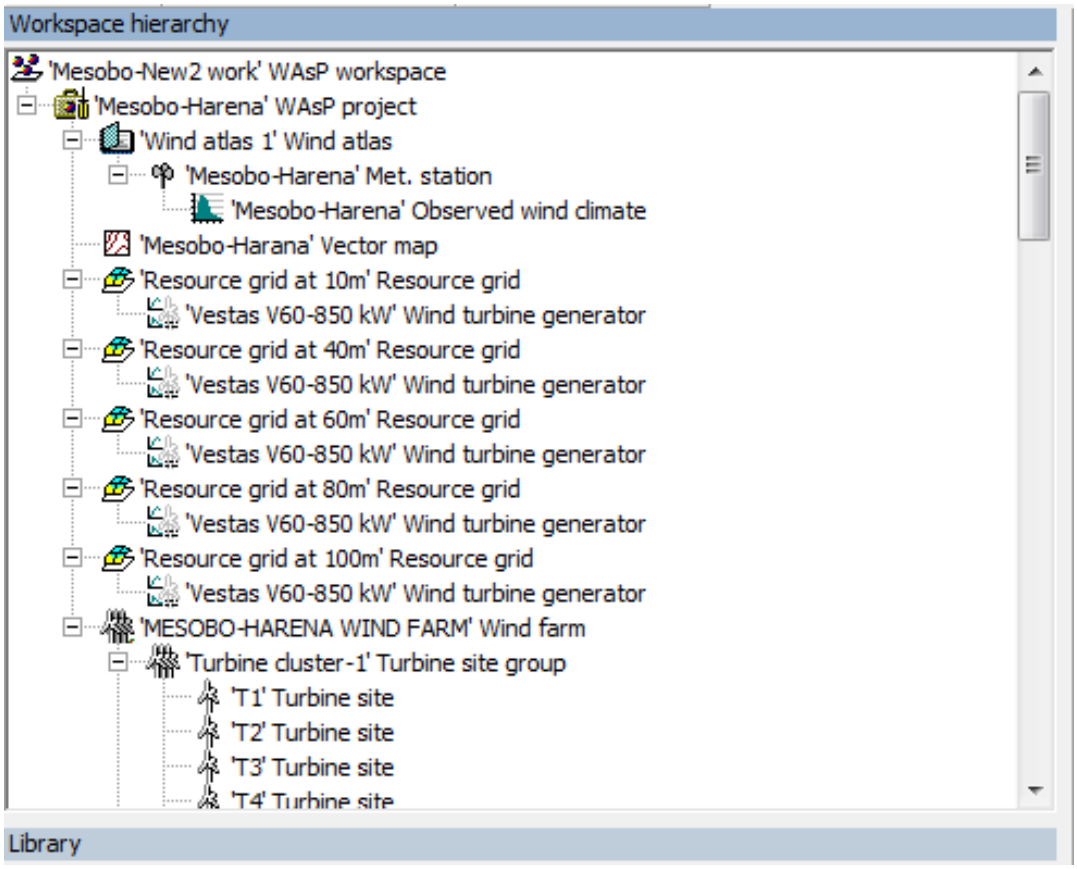


Figure 4-5: Workspace hierarchy model for Mesobo-Harena wind farm

In the workspace hierarchy, the following calculation jobs are performed by met. station, turbine sites, wind farms and resource grids.

From the collected raw wind speed and direction data of Mesobo-Harena mat-station in one year, The WAsP Climate Analyst creates site-specific statistical summary of the observed wind climate: Observed Wind Climate (OWC) Wizard. This analyzed wind data will be converted into a generalized wind climate or wind atlas data set. Using this wind atlas data set the program can estimate the wind climate at any specific point and height by introducing descriptions of the terrain around the predicted site. Then by providing WAsP with the power curve of the selected wind turbine, the total energy content of the mean wind is calculated. Furthermore, an estimate of the actual, annual mean energy production of a wind turbine can be obtained. Given the power and thrust coefficient curves of the wind turbine and the wind farm layout, WAsP can finally estimate the wake losses for each turbine in a farm and thereby the net annual energy production of each wind turbine and of the entire farm, i.e. the gross production minus the wake losses. The program thus contains analysis and application parts.

## 4.7 Result of Observed Wind Climate

Wind speed measuring mast location information

Mesobo-Harena Area

Height: 10.0 meters a.g.l.

Latitude: 13.3°

Longitude: 39.3°

Tables 4.2 and 4.3 and Figure 4.6 present the results of the observed wind climate analysis at Mesobo-Harena wind farm for the period from 1 January to 31 December 2007. The analysis is based on 10 minutes observations for this period.

Table 4.2: Summary of observed wind climate statistics

| Sector | | Wind Climate | | | | Power |
|---|---|---|---|---|---|---|
| **Number** | **Angle [°]** | **Frequency [%]** | **Weibull-A [m/s]** | **Weibull-k** | **Mean speed [m/s]** | **Power density [W/m²]** |
| 1 | 0 | 5.6 | 4 | 1.99 | 3.56 | 53 |
| 2 | 30 | 4.7 | 4.1 | 1.64 | 3.68 | 73 |
| 3 | 60 | 11.5 | 6.2 | 3.4 | 5.53 | 137 |
| 4 | 90 | 20.3 | 7 | 3.64 | 6.35 | 201 |
| 5 | 120 | 26.3 | 8.1 | 4.05 | 7.32 | 295 |
| 6 | 150 | 7.2 | 6.3 | 3.08 | 5.62 | 150 |
| 7 | 180 | 2.2 | 3.9 | 2.97 | 3.48 | 36 |
| 8 | 210 | 2.6 | 3.3 | 2.35 | 2.91 | 25 |
| 9 | 240 | 4.7 | 3.5 | 2.82 | 3.08 | 26 |
| 10 | 270 | 5.5 | 3.6 | 2.63 | 3.23 | 31 |
| 11 | 300 | 4.2 | 4.3 | 2.13 | 3.78 | 59 |
| 12 | 330 | 5.3 | 4.2 | 2.09 | 3.72 | 58 |
| All (emergent) | | | | | 5.45 | 161 |

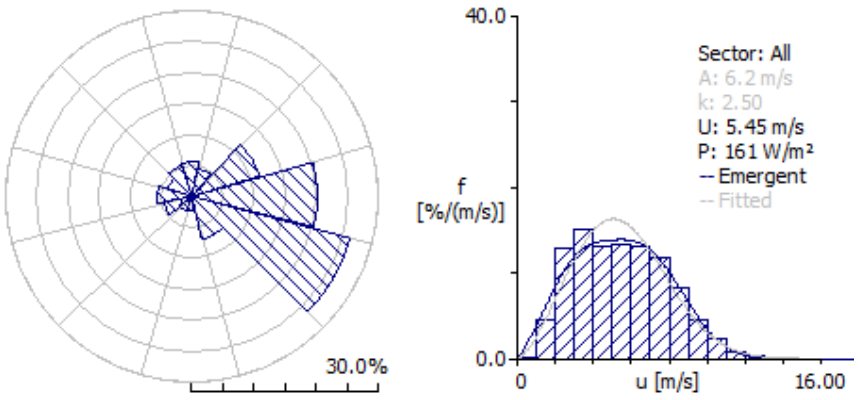


Figure 4-6: Wind rose and Weibull curve for all direction sectors.

Table 4.3: Observed wind climate statistics for each sector

| U | 0 | 30 | 60 | 90 | 120 | 150 | 180 | 210 | 240 | 270 | 300 | 330 | All |
|---|---|---|---|---|---|---|---|---|---|---|---|---|---|
| 1 | 2 | 2 | 2 | 1 | 1 | 3 | 6 | 11 | 3 | 2 | 2 | 3 | 2 |
| 2 | 91 | 85 | 22 | 15 | 9 | 36 | 112 | 152 | 102 | 95 | 95 | 92 | 45 |
| 3 | 275 | 248 | 57 | 37 | 23 | 89 | 240 | 390 | 381 | 339 | 244 | 247 | 129 |
| 4 | 286 | 280 | 119 | 68 | 39 | 132 | 316 | 292 | 342 | 347 | 244 | 260 | 150 |
| 5 | 159 | 169 | 184 | 129 | 72 | 142 | 207 | 99 | 120 | 140 | 167 | 179 | 130 |
| 6 | 101 | 74 | 221 | 177 | 124 | 169 | 90 | 32 | 39 | 47 | 112 | 100 | 132 |
| 7 | 39 | 53 | 196 | 198 | 159 | 183 | 28 | 18 | 12 | 21 | 79 | 64 | 132 |
| 8 | 21 | 40 | 116 | 179 | 198 | 122 | 1 | 6 | 2 | 6 | 43 | 34 | 118 |
| 9 | 16 | 24 | 63 | 114 | 170 | 69 | 0 | 0 | 0 | 3 | 12 | 17 | 84 |
| 10 | 5 | 13 | 14 | 51 | 111 | 40 | 0 | 0 | 0 | 0 | 2 | 4 | 45 |
| 11 | 2 | 5 | 5 | 25 | 63 | 14 | 0 | 0 | 0 | 0 | 0 | 0 | 24 |
| 12 | 1 | 4 | 2 | 5 | 23 | 2 | 0 | 0 | 0 | 0 | 0 | 0 | 8 |
| 13 | 0 | 1 | 1 | 1 | 7 | 0 | 0 | 0 | 0 | 0 | 0 | 0 | 2 |
| 14 | 0 | 0 | 0 | 0 | 1 | 0 | 0 | 0 | 0 | 0 | 0 | 0 | 0 |
| 15 | 0 | 1 | 0 | 0 | 0 | 0 | 0 | 0 | 0 | 0 | 0 | 0 | 0 |
| 16 | 0 | 0 | 0 | 0 | 0 | 0 | 0 | 0 | 0 | 0 | 0 | 0 | 0 |
| 17 | 0 | 0 | 0 | 0 | 0 | 0 | 0 | 0 | 0 | 0 | 0 | 0 | 0 |
| 18 | 0 | 0 | 0 | 0 | 0 | 0 | 0 | 0 | 0 | 0 | 0 | 0 | 0 |
| 19 | 0 | 0 | 0 | 0 | 0 | 0 | 0 | 0 | 0 | 0 | 0 | 0 | 0 |
| 20 | 0 | 0 | 0 | 0 | 0 | 0 | 0 | 0 | 0 | 0 | 0 | 0 | 0 |
| 21 | 0 | 0 | 0 | 0 | 0 | 0 | 0 | 0 | 0 | 0 | 0 | 0 | 0 |
| 22 | 0 | 0 | 0 | 0 | 0 | 0 | 0 | 0 | 0 | 0 | 0 | 0 | 0 |
| 23 | 0 | 0 | 0 | 0 | 0 | 0 | 0 | 0 | 0 | 0 | 0 | 0 | 0 |
| 24 | 0 | 0 | 0 | 0 | 0 | 0 | 0 | 0 | 0 | 0 | 0 | 0 | 0 |
| 25 | 0 | 0 | 0 | 0 | 0 | 0 | 0 | 0 | 0 | 0 | 0 | 0 | 0 |

Table 4.4: All-sector statistics

| | Weibull-A | Weibull-k | Mean speed | Power density |
|---|---|---|---|---|
| **Fitted** | 6.2 m/s | 2.5 | 5.51 m/s | 161 W/m² |
| **Emergent** | - | - | 5.45 m/s | 161 W/m² |
| **Combined** | 6.2 m/s | 2.41 | 5.45 m/s | 161 W/m² |

On an annual basis, we can see from the above tables and figure that the most frequent wind comes from east of southeast sector (90°-120°) with 26.3 %, and the next high frequent wind is from east of southeast sector (120°-150°) with 26.3 %, and the least frequent wind direction is south sector (180°) with 2.2%. Table 4.2 also shows that the strongest mean winds come from these two directions with 7.32m/s and 6.35 m/s respectively.

The diagrams below show the distribution of wind speed in most frequent wind direction (90°-120°) and in least frequent wind direction (180-210°).

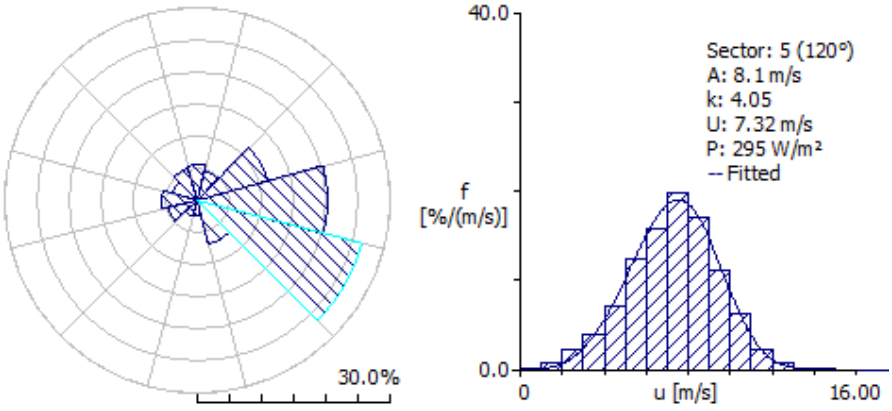


Figure 4-7: Distribution of wind speed in most frequent wind direction (120°)

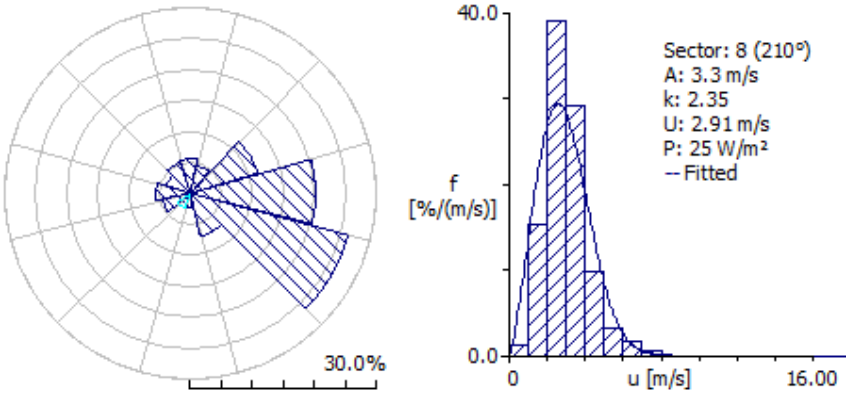


Figure 4-8: Distribution of wind speed in least frequent wind direction ($210^0$)

# CHAPTER FIVE

# SITE WIND MAP (RESOURCE GRID) PREPARATION USING WAsP SOFTWARE

## 5.1 Wind Atlas

Wind atlas is a site-independent general characterization of the wind climate for the entire 20km by 20km area of Mosobo-Harena, derived from the wind measurements at a meteorological station through the wind atlas analysis. The wind atlases show the mean wind speed and mean power density of the wind for 5 different standard heights [10 m, 40 m, 60 m, 80 m, 100 m] above ground level and 5 standard roughness lengths (classes) [0.000 m, 0.030 m, 0.100 m, 0.400 m, 1.000 m]. For each combination of a roughness length and a standard height, there is a wind rose which displays in 12 sector-wise frequencies of wind direction. For each sector in each rose, there is a graph which shows the frequency distribution of wind speeds, and the Weibull-A and Weibull-k parameters for the sector. Hence the mast site predicted Weibull wind speed distributions (wind atlas) for different heights and roughness class combination are presented below.

Table 5.1: Regional wind atlas summary

| **Height** | **Parameters** | **Roughness Classes** | | | | |
|---|---|---|---|---|---|---|
| | | **0.00 m** | **0.03 m** | **0.10 m** | **0.40 m** | **1.00 m** |
| **10 m** | Weibull A [m/s] | 6.38 | 4.55 | 3.95 | 3.09 | 2.41 |
| | Weibull k | 2.29 | 2.15 | 2.15 | 2.16 | 2.18 |
| | Mean speed U [m/s] | 5.65 | 4.03 | 3.49 | 2.73 | 2.13 |
| | Power density E [W/m²] | 186 | 72 | 47 | 22 | 10 |
| **40 m** | Weibull A [m/s] | 7.33 | 6 | 5.42 | 4.62 | 4.02 |
| | Weibull k | 2.36 | 2.31 | 2.29 | 2.3 | 2.31 |
| | Mean speed U [m/s] | 6.49 | 5.31 | 4.8 | 4.1 | 3.56 |
| | Power density E [W/m²] | 276 | 154 | 114 | 71 | 46 |
| **60 m** | Weibull A [m/s] | 7.66 | 6.56 | 5.96 | 5.16 | 4.56 |

| | | | | | | |
|---|---|---|---|---|---|---|
| | Weibull k | 2.35 | 2.4 | 2.37 | 2.38 | 2.38 |
| | Mean speed U [m/s] | 6.79 | 5.81 | 5.28 | 4.57 | 4.04 |
| | Power density E [W/m²] | 316 | 196 | 148 | 96 | 66 |
| **80 m** | Weibull A [m/s] | 7.92 | 7.03 | 6.4 | 5.58 | 4.98 |
| | Weibull k | 2.33 | 2.44 | 2.44 | 2.45 | 2.44 |
| | Mean speed U [m/s] | 7.02 | 6.23 | 5.68 | 4.95 | 4.41 |
| | Power density E [W/m²] | 352 | 238 | 180 | 119 | 84 |
| **100 m** | Weibull A [m/s] | 8.14 | 7.44 | 6.79 | 5.94 | 5.32 |
| | Weibull k | 2.32 | 2.42 | 2.43 | 2.48 | 2.51 |
| | Mean speed U [m/s] | 7.21 | 6.6 | 6.02 | 5.27 | 4.72 |
| | Power density E [W/m²] | 383 | 284 | 215 | 142 | 102 |

The figures below show predicted wind climate distributions and wind rose diagram at 10m, 40m, 60m and 80m hub heights and roughness height of 0.00m.

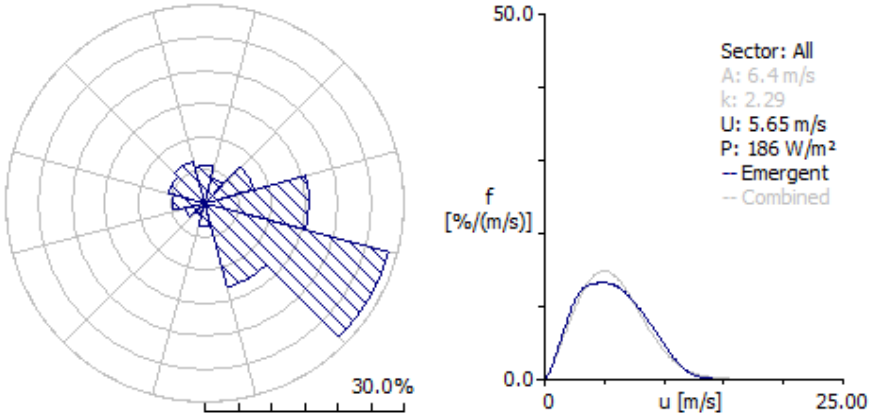


Figure 5-1: Predicted wind climate at 10m height (10m wind atlas)

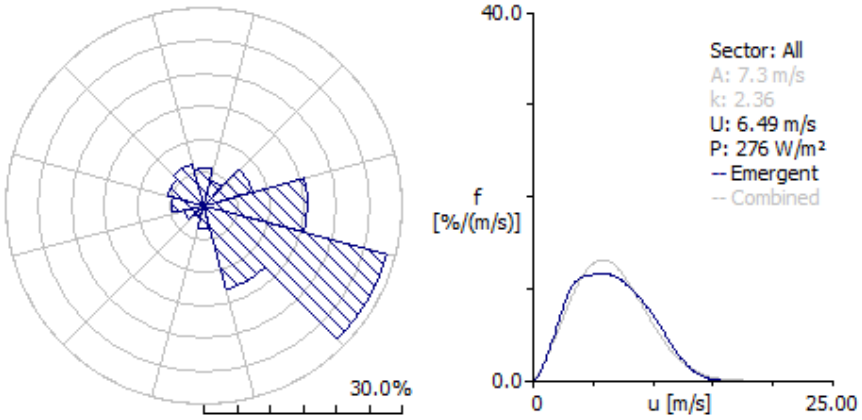


Figure 5-2: Predicted wind climate at 40m height (40m wind atlas)

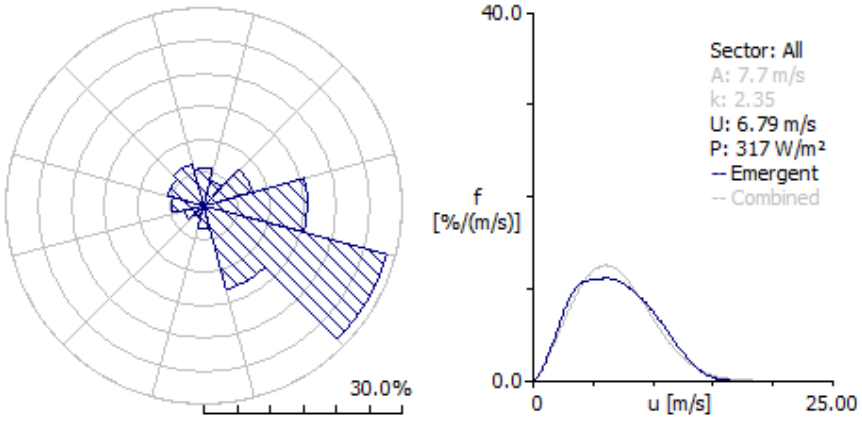


Figure 5-3: Predicted wind climate at 60m height (60m wind atlas)

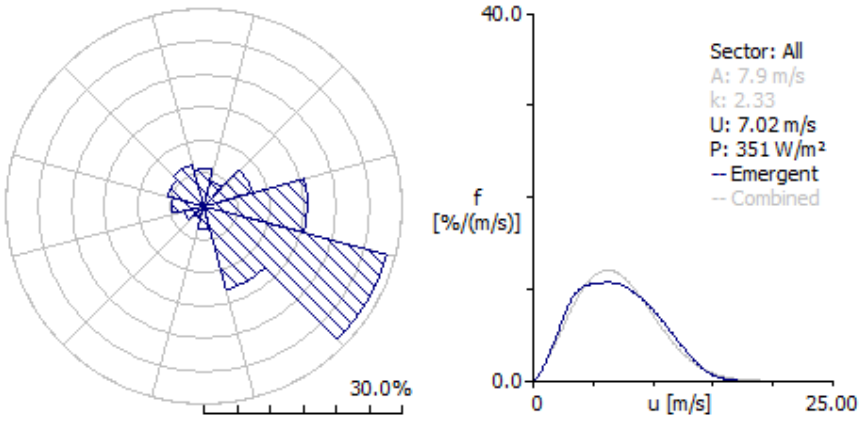


Figure 5-4: Predicted wind climate at 80m height (80m wind atlas)

## 5.2 Wind Resource Grid

One of the very important features in WAsP is the wind resource grid. Wind resource grid is a map prepared by WAsP software and used to obtain preliminary estimates of the wind energy resources of the site considering a specified hub height. This can be used to locate potentially high AEP locations.

The Wind energy resource analysis was performed for the Mosobo-Harena wind farm by considering reference hub heights of 10m, 40m, 60m, 80m and 100m. The result of the analysis is obtained from WAsP resource grid report menu in the form of table and graphics for each reference height.

Here below the figures (Figure 5.1 – Figure 5.16) presents the resources grids of the site. The presentation for all heights contains the Grid setup and the Results. The results are the resource map for Mean speed (m/s), Power density (w/m$^2$), Annual energy production (AEP) (GWhr/year) and ruggedness index (RIX) (%).

### 5.2.1 Wind resource mapping for 10m turbine hub heights

**Grid Setup**

| | |
|---|---|
| Structure: | 192 columns and 190 rows at 100 resolutions give 36480 calculation sites. |
| Boundary: | (546106, 1490993) to (565306, 1509993) |
| Nodes: | (546156, 1491043) to (565256, 1509943) |
| Height a.g.l.: | 10m |
| WTG | 'Vestas V60-850 kW' |

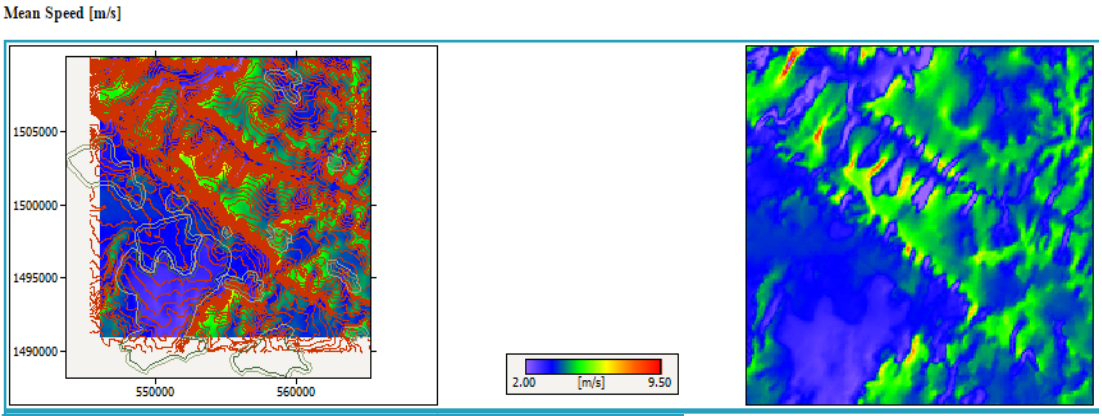


| | |
|---|---|
| Maximum Value: | 10.28 m/s at (548556, 1509243) |
| Minimum Value: | 1.03 m/s at (558456, 1501543) |
| Mean Value: | 3.95 m/s |

Figure 5-5: Wind speed resource map at 10m wind turbine heights

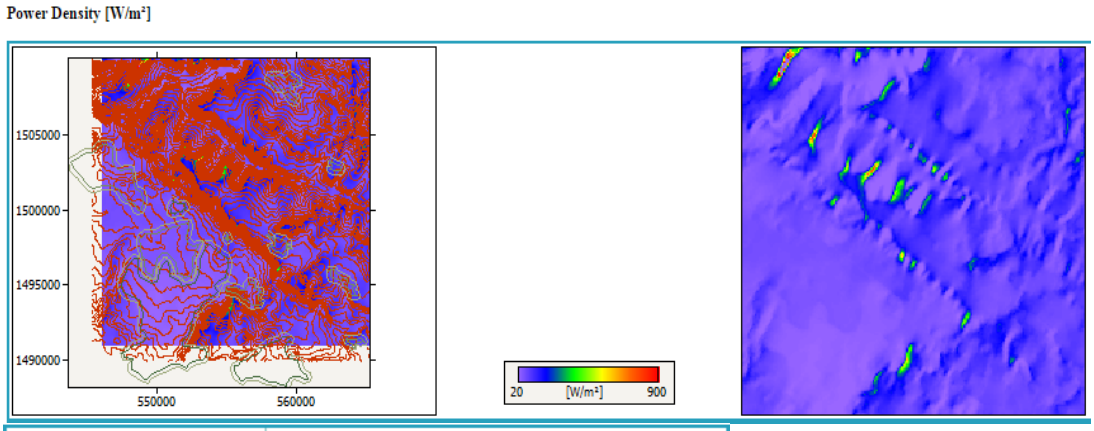


| | |
|---|---|
| Maximum Value: | 1492 W/m² at (548556, 1509243) |
| Minimum Value: | 1 W/m² at (558756, 1502043) |
| Mean Value: | 80 W/m² |

Figure 5-6: Power density resource map at 10m wind turbine hub heights

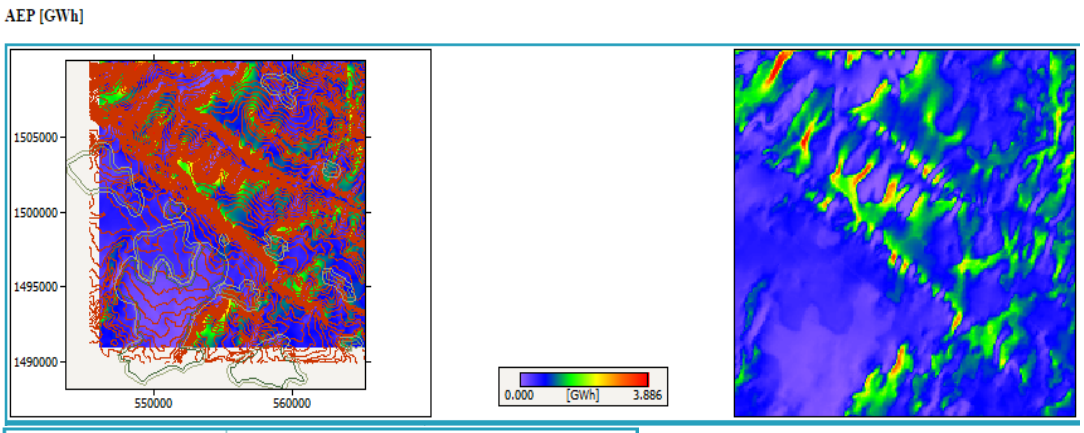


| | |
|---|---|
| Maximum Value: | 3.886 GWh at (548256, 1508743) |
| Minimum Value: | 0.000 GWh at (555756, 1504543) |
| Mean Value: | 0.768 GWh |

Figure 5-7: Annual energy production resource map at 30m wind turbine hub heights

### 5.2.2 Wind resource mapping for 40m turbine hub heights

**Grid Setup**

| | |
|---|---|
| Structure: | 192 columns and 190 rows at 100 resolutions give 36480 calculation sites. |
| Boundary: | (546106, 1490993) to (565306, 1509993) |
| Nodes: | (546156, 1491043) to (565256, 1509943) |
| Height a.g.l.: | 40m |
| WTG | 'Vestas V60-850 kW' |

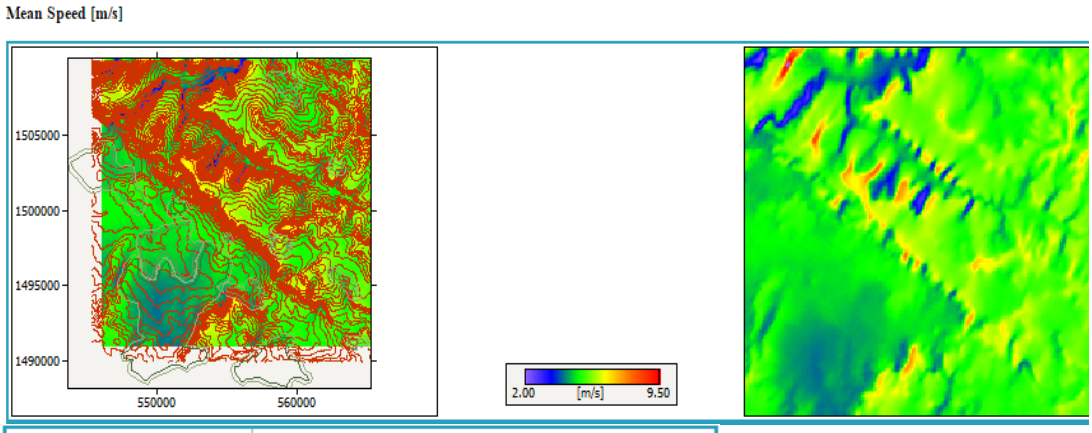


| | |
|---|---|
| Maximum Value: | 9.77 m/s at (548556, 1509243) |
| Minimum Value: | 2.36 m/s at (547056, 1509643) |
| Mean Value: | 5.21 m/s |

Figure 5-8: Wind speed resource map at 40m wind turbine heights

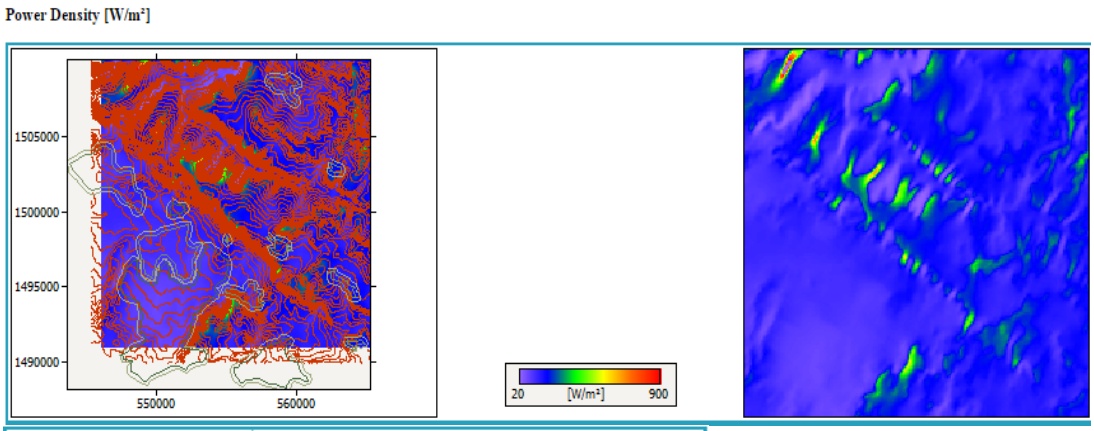


| | |
|---|---|
| Maximum Value: | 1154 W/m² at (548556, 1509243) |
| Minimum Value: | 14 W/m² at (546956, 1509343) |
| Mean Value: | 154 W/m² |

Figure 5-9: Power density resource map at 40m wind turbine hub heights

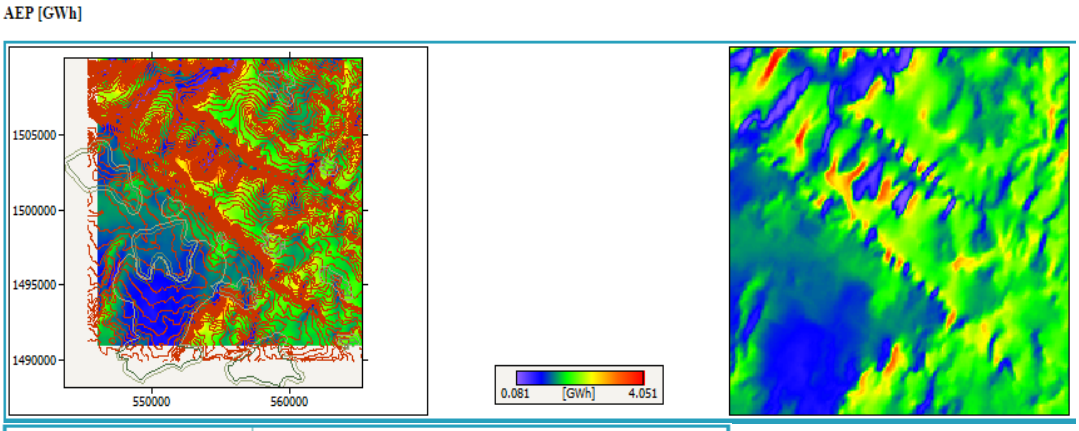


| | |
|---|---|
| Maximum Value: | 4.051 GWh at (548256, 1508743) |
| Minimum Value: | 0.081 GWh at (546956, 1509343) |
| Mean Value: | 1.536 GWh |

Figure 5-10: Annual energy production resource map at 40m wind turbine hub height

### 5.2.3 Wind resource mapping for 60m turbine hub heights

**Grid Setup**

| | |
|---|---|
| Structure: | 192 columns and 190 rows at 100 resolutions give 36480 calculation sites. |
| Boundary: | (546106, 1490993) to (565306, 1509993) |
| Nodes: | (546156, 1491043) to (565256, 1509943) |
| Height a.g.l.: | 60m |
| WTG | 'Vestas V60-850 kW' |

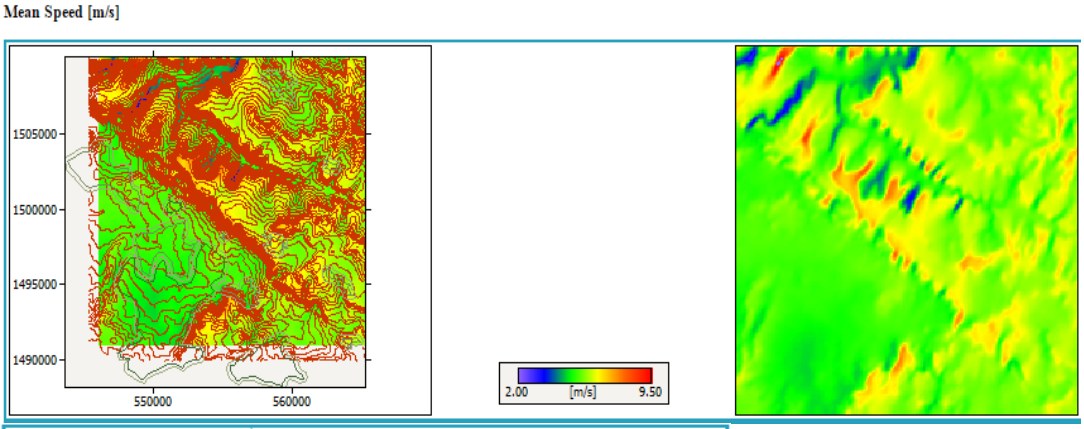


| | |
|---|---|
| Maximum Value: | 9.75 m/s at (548556, 1509243) |
| Minimum Value: | 3.06 m/s at (547056, 1509643) |
| Mean Value: | 5.71 m/s |

Figure 5-11: Wind speed Resource map at 60m wind turbine hub heights

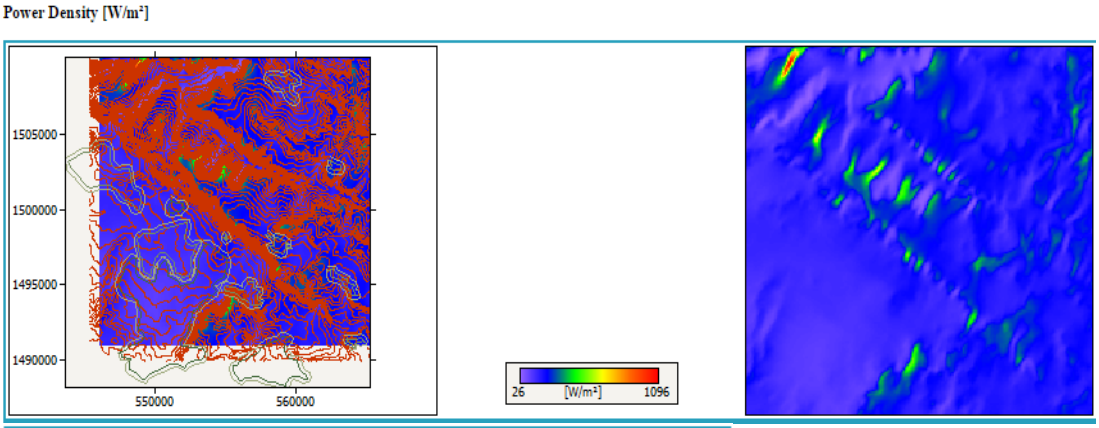


| | |
|---|---|
| Maximum Value: | 1096 W/m² at (548556, 1509243) |
| Minimum Value: | 26 W/m² at (547056, 1509643) |
| Mean Value: | 194 W/m² |

Figure5-12: Power density resource map at 60m wind turbine hub heights

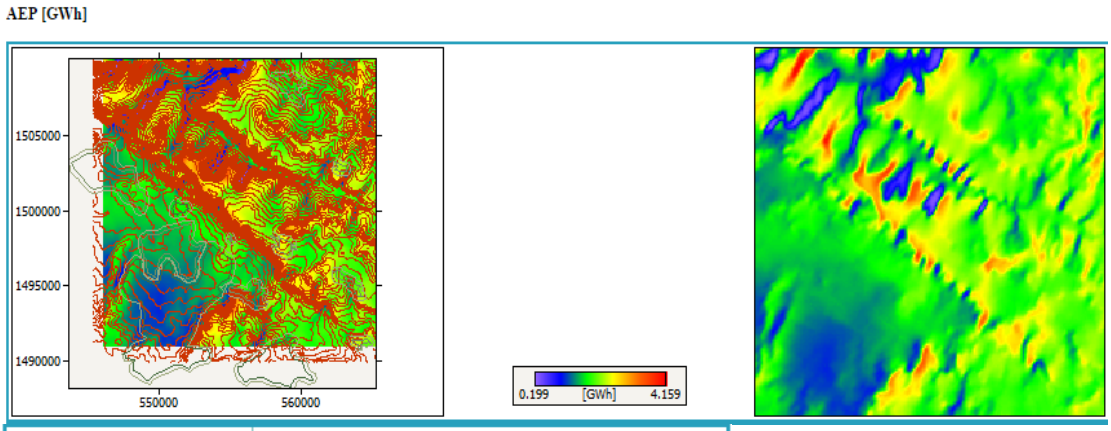


| | |
|---|---|
| Maximum Value: | 4.159 GWh at (548256, 1508743) |
| Minimum Value: | 0.199 GWh at (547056, 1509643) |
| Mean Value: | 1.903 GWh |

Figure 5-13: Annual energy production resource map at 80m wind turbine hub heights

### 5.2.4 Wind resource mapping for 80m turbine hub heights

**Grid Setup**

| | |
|---|---|
| Structure: | 192 columns and 190 rows at 100 resolutions give 36480 calculation sites. |
| Boundary: | (546106, 1490993) to (565306, 1509993) |
| Nodes: | (546156, 1491043) to (565256, 1509943) |
| Height a.g.l.: | 80m |
| WTG | 'Vestas V60-850 kW' |

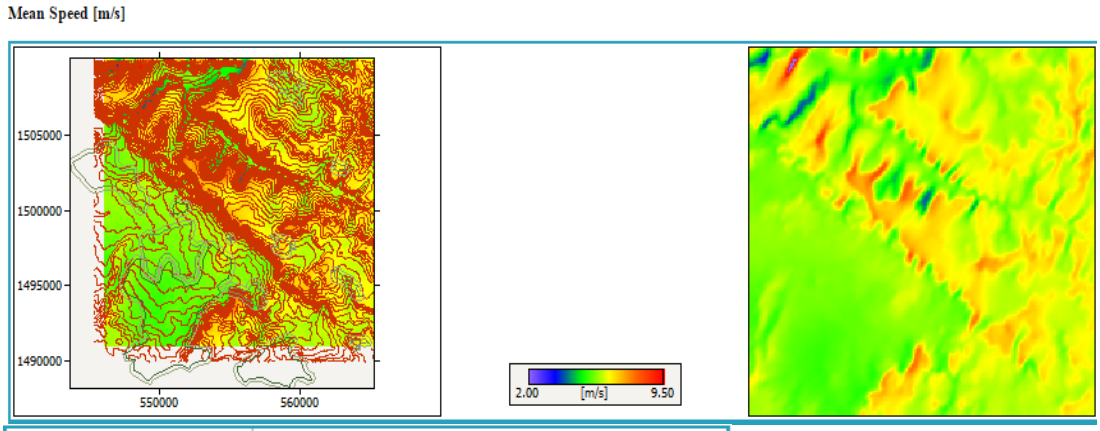


| | |
|---|---|
| Maximum Value: | 9.79 m/s at (548556, 1509243) |
| Minimum Value: | 3.65 m/s at (547056, 1509643) |
| Mean Value: | 6.13 m/s |

Figure 5-14: Wind speed Resource map at 80m wind turbine hub heights

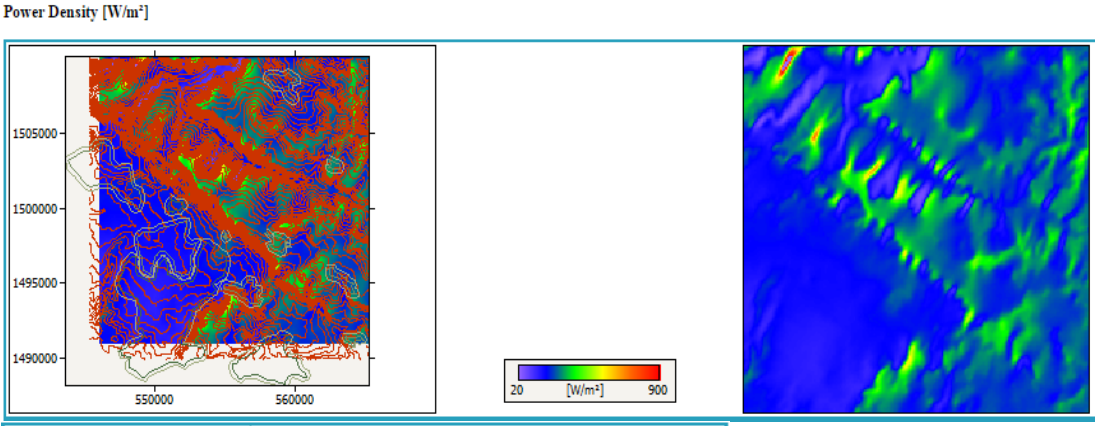


| | |
|---|---|
| Maximum Value: | 1082 W/m² at (548556, 1509243) |
| Minimum Value: | 41 W/m² at (546956, 1509443) |
| Mean Value: | 234 W/m² |

Figure5-15: Power density resource map at 80m wind turbine hub heights

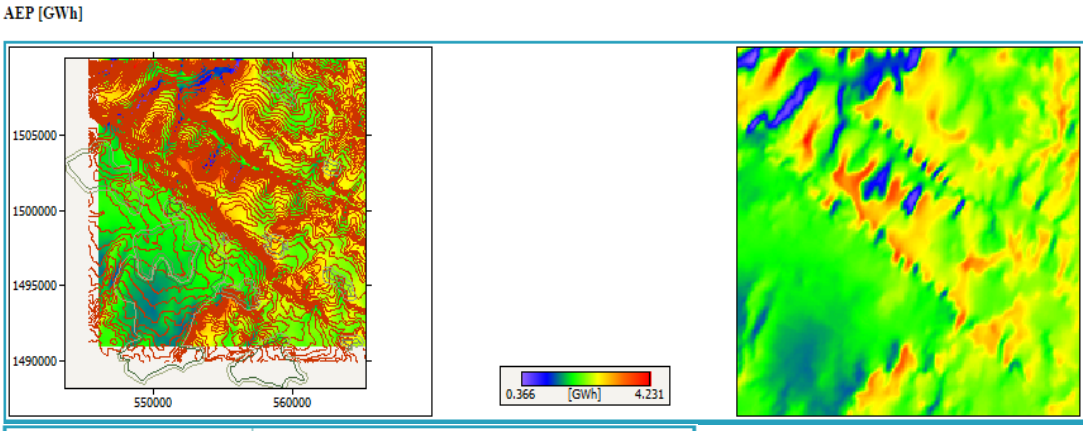


| | |
|---|---|
| Maximum Value: | 4.231 GWh at (548356, 1508843) |
| Minimum Value: | 0.366 GWh at (546956, 1509443) |
| Mean Value: | 2.236 GWh |

Figure 5-16: Annual energy production resource map at 80m wind turbine hub height

### 5.2.5 Wind resource mapping for 100m turbine hub heights

**Grid Setup**

| | |
|---|---|
| Structure: | 192 columns and 190 rows at 100 resolutions give 36480 calculation sites. |
| Boundary: | (546106, 1490993) to (565306, 1509993) |
| Nodes: | (546156, 1491043) to (565256, 1509943) |
| Height a.g.l.: | 100m |
| WTG | 'Vestas V60-850 kW' |

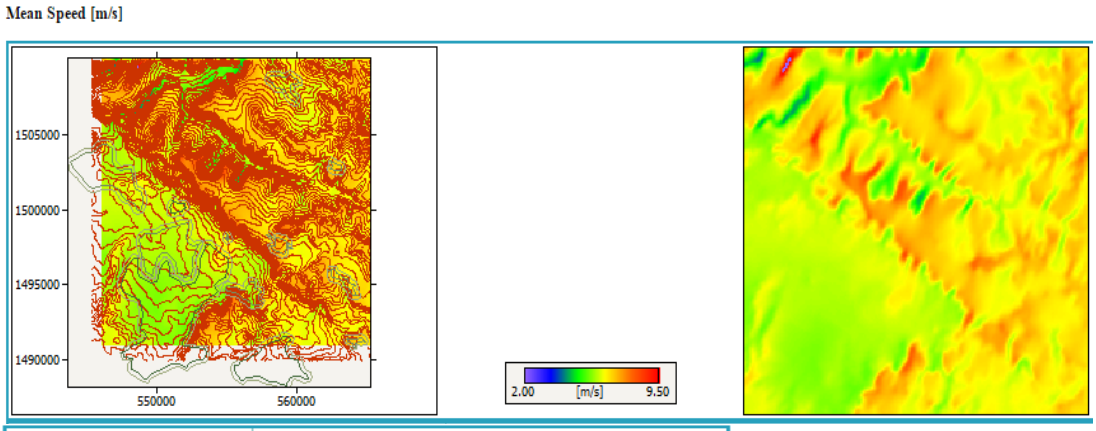


| | |
|---|---|
| Maximum Value: | 9.86 m/s at (548556, 1509243) |
| Minimum Value: | 4.15 m/s at (546856, 1509343) |
| Mean Value: | 6.49 m/s |

Figure 5-17: Wind speed resource map at 100m wind turbine hub heights

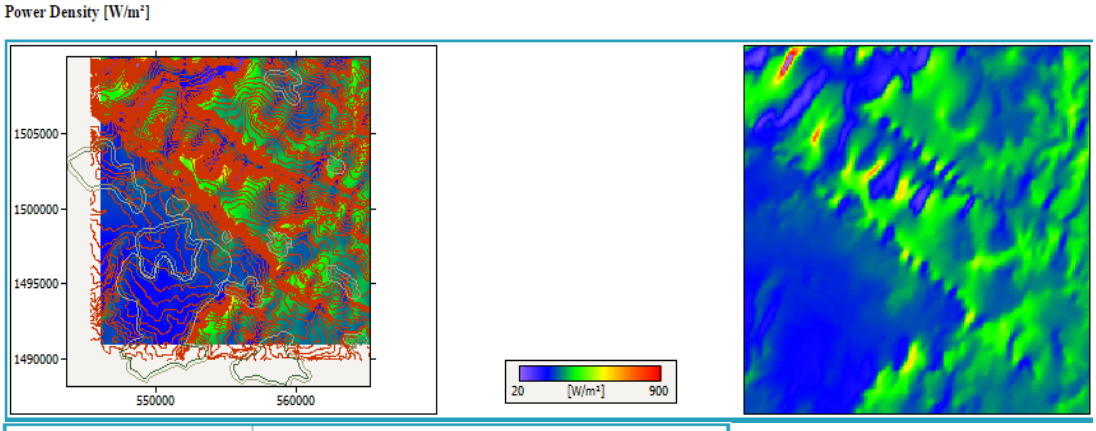


| | |
|---|---|
| Maximum Value: | 1096 W/m² at (548556, 1509243) |
| Minimum Value: | 60 W/m² at (546956, 1509443) |
| Mean Value: | 277 W/m² |

Figure 5-18: Power density resource map at 100m wind turbine hub heights

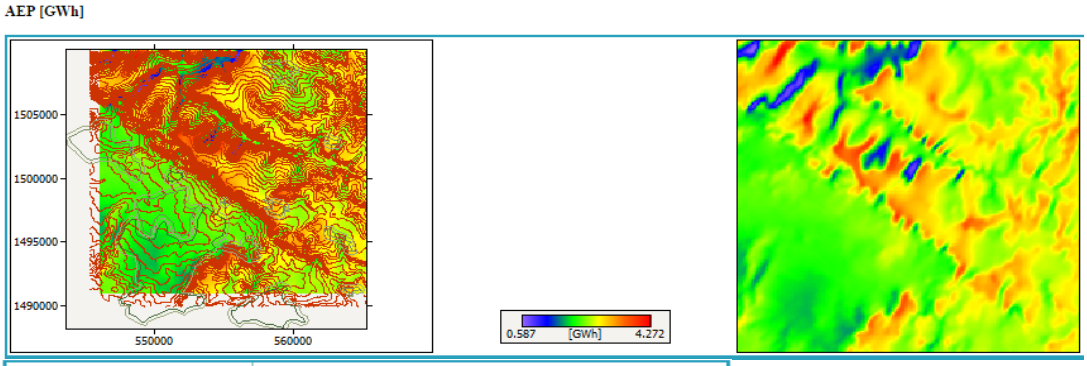


| | |
|---|---|
| Maximum Value: | 4.272 GWh at (548356, 1508843) |
| Minimum Value: | 0.587 GWh at (546956, 1509443) |
| Mean Value: | 2.540 GWh |

Figure 5-19: Annual energy production resource map at 100m wind turbine hub heights

### 5.2.6 The ruggedness index of the site

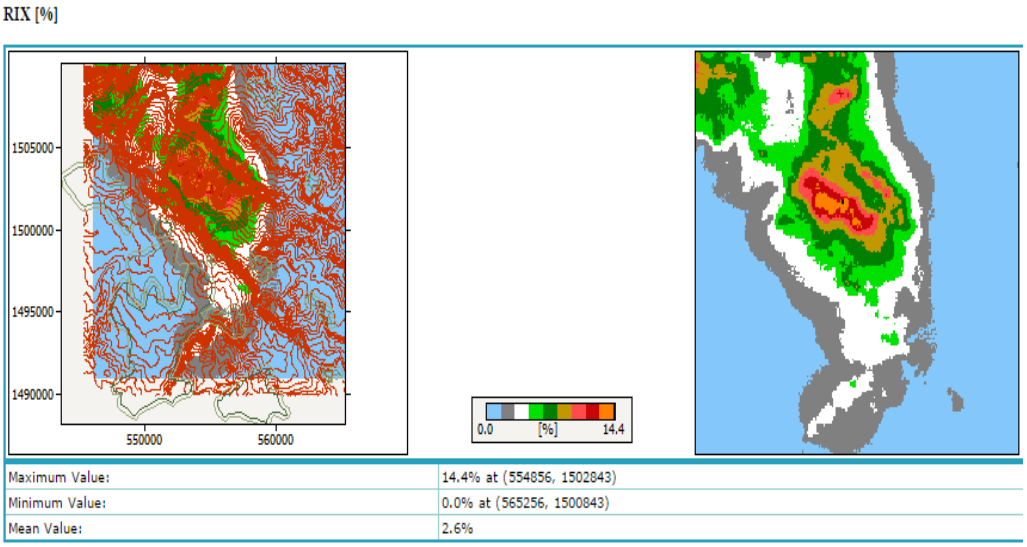


| | |
|---|---|
| Maximum Value: | 14.4% at (554856, 1502843) |
| Minimum Value: | 0.0% at (565256, 1500843) |
| Mean Value: | 2.6% |

Figure5-20: the ruggedness index (RIX) of Mesobo-Harena wind farm

The topographic ruggedness index (RIX) is a measurement to express the amount of elevation difference between adjacent cells of a digital elevation grid. According to WAsP reference manual landscapes are characterized by the following different ruggedness index values as: flat and hilly 0%, more complex about 10% or less, mountainous from about 10 to 50% or more. Hence Mosobo-Harena win farm within area coverage of 20km x 20km has average ruggedness index of 2.6% as shown in figure 5.20 implying the location is complex terrain.

# CHAPTER SIX

# TURBINE SITING AND WIND FARM LAYOUT

## 6.1 Introduction

Before wind turbines are installed, a sitting study needs to be undertaken to determine where to locate them. Turbine sitting involves laying out the turbine at optimum locations at the selected site. The major objective of a sitting study is optimally positioning the turbines within the wind farm so that the wake effect is minimized and therefore the expected power production maximized.

The rotation of blades of one turbine will cause turbulence to be induced on the nearby turbines. As proposed by Mathew, 2006, in order to minimize the effect of induced turbulence, wind turbines need to be positioned in such a way that a spacing of 3 - 4 rotor diameter within the rows perpendicular to the main wind direction, and the spacing in prevailing wind direction should be around 10 rotor diameter, so that the wind stream passing through one turbine is restored before it interacts with the next turbine.

Therefore, for this project turbines were placed in rows with minimum values of 540m of spacing in prevailing wind direction and 210 m spacing in direction perpendicular to prevailing winds, as shown in Figure 6.1.

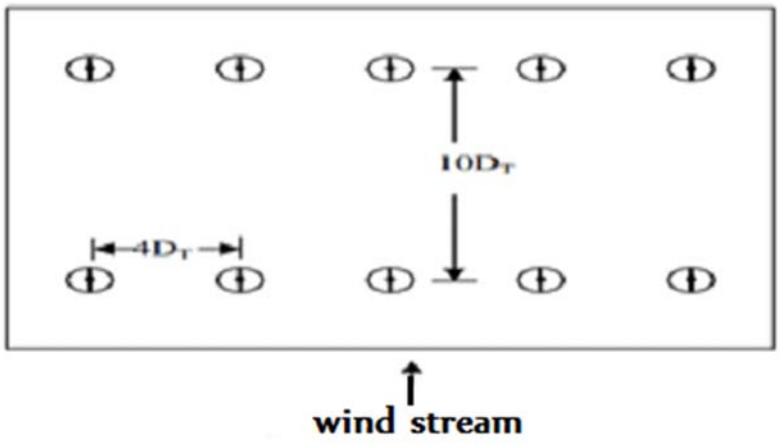


Figure 6-1: Typical layout of a wind farm [6]

But in practice, depending on some factors like the shape and size of the available land, existing electrical network, etc. the final placement of individual turbines at a given site may violate the above norms.

## 6.2 Mesobo-Harena Wind Farm Layout

For this project areas with high average wind speeds within the region of interest are identified and the wind farm layouts have been developed considering the effect of induced turbulence among turbines. Since wind resource is the most important factor when choosing a wind turbine location, the wind resource map of the site which had been generated by WAsP modeling was used for the sitting of individual turbines.

Figure 6.2 below - Resource Grid Map in WAsP, showing the AEP potential for seventy two 850 MW Vestas V60 turbines within the wind farm boundary, was used to locate high AEP sites and low wake losses. In the map, the colors denote the energy content of the wind farm, red high and blue low energy content.

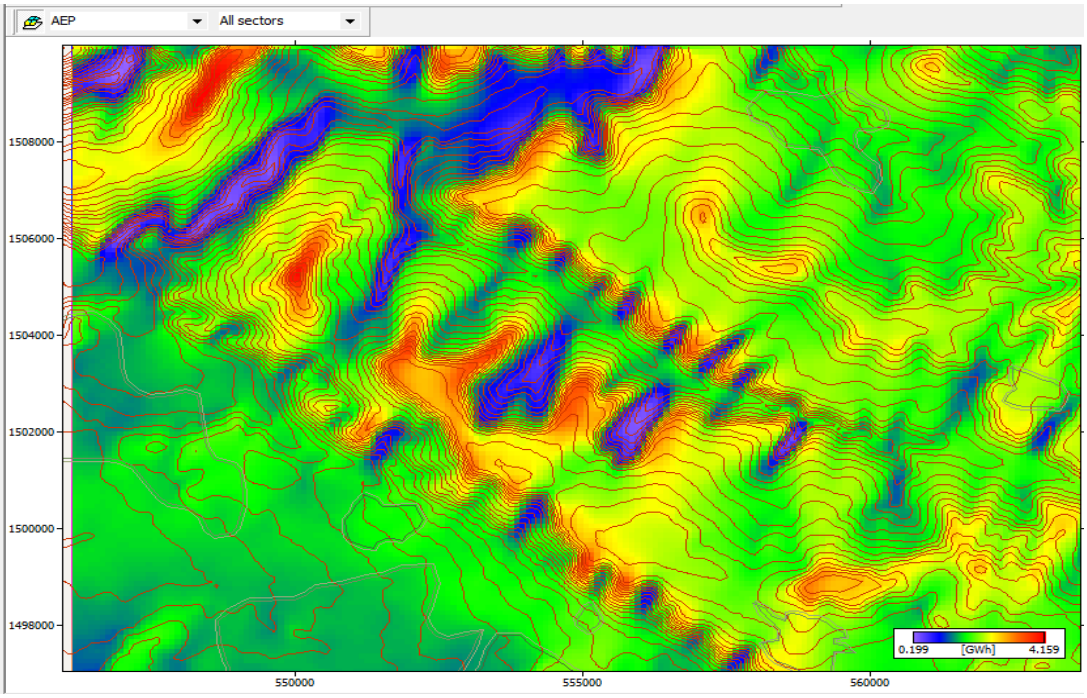


Figure 6-2: WAsP Resource Grid Map, showing the AEP potential of Mosobo-Harena wind farm

In order to simplify the installation, operation, maintenance and for efficient power transmission of Mesobo-Harena wind park, groups of wind turbines are locally concentrated and installed forming a turbine cluster. A turbine cluster consists of a set of turbine sites which differ from each other in their map location. The proposed wind site has area coverage of 20km x 20km. In this area total of 72 turbines were installed in 4 groups (turbine clusters). Turbine cluster 1 and turbine cluster 2 are found in North-West direction of the site and consists of 13 turbines each. Turbine cluster 3 with 25 turbines and turbine cluster 4 with 21 turbines are found around the center of the site. Therefore several rows of wind turbines are placed within the area and formed the layouts shown in Figure 6.3 and Figure 6.4.

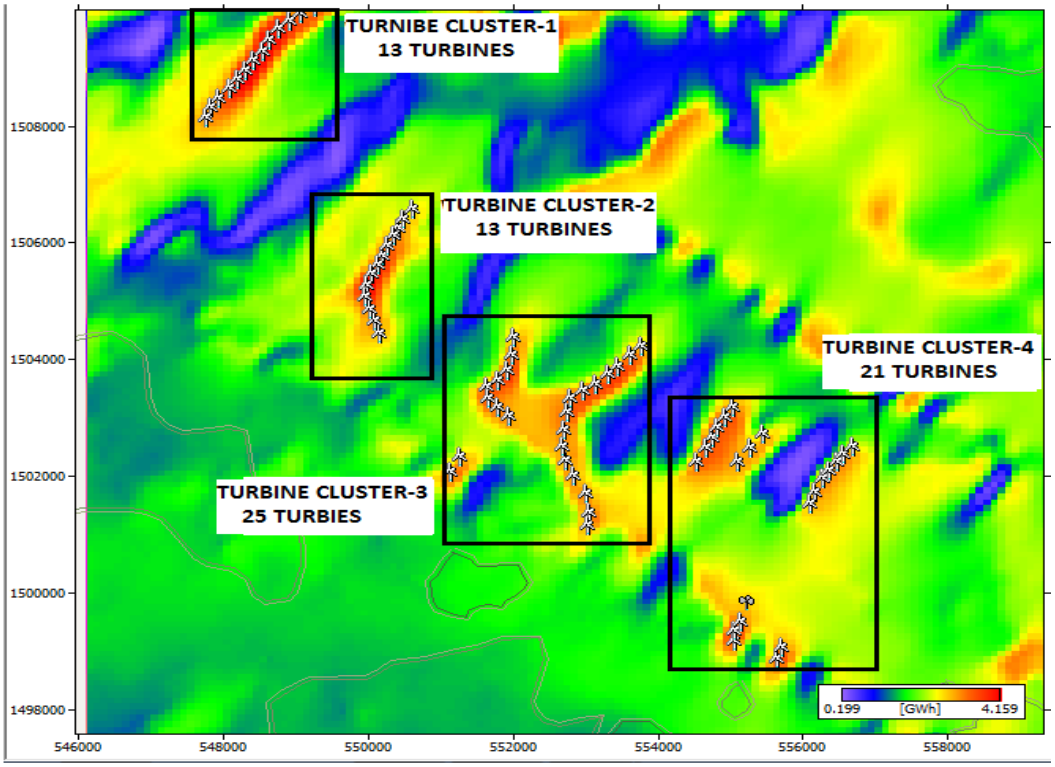


Figure 6-3: Mosobo-Harena Wind Park, Layout Vestas V60 turbines

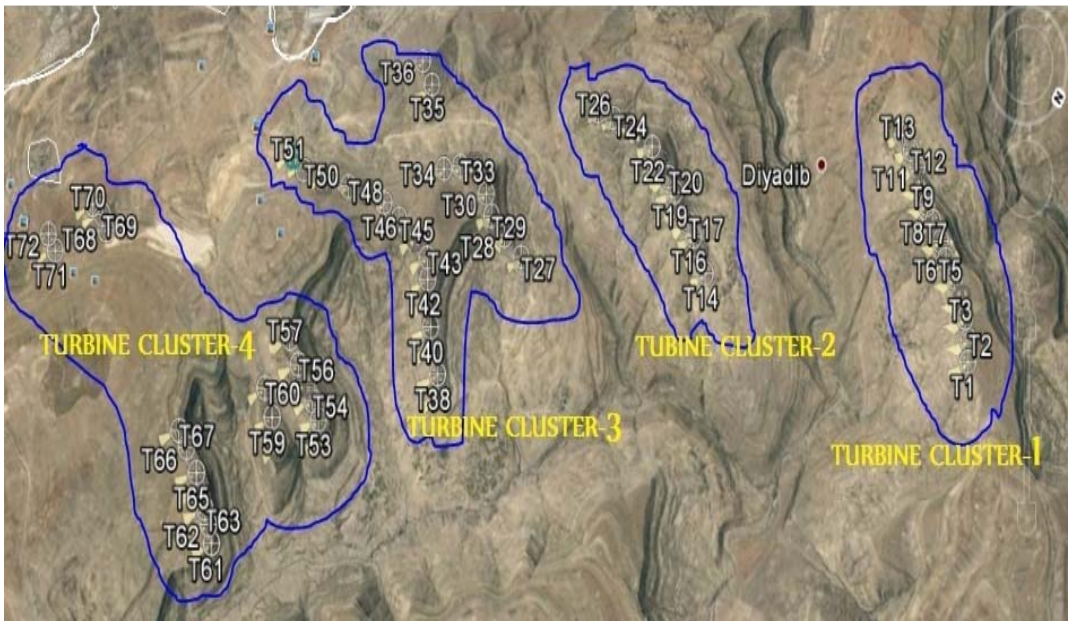


Figure 6-4: Mosobo-Harena Wind Park, Layout Vestas V60 -850Kw turbines, (Google earth image)

## 6.3 Summary Results of Mesobo-Harena Wind Farm Analysis

WAsP wind farm analysis report genereted the following summary results of the Mosebo-Harena wind farm. Table 6.2 shows the wind climate characteristics of individual turbine installed at recommended location in the farm.

Table 6.1: Mesobo-Harena wind farm summary results of basic parameters

| Parameter | Maximum Value: | Minimum Value: | Mean Value: | Farm Total |
|---|---|---|---|---|
| **Mean Speed [m/s]** | 9.66 m/s | 6.7 m/s | 7.68 m/s | _ |
| **Power Density [W/m²]** | 1059 W/m² | 296 W/m² | 491 W/m² | _ |
| **RIX [%]** | 14.10% | 4.00% | 8.10% | _ |
| **Net AEP [GWh]** | 4.143 | 2.665 | 3.282 | 236.301 |
| **Gross AEP [GWh]** | 4.158 | 2.749 | 3.383 | 243.583 |
| **Wake loss [%]** | _ | _ | _ | 2.99 |
| **Eff. [%]** | _ | _ | _ | 97.01 |

Table 6.2: Mesobo-Harena wind farm individual turbine site result and wind climate characteristics

| Turbine | Location [m] | A [m/s] | k | U [m/s] | E [W/m²] | Gross AEP [MWh] | Net AEP [GWh] | Wake loss [%] | Eff. [%] | RIX [%] |
|---|---|---|---|---|---|---|---|---|---|---|
| T1 | (549294.4,1509900) | 8.8 | 2.1 | 7.77 | 523 | 3444.11 | 3.436 | 0.23 | 99.77 | 4.7 |
| T2 | (549097.5,1509798) | 8.8 | 2.15 | 7.82 | 523 | 3488.755 | 3.434 | 1.56 | 98.44 | 5.4 |
| T3 | (548929.3,1509658) | 9.7 | 2.04 | 8.57 | 721 | 3839.45 | 3.802 | 0.99 | 99.01 | 5.9 |
| T4 | (548780, 1509531) | 10.2 | 2.02 | 9 | 845 | 3985.523 | 3.946 | 0.98 | 99.02 | 6.2 |
| T5 | (548657, 1509345) | 10.7 | 1.99 | 9.5 | 1004 | 4105.541 | 4.089 | 0.41 | 99.59 | 6.3 |
| T6 | (548555, 1509146) | 10.9 | 1.99 | 9.66 | 1059 | 4129.987 | 4.119 | 0.28 | 99.72 | 6.8 |
| T7 | (548440, 1508997) | 10.8 | 2.01 | 9.6 | 1028 | 4137.579 | 4.116 | 0.52 | 99.48 | 7.8 |
| T8 | (548322.3,1508809) | 10.7 | 2.06 | 9.45 | 957 | 4157.959 | 4.143 | 0.37 | 99.63 | 8.8 |
| T9 | (548219.8,1508658) | 10.4 | 2.06 | 9.2 | 882 | 4083.002 | 4.06 | 0.56 | 99.44 | 8.1 |
| T10 | (548104.9,1508506.) | 9.5 | 2.04 | 8.45 | 691 | 3781.642 | 3.755 | 0.71 | 99.29 | 5.9 |
| T11 | (547850.7,1508186) | 8.4 | 2.14 | 7.4 | 444 | 3217.311 | 3.185 | 1.01 | 98.99 | 6.1 |
| T12 | (547776.9,1508010) | 8 | 2.17 | 7.11 | 390 | 3027.899 | 2.992 | 1.19 | 98.81 | 6 |
| T13 | (547957.3,1508350) | 8.7 | 2.07 | 7.69 | 515 | 3391.346 | 3.358 | 0.99 | 99.01 | 6.2 |
| T14 | (550634.6,1506444) | 7.6 | 2.24 | 6.7 | 318 | 2748.781 | 2.72 | 1.03 | 98.97 | 4.6 |
| T15 | (550509.3,1506264) | 7.9 | 2.26 | 6.97 | 354 | 2947.741 | 2.907 | 1.38 | 98.62 | 4.2 |
| T16 | (550433.1,1506112) | 8.1 | 2.26 | 7.21 | 392 | 3125.291 | 3.082 | 1.37 | 98.63 | 4.1 |
| T17 | (550367.8,1505981) | 8.4 | 2.26 | 7.41 | 426 | 3256.338 | 3.204 | 1.62 | 98.38 | 4.1 |
| T18 | (550296.9,1505823) | 8.7 | 2.21 | 7.75 | 496 | 3466.877 | 3.42 | 1.36 | 98.64 | 4.2 |
| T19 | (550220.7,1505649) | 9.2 | 2.17 | 8.14 | 584 | 3693.182 | 3.648 | 1.23 | 98.77 | 4.7 |
| T20 | (550144.5,1505497) | 9.6 | 2.19 | 8.48 | 656 | 3876.196 | 3.824 | 1.35 | 98.65 | 5.3 |
| T21 | (550068.2,1505339) | 9.9 | 2.25 | 8.77 | 708 | 4056.357 | 4.002 | 1.34 | 98.66 | 7.2 |
| T22 | (550008.4,1505137) | 9.6 | 2.38 | 8.54 | 626 | 4011.181 | 3.943 | 1.7 | 98.3 | 7.7 |
| T23 | (549986.6,1504936) | 8.7 | 2.42 | 7.73 | 457 | 3533.535 | 3.41 | 3.5 | 96.5 | 5.3 |
| T24 | (550106.4,1504527) | 8.1 | 2.51 | 7.15 | 353 | 3111.914 | 2.954 | 5.06 | 94.94 | 4.4 |
| T25 | (550041.0,1504718) | 8.2 | 2.46 | 7.31 | 383 | 3241.01 | 3.087 | 4.75 | 95.25 | 4.5 |
| T26 | (550171.7,1504315) | 7.6 | 2.54 | 6.77 | 296 | 2795.196 | 2.665 | 4.65 | 95.35 | 4 |
| T27 | (552037.0,1504250) | 8 | 2.3 | 7.09 | 367 | 3061.637 | 2.95 | 3.65 | 96.36 | 6.8 |
| T28 | (552005.2,1503941) | 8.7 | 2.25 | 7.73 | 484 | 3502.256 | 3.369 | 3.8 | 96.2 | 6.9 |
| T29 | (551949.8,1503687) | 9 | 2.4 | 7.98 | 506 | 3687.617 | 3.532 | 4.22 | 95.78 | 8.7 |
| T30 | (551814.9,1503505) | 8.7 | 2.52 | 7.71 | 440 | 3514.517 | 3.3 | 6.11 | 93.89 | 8.4 |
| T31 | (551648.2,1503401) | 8.6 | 2.62 | 7.68 | 423 | 3503.725 | 3.108 | 11.29 | 88.71 | 7.6 |
| T32 | (551680.0,1503203) | 8.4 | 2.68 | 7.46 | 383 | 3362.423 | 2.936 | 12.69 | 87.31 | 6.9 |
| T33 | (551806.9,1503052) | 8.2 | 2.72 | 7.29 | 353 | 3224.456 | 2.834 | 12.12 | 87.88 | 6.4 |

| | | | | | | | | | | |
|---|---|---|---|---|---|---|---|---|---|---|
| T34 | (551965.6,1502886) | 8 | 2.77 | 7.13 | 327 | 3086.129 | 2.836 | 8.1 | 91.9 | 6.7 |
| T35 | (551295.2,1502200) | 8.2 | 2.18 | 7.25 | 410 | 3118.736 | 3.019 | 3.21 | 96.79 | 6.5 |
| T36 | (551150.2,1501932) | 8.3 | 2.29 | 7.34 | 410 | 3191.167 | 3.104 | 2.73 | 97.27 | 7.8 |
| T37 | (553782.2,1504084) | 8.3 | 2.15 | 7.31 | 426 | 3164.561 | 3.106 | 1.86 | 98.14 | 8.9 |
| T38 | (553639.4,1503949) | 8.9 | 2.1 | 7.86 | 542 | 3489.478 | 3.404 | 2.45 | 97.55 | 10.9 |
| T39 | (553472.9,1503743) | 9.3 | 2.07 | 8.25 | 635 | 3681.517 | 3.608 | 2.01 | 97.99 | 12.2 |
| T40 | (553330.1,1503616) | 9.3 | 2.08 | 8.21 | 623 | 3659.27 | 3.563 | 2.63 | 97.37 | 12.3 |
| T41 | (553155.6,1503449) | 9.1 | 2.08 | 8.09 | 596 | 3589.396 | 3.501 | 2.48 | 97.52 | 11.7 |
| T42 | (552981.0,1503322) | 8.9 | 2.16 | 7.9 | 536 | 3503.886 | 3.393 | 3.17 | 96.83 | 10.9 |
| T43 | (552814.4,1503195) | 8.6 | 2.3 | 7.63 | 458 | 3386.726 | 3.249 | 4.07 | 95.93 | 9.9 |
| T44 | (552758.6,1502950) | 8.4 | 2.38 | 7.47 | 419 | 3337.516 | 3.23 | 3.22 | 96.78 | 9.4 |
| T45 | (552731.9,1502657) | 8.1 | 2.56 | 7.2 | 355 | 3164.393 | 3.049 | 3.66 | 96.34 | 7.8 |
| T46 | (552714.2,1502382) | 7.9 | 2.67 | 7.03 | 320 | 3019.254 | 2.9 | 3.96 | 96.04 | 6.9 |
| T47 | (552749.7,1502125) | 8 | 2.65 | 7.09 | 330 | 3070.926 | 2.957 | 3.72 | 96.28 | 6.8 |
| T48 | (552858.6,1501864) | 8 | 2.69 | 7.1 | 330 | 3083.44 | 2.969 | 3.72 | 96.28 | 6.2 |
| T49 | (553033.7,1501557) | 8.1 | 2.71 | 7.18 | 338 | 3137.255 | 3.041 | 3.06 | 96.94 | 6.8 |
| T50 | (553078.1,1501237) | 8.4 | 2.53 | 7.45 | 396 | 3323.927 | 3.237 | 2.6 | 97.4 | 6.9 |
| T51 | (553051.0,1501026) | 7.8 | 2.28 | 6.94 | 347 | 2905.343 | 2.836 | 2.38 | 97.62 | 5.3 |
| T52 | (555046.4,1503038) | 8.6 | 2.24 | 7.62 | 467 | 3410.182 | 3.296 | 3.35 | 96.65 | 13.2 |
| T53 | (554942.8,1502876) | 8.8 | 2.30 | 7.78 | 485 | 3519.5472 | 3.358 | 4.59 | 95.41 | 14.1 |
| T54 | (554848.2,1502705) | 8.7 | 2.27 | 7.72 | 479 | 3475.482 | 3.269 | 5.95 | 94.05 | 14 |
| T55 | (554776.1,1502529) | 8.8 | 2.19 | 7.82 | 514 | 3517.418 | 3.295 | 6.33 | 93.67 | 13.3 |
| T56 | (554681.6,1502349) | 8.8 | 2.17 | 7.75 | 504 | 3463.157 | 3.236 | 6.56 | 93.44 | 11.6 |
| T57 | (554550.9,1502110) | 8.5 | 2.13 | 7.53 | 470 | 3300.6978 | 3.169 | 3.99 | 96.01 | 10.2 |
| T58 | (555480.6,1502590) | 8 | 2.29 | 7.1 | 370 | 3010.332 | 2.868 | 4.73 | 95.27 | 12.8 |
| T59 | (555289.8,1502351) | 8 | 2.29 | 7.11 | 373 | 3035.671 | 2.855 | 5.95 | 94.05 | 12.7 |
| T60 | (555127.4,1502110) | 7.9 | 2.26 | 7 | 359 | 2968.618 | 2.8 | 5.67 | 94.33 | 11.2 |
| T61 | (556703.3,1502378) | 7.9 | 2.26 | 7.01 | 361 | 2989.132 | 2.978 | 0.37 | 99.63 | 10 |
| T62 | (556586.9,1502241) | 8.2 | 2.26 | 7.26 | 400 | 3146.651 | 3.107 | 1.27 | 98.73 | 11.1 |
| T63 | (556499.5,1502113) | 8.2 | 2.25 | 7.28 | 404 | 3155.095 | 3.117 | 1.22 | 98.78 | 12 |
| T64 | (556386.0,1501964) | 8.2 | 2.26 | 7.24 | 396 | 3130.863 | 3.091 | 1.26 | 98.74 | 12.1 |
| T65 | (556298.6,1501824) | 8.2 | 2.26 | 7.22 | 394 | 3119.202 | 3.082 | 1.2 | 98.8 | 12.1 |
| T66 | (556190.9,1501580) | 8 | 2.2 | 7.08 | 379 | 3014.544 | 2.986 | 0.95 | 99.05 | 11.2 |
| T67 | (556121.9,1501402) | 7.8 | 2.19 | 6.88 | 350 | 2867.463 | 2.837 | 1.08 | 98.92 | 10.1 |
| T68 | (555169.7,1499365) | 8.6 | 2.42 | 7.59 | 433 | 3407.451 | 3.327 | 2.35 | 97.65 | 6.8 |
| T69 | (555074.2,1499214) | 9.1 | 2.29 | 8.03 | 536 | 3656.25 | 3.53 | 3.45 | 96.55 | 8 |
| T70 | (555070.9,1499029) | 8.3 | 2.28 | 7.34 | 410 | 3217.051 | 3.085 | 4.12 | 95.88 | 7.7 |
| T71 | (555735.1,1498923) | 8.6 | 2.45 | 7.66 | 441 | 3476.55 | 3.447 | 0.84 | 99.16 | 7.6 |
| T72 | (555660.6,1498726) | 8.4 | 2.23 | 7.44 | 436 | 3277.997 | 3.239 | 1.18 | 98.82 | 7 |

The following four figures are illustrations of turbine sittings for each turbine clusters in the proposed wind park one by one. The left half of each figure was copied from the vector map which contains multiple of turbines with site mean speed distribution and wind frequency rose, and the corresponding three-dimensional model of the turbines is shown in the right half of the figure which was obtained by Synchronizing with Google-Earth.

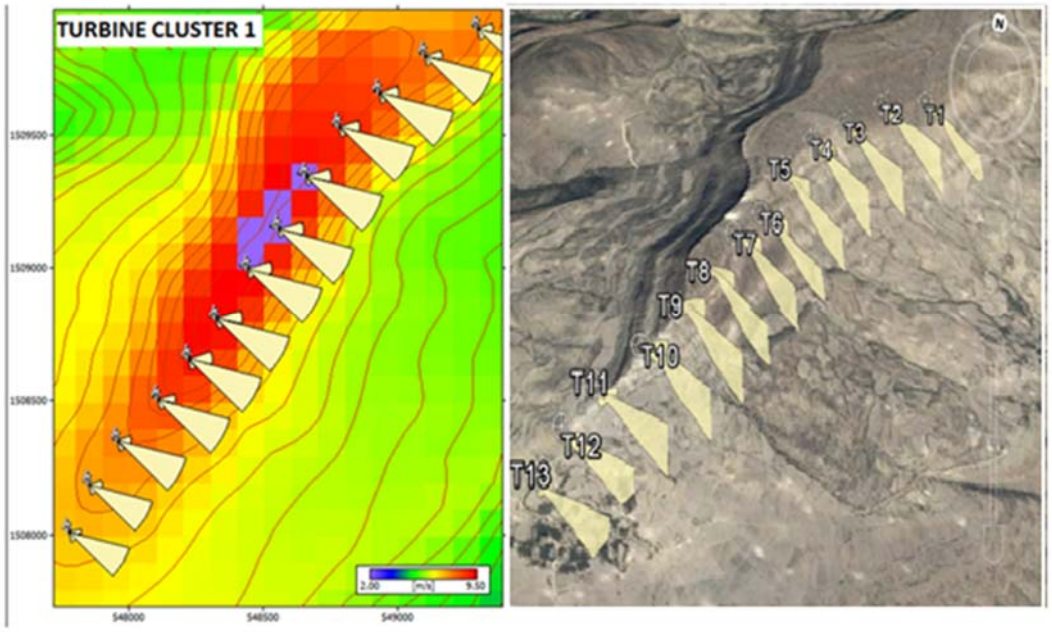


Figure 6-5: Wind turbines sitting with site mean wind speed and wind frequency rose for turbine cluster-1

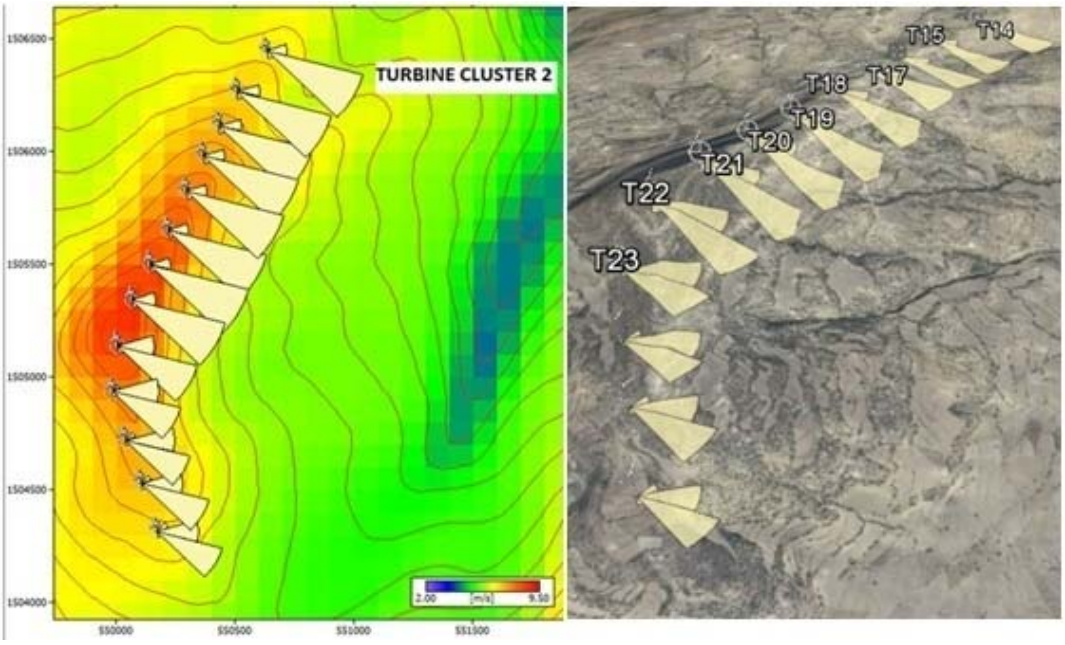


Figure 6-6: Wind turbines sitting with site mean wind speed and wind frequency rose for turbine cluster-2

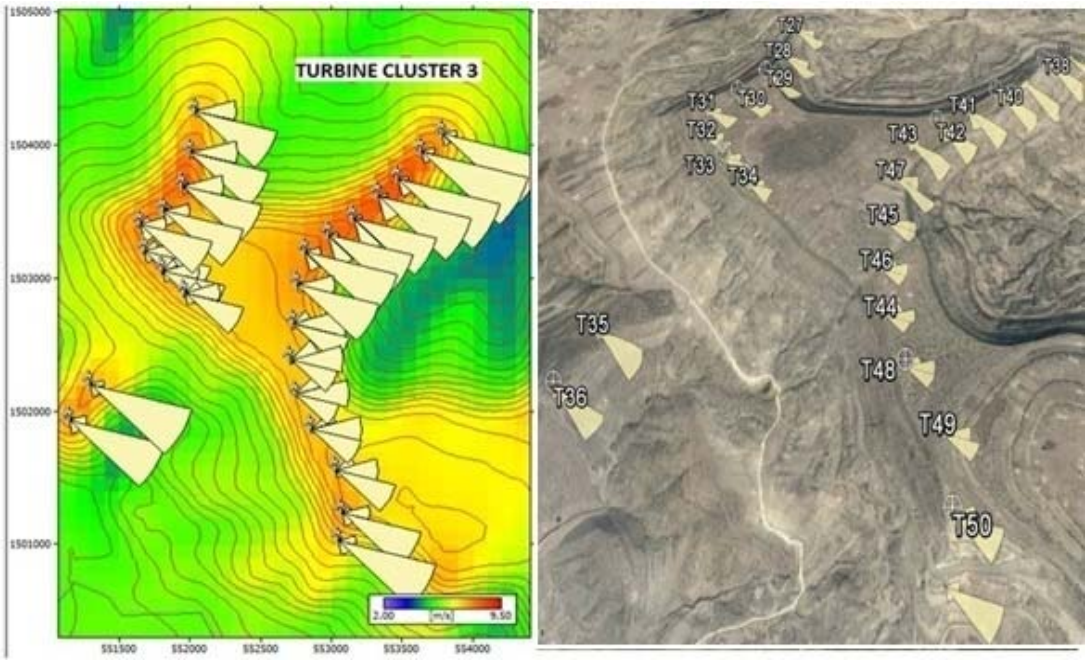


Figure 6-7: Wind turbines sitting with site mean wind speed and wind frequency rose for turbine cluster-3

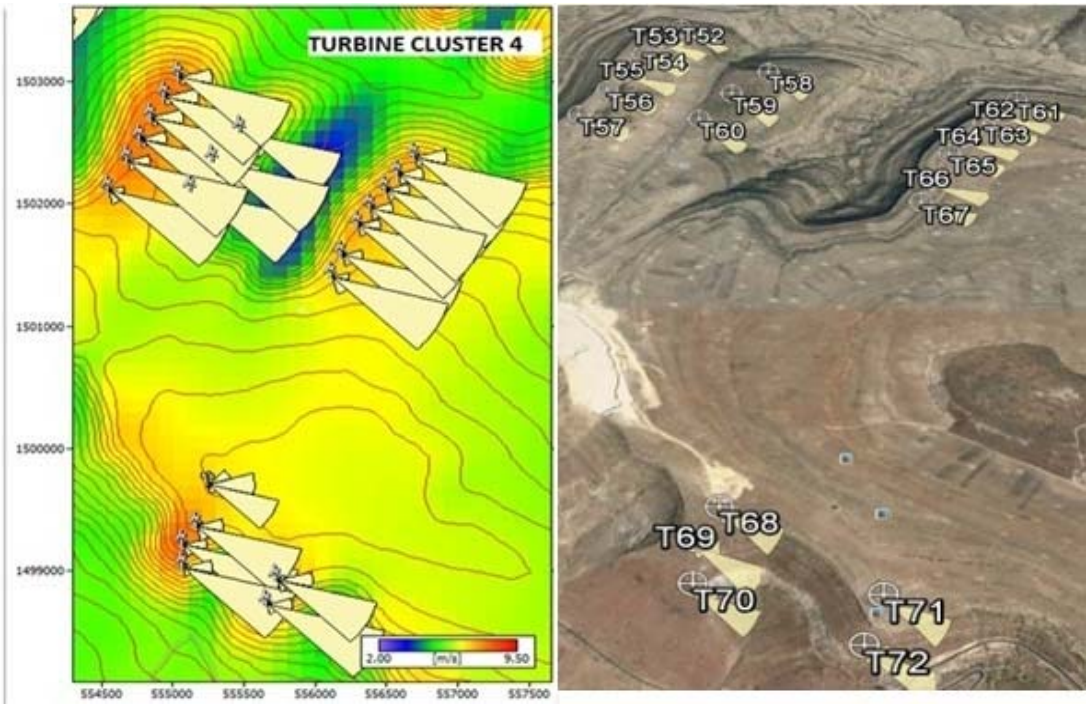


Figure 6-8: Wind turbines sitting with site mean wind speed and wind frequency rose for turbine cluster-4

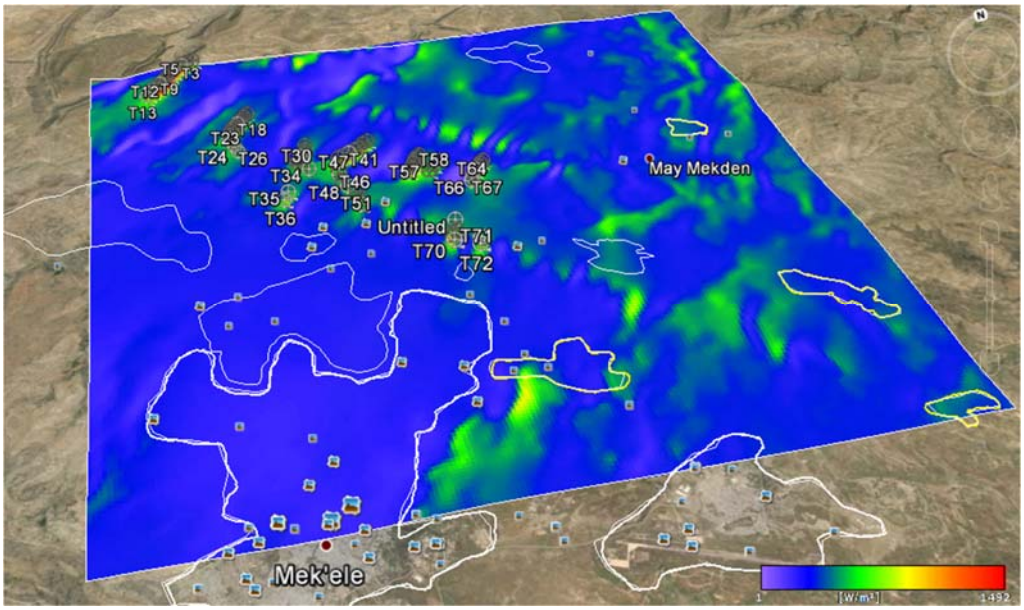


Figure 6-9: Google-Earth 3D image synchronized with power density distribution

The following figures are some of the turbine sitting's 3D views of Google-Earth Synchronized with site AEP distribution for each turbine clusters. .

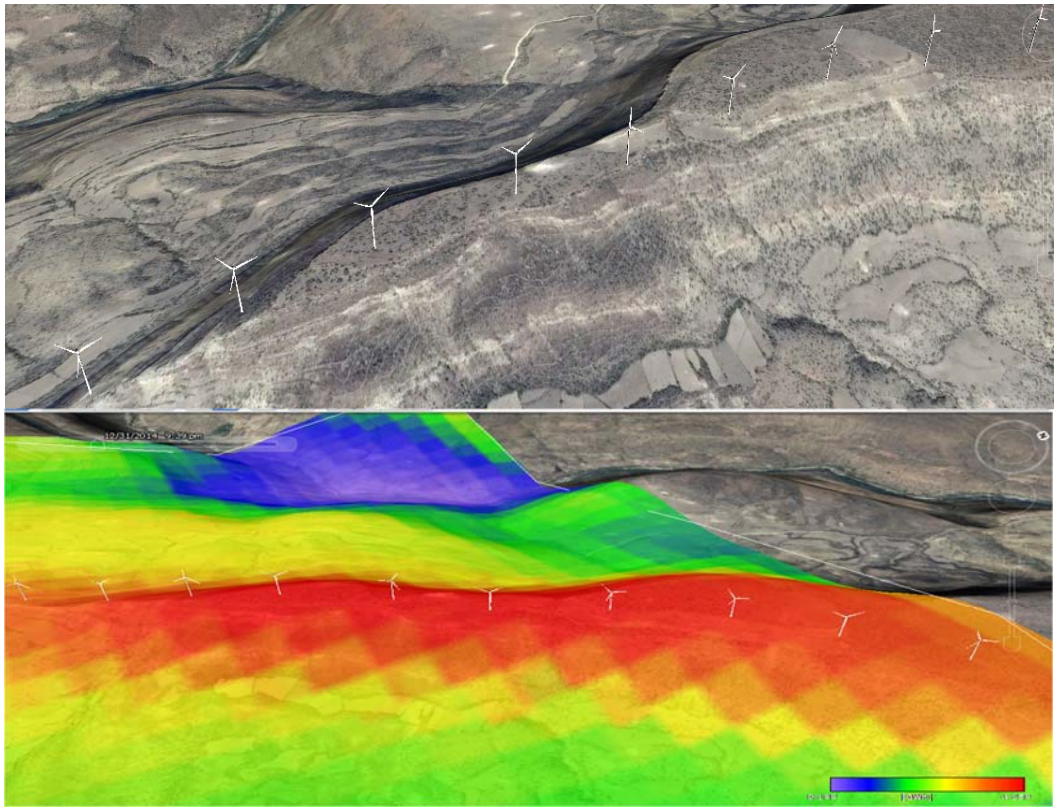

Figure 6-10: Google earth 3D view of wind turbines sitting with site AEP for turbine cluster-1

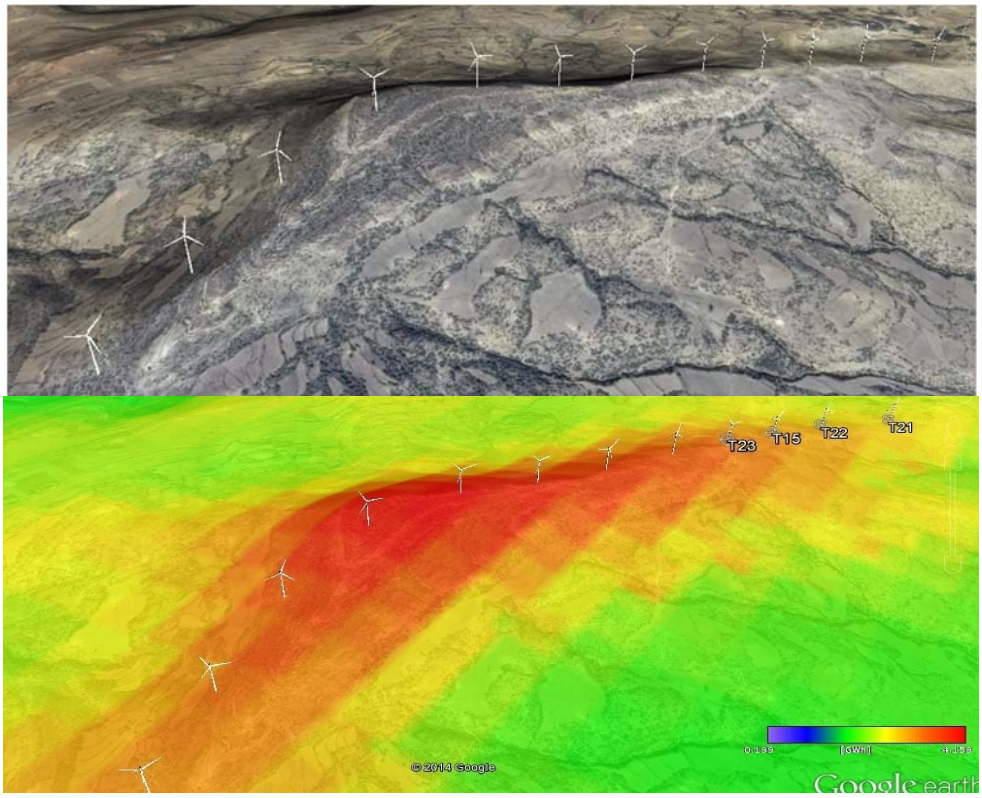


Figure 6-11: Google earth 3D view of wind turbines sitting with site AEP for turbine cluster-2

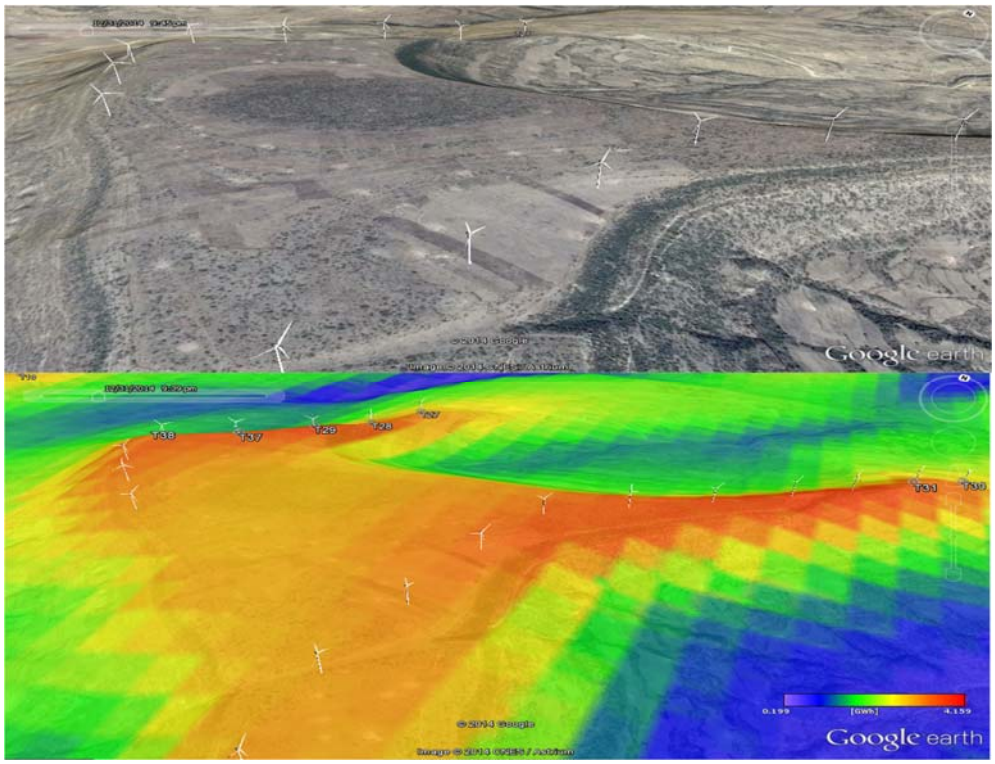


Figure 6-12: Google earth 3D view of wind turbines sitting with site AEP for turbine cluster-3

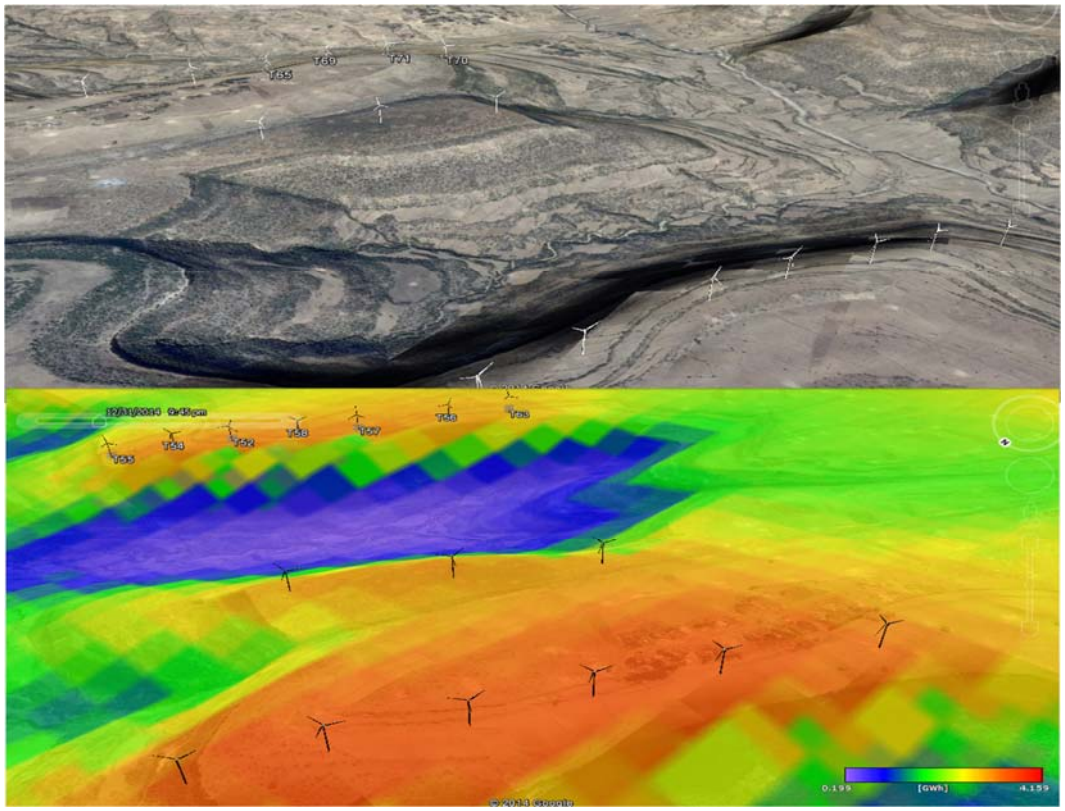

Figure 6-13: Google earth 3D view of wind turbines sitting with site AEP for turbine cluster-4

## 6.4 Energy and Capacity Factor Calculation for Mesobo-Harena Wind Farm

As discussed above, the wind turbine V60 with rated power of 850kW was selected. Rated AEP of the turbine can be calculated as:

Rated AEP = Rated power x the number of hours in one year ;

= 850kW x 8760 = 7,446,000kWhr = 7.446GWhr

Rated AEP of the total number of 72 turbine is = 72 x 7.446 = 536.112GWhr.

As indicated in Table 6.2 net average AEP per turbine is 3.282GWhr and the total net AEP of the farm with total number of 72 turbines is 236.301GWhr. Therefore, the capacity factor (CF) of the farm is calculated as:

CF = Net total AEP of the farm divided by Total rated AEP of the turbines

= 236.301 / 536.112 = 44 %

The energy calculation by WAsP above using table 6.1 considers only the wind farm wake loss. But in practice there are also various unfavorable causes occurring along electro

mechanical drive which reduce the park efficiency considerably so that the total net annual energy production of the farm will be lower than this calculated value. As presented by [Erich H.], these losses may have following approximate values.

- The tower shadow effect loss (wake loss) = 2 to 3% in our cause it is 2.99%.
- Bearing efficiency = 99.60%
- Gearbox efficiency = 97.20%
- Generator efficiency = 96.50%
- Efficiency of Frequency converter = 97.50%
- Transformer and other transmission accessories = 98.00%

Therefore, the estimated total system efficiency would be 82.8%.

Then the new actual net AEP is calculated to be **201686.7 MWh.** And therefore the actual CF would be **37.6%.**

The overall energy characteristics of the farm are summarized in Table 6.3 below.

Table 6.3 Energy Calculations for Mesobo-Harena Wind farm with Vestas V850 layout

| | | |
|---|---|---|
| Turbine type | | Vestas V60-850Kw |
| Hub height | m | 60 |
| Rotor diameter | m | 60 |
| Rated Turbine power capacity | kW | 850 |
| No. of turbines | | 72 |
| Installed farm capacity | MW | 61.2 |
| Rated AEP per turbine | MWh | 7446 |
| Total turbines rated AEP | MWh | 536,112 |
| Farm Gross AEP | MWh | 243583 |
| Wind farm wake loss | % | 2.99 |
| Bearing efficiency | % | 99.60 |
| Gearbox efficiency | % | 97.20 |
| Generator efficiency | % | 96.50 |
| Efficiency Frequency converter | % | 97.50 |
| Transformer and other transmission accessories | % | 98.00 |
| Farm Net AEP | MWh | **201686.7** |
| Capacity factor | % | **37.6%.** |

# CHAPTER SEVEN

# CONCLUSION AND RECOMMENDATION

## 7.1. Conclusion

Ethiopia has been relying much on hydroelectric plants for its power demand. But hydro power is exposed to the effects of climatic change. Recently the country faced major challenges in electricity as a result of industrial development and population growth. At the same time the problem of water level fluctuation is increasing continuously in most of the hydropower dams resulting from climate change. Therefore searching other local renewable energy sources, particularly wind energy, is greatly helpful to Ethiopia to meet its growing massive energy demand and to promote sustainable development.

In this paper, wind energy resource assessment was conducted for Mosobo-Harena wind farm with the help of different statistical methods and software such as MS Excel, MATLAB and WAsP (the Wind Atlas Analysis and Application Program). For this purpose, one year 10 minutes interval wind speed data from mast at Mosobo-Harena is used. According to the result of the WAsP wind atlas modeling, in this wind farm, the annual mean wind speed at the selected hub height of 60m is 6.79m/s and the annual wind power density is 316W/$m^2$. This is lower wind resource potential compared to that of Adama and Ashegoda wind farms. According to the IEC wind class regulations, wind turbine class-III is found to be more suitable for the farm at 60m hub height. And thus wind turbine Vestas V60-850kW was selected from WAsP documentation catalogue. The result also shows that both the most frequent wind and the major wind energy in Mosobo-Harena wind park come from east of southeast direction (ESE); and therefore this should be considered during installation of turbines.

The seasonal pattern of the wind in the study area at 10m height shows that relatively high mean speeds were recorded in March, April, November and December. These months are the dry season in Ethiopia so that the water level in hydropower reservoirs will be low. And very low wind speeds were recorded in July, August and September. These months are rainy and cold season so that hydropower reservoirs will rapidly filling up with water in this period. Therefore, in the context of the Ethiopian power system, wind power will play a vital complementary role with hydro power. This will make wind power a crucial ingredient of the grid energy mix by improving the reliability of the system even in dry seasons.

## 7.2. Recommendation

In this paper, wind energy resource assessment for Mesobo-Harena wind farm was conducted using WAsP modeling. WAsP software is found to be successful and suitable for predicting wind climate, wind resources, wind potential sites, and power production from each wind turbine and the wind farm.

However, the present work is only a preliminary study in order to estimate the wind energy potential at different locations in the farm and does not include environmental, economic and financial issues. For a comprehensive study prior to construction and installing wind energy conversion systems, a detail environmental, economic and financial feasibility analysis for the proposed wind farm should be performed.

It is recommended that on-site observation be carried out for each wind turbine candidate site separately in order to examine the challenges of individual turbines installation and control at highly potential sites which are marked by red color in the resource grid map. This is maybe due to complex orographic conditions.

A density correction should be made for wind farm (at the selected hub height of the turbine a.s.l) as the air density change with elevation. This paper has not considered the site specific power curve adjustment of the air density.

# References


1. Dan Chiras, 2010, ***Wind Power Basics, A Green Energy Guide,*** Canada

2. Danish Wind Industry Association, 2002, ***Guided Tour on Wind Energy***.

3. Erich H., 2006, ***Wind Turbines: Fundamentals, Technologies, Application, Economics***, Springer-Verlag, Berlin Heidelberg.

4. International Electrotechnical Commission (61400-12-1 IEC), 2005***, International Standard Wind Turbines***, Geneva, Switzerland.

5. Manwell J.F., McGowan J.G. and Rogers and A.L. 2002, ***Wind Energy Explained-Theory, Design, and Application***, New York, USA

6. Mathew Sathyajith, 2006, ***Wind Energy Fundamentals, Resource Analysis and Economics***, Springer-Verlag Berlin Heidelberg.

7. Michael Green, 2005, ***Using Mesoscale Meteorological Models to Assess Wind Energy Potential***, University of Canterbury.

8. National Renewable Energy Laboratory (NREL), 1997, ***Wind Resource Assessment Handbook: Fundamentals for Conducting A Successful Monitoring Program***, USA

9. Risø National Laboratory, ***Wasp10 software Help Documentation***, 2010, Technical University of Denmark, Denmark.

10. Thomas Ackermann (ed.), ***Wind Power in power system***, Royal Institute of Technology Stockholm, Sweden.

11. Wei Tong (ed.), ***Wind Power Generation and Wind Turbine Design***, Kollmorgen Corp, USA.

12. Wind Energy Guide; Wind Energy Development Programmatic IEC
Available: http//www.windeis.anl.gov/guide/basics Accessed: October 2014.